

1-(C-11)L-LEUCINE AND THE PRINCIPLE OF METABOLIC TRAPPING FOR THE TOMOGRAPHIC MEASUREMENT OF CEREBRAL PROTEIN SYNTHESIS IN MAN

J.R. Barrio, M.E. Phelps, S.-C. Huang, R.E. Keen, and N.S. MacDonald.  
 UCLA School of Medicine, Division of Biophysics, Los Angeles, California 90024.

We describe herein the development of a remote controlled, semiautomated synthesis of non-carrier added (NCA) 1-(C-11)L-leucine and the investigation of its use by application of tracer kinetic principles to the measurement of local rates of cerebral protein synthesis (CPR) with positron computed tomography (PCT) using a model developed by Smith et al (1) for autoradiography studies with 1-(C-14)leucine.

1-(C-11)L-leucine was synthesized from NCA C-11 labeled HCN using a modification of the Bucherer-Strecker reaction (2) with subsequent purification of the L-leucine stereoisomer by treating the enantiomers with immobilized D-amino acid oxidase, an enzyme that deaminates D-amino acids without affecting L-amino acids (3). In all cases the resultant 1-(C-11)L-leucine was easily separated from the radiolabeled alpha-ketoisocaproic acid, formed by deamination of D-leucine, using an AG 1-X4 anion exchange column and obtained with >99% radiochemical purity. (Ultrasphere ODS, 5  $\mu$ m, 4.6 X 150 mm column; mobile phase: 90% 30 mM sodium acetate, 17 mM L-proline, 8 mM CuCl<sub>2</sub> and 10% MeOH; flow rate 1.0 mL/min; radioactivity detector; retention time for L-leucine: 12.5 min). Typically the synthesis was accomplished 30 min after cyclotron production of NCA C-11 labeled HCN with radiochemical yields of >20 mCi (25%). The use of a remote, semiautomated system assures less than 1 mR radiation exposure to the chemist. Use of immobilized enzymes eliminates the possibility of protein contamination, assures sterile, pyrogen free products, and allows rapid separation of D and L-isomers.

Two distinctive biochemical features make 1-(C-11)L-leucine attractive for the measurement of CPR in man with PCT. a) L-leucine is transported across the blood brain barrier (BUI =  $54 \pm 2$ ) with L-phenylalanine (BUI =  $55 \pm 5$ ) being the only other amino acid with a higher brain uptake in rats (4), b) In addition to its incorporation into proteins, L-leucine is also oxidatively decarboxylated in mitochondria (5,6). This metabolic pathway results in labeled CO<sub>2</sub>, which is removed from the tissue by the cerebral blood flow leaving the major portion of the C-11 in the form of labeled proteins at times > 40 min after injection.

Initial kinetic PCT studies after I.V. injections of 1-(C-11)L-leucine, plasma sampling and the application of a tracer kinetic model allow for the calculation of transport, pool turnover rates, ratio metabolism/CPR, rate constants for each process and CPR in monkeys and man. In 3 adult monkeys, the global CPR was  $0.61 \pm 0.18$  (S.D.) nmole/g/min. In a normal volunteer, CPR was gray matter = 1.05 white matter = 0.49 and global = 63 nmole/g/min, in good agreement with above PCT and in vitro monkey data.

- (1) Smith, C.B., Davidson, L., Deibler, G., Patlak, C., Pettigrew, K, and Sokoloff, L., *Trans. Am. Soc. Neurochem.*, 11, 94 (1980).
- (2) Washburn, L.C., Sun, T.T., Byrd, B.L., Hayes, R.L., Butler, T.A. and Callahan, A.P., *Radiopharmaceuticals II*, 767 (1979).
- (3) Bright, H.J., Porter, D.J.T., *The Enzymes*, P.D. Boyer, ed., 3rd edition, vol. 12, p 445 (1975).
- (4) Oldendorf, W.H., *Am. J. Phys.*, 221, 1629 (1971).
- (5) Chaplin, E.R., Goldberg, A.L. and Diamond, I., *J. Neurochem.*, 26, 701 (1976).
- (6) Williamson, J.R., Walajtys-Rode, E. and Coll, K.E., *J. Biol. Chem.*, 254, 11511 (1979).

Table 1. Kinetic Rate Constants for Leucine and Cerebral Protein Synthesis Rate (CPR)

	$k_1$	$k_2$	$k_3$	$k_4$	$k_5$	(a)	(b)	(c)	(d)	CPR
						$k_5/k_3$	$\frac{\ln 2}{k_2+k_3+k_5}$	$\frac{\ln 2}{k_4}$	Leu	
							(min)	(min)	( $\mu M$ )	(nmole/min/g)
Human (Gray Matter)	0.176 (0.039)	1.12 (0.25)	0.124 (0.002)	0.058 (0.013)	0.085 (0.008)	0.680 (0.072)	0.481 (0.081)	12.3 (2.7)	104	1.05 (0.04)
(White Matter)	0.320	7.15	0.293	0.036	0.112	0.382	0.092	19.3		0.49
(Global)	0.138 (0.040)	1.08 (0.35)	0.144 (0.025)	0.037 (0.001)	0.057 (0.011)	0.41 (0.15)	0.56 (0.16)	18.7 (0.3)		0.63 (0.13)

(a) Ratio of protein synthesis to metabolic rate. (b) Half time of leucine precursor pool.  
(c) Half time of metabolic pool. (d) Plasma leucine concentration. (e) Values in parenthesis  
are standard deviations.

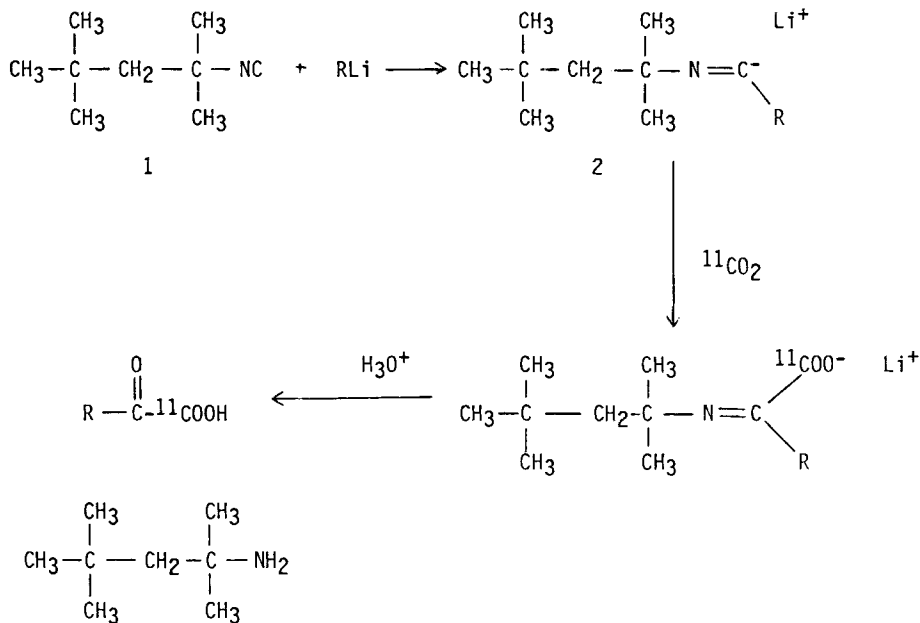
NEW REACTIONS FOR CARBON-11 LABELING

M.R. Kilbourn and M.J. Welch.

Washington University School of Medicine, St. Louis, MO 63110.

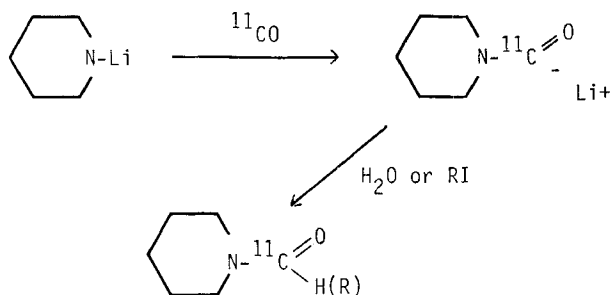
Although a large number of organic compounds have now been prepared in carbon-11 labeled form, only a limited effort has been expended in the development of new methods of organic syntheses with carbon-11. Simultaneously with our efforts into preparing radiopharmaceuticals for PETT studies, we have begun to examine new chemical reactions for labeling with carbon-11: our goals are to develop new classes of compounds labeled with carbon-11, or improve on syntheses of labeled compounds already of interest. We report here developments in new radiolabeling reactions for use in labeling with carbon-11.

Metallo Aldimines: "Masked" Acyl Carbanions. The reaction of an organolithium or Grignard reagent with a suitable isonitrile (one lacking  $\alpha$ -hydrogens: we have used 1,1,3,3-tetramethylbutylisonitrile, 1) yields the unstable metallo aldimine 2, which readily adds to  $^{11}\text{C}^{12}\text{O}_2$  to form the labeled  $\alpha$ -imino acid 3:



acidic hydrolysis then yields the C-11 labeled  $\alpha$ -keto acid (1). This reaction sequence can be used to prepare a wide variety to  $\alpha$ -keto acids: we have prepared C-11 labeled pyruvic acid ( $\text{R}=\text{CH}_3$ ),  $\alpha$ -ketobutyric acid ( $\text{R}=\text{CH}_3\text{CH}_2\text{CH}_2$ ), and  $\alpha$ -keto pentanoic acid ( $\text{R}=\text{CH}_3\text{CH}_2\text{CH}_2\text{CH}_2$ ). Radiochemical yields are good (up to 30%) and radiochemical purity excellent (> 90%).

Lithium Dialkylamides and  $^{11}\text{C}$ O: "Naked" Acyl Carbanions. We have recently found that C-11 carbon monoxide will react with lithium dialkylamides at  $-78^\circ\text{C}$  to form the intermediate unstable acyl carbanion:



This intermediate can then be quenched with water (to form the formamide) or an alkyl halide (to form the dialkylamide)(2). In this fashion we have prepared N-formylpiperidine, N-acetylpiperidine and N-propionyl piperidine in yields of 12-15% and radiochemical purities of greater than 95%. Synthesis times are very short (5-7 minutes). Yields appear limited by trapping efficiency of a single pass of  $^{11}\text{C}$ O through the solution of lithium dialkylamide, and should be increased by use of a recirculating  $^{11}\text{C}$ O system. This synthesis makes possible the preparation of a wide variety of C-11 labeled amides. Further reduction of the amide to the amine (diborane in THF) would yield the C-11 labeled tertiary amine; we have successfully prepared [ $^{11}\text{C}$ -methyl]-N-methyl piperidine in 5% overall yield by a one-pot procedure of carbonylation and reduction. This reaction sequence thus is a new method for amine methylation, but also an unprecedented method for amine alkylation with a C-11 labeled substituent.

The use of  $^{11}\text{C}$ O to label organic molecules may yield products of very high specific activity. Firstly, as carbon monoxide is the initial product formed in recoil syntheses of carbon-11 labeled gases, appropriate targetry might yield  $^{11}\text{C}$ O of higher specific activity than that for  $^{11}\text{C}$ O<sub>2</sub>. Secondly, the use of  $^{11}\text{C}$ O minimizes isotopic dilution by environmental sources of  $^{12}\text{C}$ O<sub>2</sub>, a problem prevalent in handling of reactive organometallic precursors.

These reactions are examples of interesting new methods for the carbon-11 labeling of organic molecules. The possible use of these and other reactions to the labeling of compounds for PETT studies will be discussed.

- (1) Niznik G.E., Morrison W.H. and Walborsky H.M., *J. Org. Chem.*, **39**, 600 (1979).
- (2) Rautenstrauch V. and Joyeux M., *Angew. Chem. I.E.E.* **18**, 83 (1979).

PREPARATION OF CARBON-11 LABELLED ERYTHROMYCIN A LACTOBIONATE FOR THE STUDY OF THE ANTIBIOTIC IN VIVO

A.J. Palmer, V.W. Pike, P.L. Horlock, T.J. Perun, L.A. Freiberg, D.A. Dunnigan and R.H. Liss.

M.R.C. Cyclotron Unit, Hammersmith Hospital, Ducane Road, London W12 OHS. U.K.

Erythromycin A is produced by a strain of *Streptomyces erythreus* and is the best known of the medicinally important macrolide antibiotics (1). (<sup>14</sup>C)-Erythromycin A has been prepared (2) but carbon-11 ( $t_{1/2}$ , 20.4 min) is the natural choice of label to enable the behaviour of the antibiotic to be studied in patients by positron emission tomography. The erythromycin A molecule (Figure 1) contains the sugars L-cladinose and D-desosamine, linked to the aglycone, erythronolide A. We considered that the single dimethylamino group could be usefully labelled with carbon-11 by the reductive methylation of N-demethylerythromycin A with (<sup>11</sup>C)-formaldehyde, provided that a fast reaction could be achieved. (The reported method of labelling the dimethylamino group with carbon-14 used a reaction time of 72 hr and an excess of formaldehyde, conditions which are impractical for carbon-11 labelling).

N-Demethylerythromycin A was prepared by a reported procedure (3). From kinetic studies we found that the reductive methylation of N-demethylerythromycin A in methanol using one equivalent of formaldehyde in the presence of hydrogen and palladium on charcoal at 18°C gives erythromycin A in 50% yield after only ca 20 min of reaction. Hence we next explored the labelling of erythromycin A with (<sup>11</sup>C)-formaldehyde, which can be prepared from cyclotron-produced (<sup>11</sup>C)-carbon dioxide (4,5).

In order to reduce radiation exposure to personnel and also to enhance reliability, a semi-automated and remotely-controlled system (Figure 2) was built to perform the preparation. All connecting tubes are ptfe (3 mm or 1.5 mm o.d.). The solenoid-actuated valves (constructed in ptfe) are automatically controlled by relays, which in turn are manually controlled by a single wafer switch. For the preparation, (<sup>11</sup>C)-carbon dioxide (3-10 GBq) was produced on the M.R.C. Cyclotron by the <sup>14</sup>N(p,α)<sup>11</sup>C nuclear reaction on nitrogen (1 bar) using 7.5 MeV protons at 40μA for 1 hr (6) and swept (80 ml/min) directly from the target into a solution (2 ml) of lithium aluminium hydride (20 mg) in tetrahydrofuran (redistilled from potassium). The solvent (under N<sub>2</sub>) was then evaporated off and the radioactive residue hydrolysed with water (0.8 ml). The resultant (<sup>11</sup>C)-methanol was distilled from the flask and carried in N<sub>2</sub> (flow rate 80 ml/min) through a Porapak P column (2.0 x 1.0 cm i.d.) and over heated (v 450°C) silver wool catalyst (1.0 g). The generated (<sup>11</sup>C)-formaldehyde/(<sup>11</sup>C)-methanol mixture was carried by nitrogen into the receiver pot containing cold (0-5°C) ethanol (2.3 ml), N-demethylerythromycin A (10 mg) and palladium on charcoal catalyst (18 mg). The latter had been pre-activated by passing hydrogen through the suspension at 40 ml/min at atmospheric pressure for 10 min. After 10 min distillation time the suspension was warmed to 40°C and hydrogenated for 10 min as before. The solution was then automatically filtered (Millex F.G. filter), transferred by air pressure from the manual syringe to the injector loop (vol, 2 ml) of the HPLC, and injected onto a silica column (μ-Porasil, 30 cm x 3.9 mm i.d.) eluted at 5.0 ml/min with CH<sub>2</sub>Cl<sub>2</sub>: EtOH: conc. NH<sub>4</sub>OH (97.5: 2.5: 0.25 by volume). The column had been pre-conditioned by elution with CH<sub>2</sub>Cl<sub>2</sub>: EtOH: conc. NH<sub>4</sub>OH (50:50:5 by volume). (<sup>11</sup>C)-Erythromycin A, which was well-separated from other radioactive components, eluted in 5-8 min and was collected. Unchanged N-demethylerythromycin A was retained on the column.

The (<sup>11</sup>C)-erythromycin A was formulated for human injection as follows. The solvent was removed on a rotary evaporator (water pump, bath temperature 50°C) and the flask containing the activity was then evacuated to 0.1 mm Hg to remove any traces of solvent. The residue was dissolved in dextrose solution for injection (5% w/v: 5 ml) containing lactobionic acid (6.7 mg, 18.7 μmol.). This solution was added to unlabelled erythromycin A (12.8 mg, 17.4 μmol.) and shaken thoroughly until the solid dissolved. Finally the solution was sterilised by filtration (0.22 μ pore size). Preparations of (<sup>11</sup>C)-erythromycin A lactobionate passed

independent tests for sterility and apyrogenicity.

From the end of ( $^{11}\text{C}$ )-carbon dioxide production the preparation requires only about 45 min and provides an injectable solution of ( $^{11}\text{C}$ )-erythromycin A lactobionate in 4-12% radiochemical yield (corrected for radioactive decay) and based on the activity of ( $^{11}\text{C}$ )-carbon dioxide used at the end of proton irradiation). Data for five preparations are given in Table 1. The proportion of activity distilled from the hydrolysed lithium aluminium hydride complex varied between 40 and 75%. Some of this activity was retained on the Porapak P column which serves to remove any traces of tetrahydrofuran solvent still present. Tetrahydrofuran must not be allowed to come in contact with the silver catalyst since this results in the production of aldehydes which can compete with subsequent reactions of the ( $^{11}\text{C}$ )-formaldehyde (7). The silver wool catalyst was preactivated by distilling methanol (1 ml) over it in air at  $450^\circ\text{C}$ . It was neither changed nor reactivated between runs. The conversion of ( $^{11}\text{C}$ )-methanol to ( $^{11}\text{C}$ )-formaldehyde was the most variable factor in the preparation and the temperature of the catalyst had to be gradually increased between runs in order to off-set a gradual decline in its activity. In our hands the conversion to ( $^{11}\text{C}$ )-formaldehyde was only satisfactory using 99.9 % nitrogen as carrier gas. Using 2-5% oxygen in nitrogen as carrier the conversion to ( $^{11}\text{C}$ )-formaldehyde was only  $\sim 2\%$  and the unwanted production of ( $^{11}\text{C}$ )-carbon dioxide substantial.

TLC/autoradiography [silica gel, mobile phase  $\text{CHCl}_3\text{-MeOH-conc. NH}_4\text{OH}$  (9:1:0.2 by volume)] of the collected HPLC fraction verified the ( $^{11}\text{C}$ )-erythromycin A to be radiochemically pure (Rf, 0.74). Erythromycin A was the only stable compound detected in chromatographed samples by an aqueous solution of  $\text{Ce}(\text{SO}_4)_2 \cdot 4\text{H}_2\text{O}$  (20 g/l) and  $(\text{NH}_4)_6\text{Mo}_7\text{O}_{24} \cdot 4\text{H}_2\text{O}$  (50 g/l) spray reagent. The specific activity of the ( $^{11}\text{C}$ )-erythromycin A after HPLC was estimated to be  $\sim 56 \text{ MBq}/\mu\text{mol}$ . This low value derives from the low specific activity of the prepared ( $^{11}\text{C}$ )-formaldehyde and the presence of stable erythromycin A in the N-demethylerythromycin A preparation. No attempt was made however to optimise the specific activity of the product since for clinical studies 20 mg of ( $^{11}\text{C}$ )-erythromycin A lactobionate were to be administered with a therapeutic dose of the antibiotic (250 mg). The results of studies of the uptake of erythromycin A into the normal and infected lung are the subject of a forthcoming publication (8).

- (1) Nicolaou K.C., *Tetrahedron*, **33**, 683 (1977).
- (2) Flynn E.H., Murphy H.W. and McMahon R.E., *J. Am. Chem. Soc.*, **77**, 3104 (1955).
- (3) Freiberg L.A., U.S. Patent 3,725, 385 (1973).
- (4) Christman D., Crawford E.J., Friedkin M. and Wolf A.P., *Proc. Nat. Acad. Sci. U.S.A.*, **69**, 988 (1972).
- (5) Berger G., Maziere M., Knipper R., Prenant C., and Comar D. *Int. J. Appl. Radiat. Isotop.*, **30**, 393 (1979).
- (6) Clark J.C. and Buckingham P.D., "Short-Lived Radioactive Gases for Clinical Use", Butterworths, London, 1975, p218.
- (7) Berger G., Maziere M., Sastre J. and Comar D., *J. Lab. Comp. Radiopharm.*, **17**, 59 (1980).
- (8) Wollmer P., Pride N.B., Rhodes C.G., Sanders A., Palmer A.J., Pike V.W., Silvester D.J. and Liss R.H., *New Engl. J. Med.*, submitted.

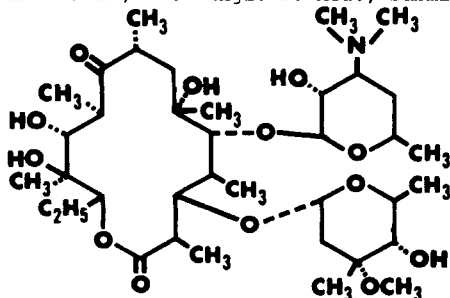


Figure 1. Molecular structure of erythromycin A.

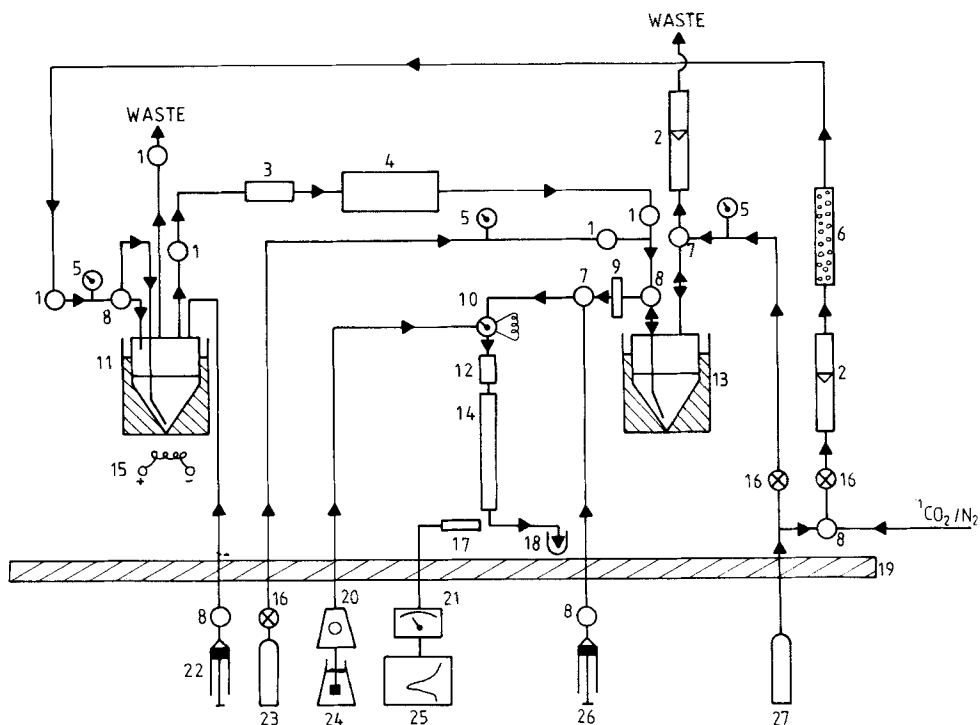


Figure 2. Semi-automated and remotely controlled apparatus for the preparation and purification of (<sup>11</sup>C)-erythromycin A. 1 - two-way solenoid valve, 2 - rotameter, 3 - Porapak P, 4 - furnace to heat silver catalyst, 5 - pressure gauge, 6 - Mg(ClO<sub>4</sub>)<sub>2</sub>.2H<sub>2</sub>O, 7 - three-way solenoid valve, 8 - three-way disposable tap, 9 - filter, 10 - sample injector, 11 - reaction pot (for LiAlH<sub>4</sub> - THF soln.) in oil bath, 12 - pre-column (Corasil), 13 - reaction flask (for N-demethylerythromycin A and catalyst in EtOH) in water bath, 14 - μ-Porasil column, 15 - electrical heater, 16 - needle-valve, 17 - lead shielded G-M tube, 18 - receiver, 19 - lead wall, 20 - HPLC pump, 21 - G-M-tube electronics, 22 - syringe for water, 23 - H<sub>2</sub> supply, 24 - solvent reservoir, 25 - chart recorder, 26 - syringe for air, 27 - N<sub>2</sub> supply.

Table 1: Yields for <sup>11</sup>C-Erythromycin A Lactobionate ((<sup>11</sup>C)-E) Preparation

EOB starting activity (GBq)	% Out of LiAlH <sub>4</sub> pot	% In receiver	% transferred to HPLC	of which % ( <sup>11</sup> C)-E	( <sup>11</sup> C)-E for inj. (MBq)	Time for prep (min)
9.81	42	30	63	49	120	52
6.70	70	48	75	20	104	42
5.59	63	46	71	39	155	42
7.25	51	45	74	24	89	50
3.07	74	43	74	25	52	44

SYNTHESIS AND HIGH PRESSURE LIQUID CHROMATOGRAPHY OF CARBON-11 LABELED CARBOXYLIC ACIDS: VALPROIC ACID AND PALMITIC ACID

B. Schmall, P.S. Conti, B. Sundoro-Wu, J.R. Dahl, J.K. Jacobsen, and R. Lee.  
Biophysics Laboratory, Memorial Sloan-Kettering Cancer Center, New York, N.Y. 10021.

The Grignard reaction has provided a convenient route for the production of C-11 labeled carboxylic acids starting with C-11 CO<sub>2</sub> and the appropriate aryl or alkyl magnesium bromide (1). Carbon-11 labeled palmitic acid (2-6) and other fatty acid derivatives (7) are useful agents for imaging the myocardium and for studying fatty acid metabolism *in vivo*. Sodium benzoate labeled with carbon-11 has been used for renal and tumor visualization (1,8). Sodium C-11 benzoate with no-carrier-added has been synthesized at SKI and evaluated for renal and tumor imaging in a dog bearing an osteogenic sarcoma (9). In order to further evaluate C-11 carboxylates for organ and tumor visualization we have synthesized C-11 palmitic acid and C-11 valproic acid (di-n-propyl-acetic acid). Palmitic acid, a straight chain fatty acid, is known to undergo metabolism primarily through  $\beta$ -oxidation to CO<sub>2</sub> and acetate, while valproic acid, a branched chain fatty acid, is thought to be metabolized mainly by  $\omega$ -oxidation (10) and excreted via the urine as various glucuronide conjugates (10,11). Sodium valproate is an anticonvulsant drug used in the treatment of epilepsy (11).

Carbon-11 was produced by the proton irradiation of N<sub>2</sub> using the nuclear reaction N-14(p, $\alpha$ )C-11 and converted to C-11 CO<sub>2</sub>. This was used to produce C-11 valproate and C-11 palmitate with no-carrier-added. C-11 CO<sub>2</sub> in dry nitrogen gas was bubbled into 20 ml of anhydrous ether (0°C) containing 400-500 mg of the Grignard reagent, di-n-propyl-methylmagnesium bromide or pentadecylmagnesium bromide, respectively. Nitrogen was passed into the reaction flask for ten minutes. Following the carbonation reaction, 1 ml of 6N HCl was added to hydrolyze the mixture while nitrogen continued to pass through the vessel. After three minutes, the nitrogen flow was stopped and the aqueous and organic phases were separated. To prepare C-11 valproate, 5 ml of a 6% aqueous NaHCO<sub>3</sub> solution was added to the organic phase. Nitrogen was passed through the mixture for 5 minutes. The nitrogen flow was stopped and the aqueous layer collected. The aqueous layer containing the C-11 valproate was heated to remove traces of ether, cooled and filtered through a 0.22 $\mu$  Millipore filter. By this procedure, 2-20 mCi of C-11 valproate were produced in reaction times of approximately 35 minutes. Analysis by TLC (silica gel, MeOH:CHCl<sub>3</sub>, 1:1) gave a radioactive peak with R<sub>f</sub>=0.74 which was identical to that of commercial material. In one experiment, HPLC analysis showed a radioactive peak which eluted (15 min) with commercial material. Two unidentified radioimpurities were also observed (Figure 1A). These impurities were removed on acidification of the aqueous bicarbonate solution and back-extraction of the material into 5 ml of fresh ether. Evaporation of the ether and dissolution of the material into 5 ml of fresh bicarbonate solution afforded C-11 valproate in >99% radiopurity as indicated by HPLC (Figure 1B).

An adaptation of a known procedure (3,6) was used to produce C-11 palmitic acid. Following the introduction of C-11 CO<sub>2</sub> with no-carrier-added and hydrolysis with 1 ml of 6N HCl, the organic phase was separated from the aqueous layer and the ether reduced to a volume of 2 ml by evaporation under a stream of nitrogen. Ethanol (1 ml) was added and the remainder of the ether was removed by heating. Analysis of this solution by TLC (silica gel, hexane:ether:HOAc, 70:30:1) gave a radioactive peak with R<sub>f</sub>=0.31, which was identical to that of commercial material. HPLC analysis showed a radioactive peak (>99% radiopurity) which eluted (11 min) with commercial material (Figure 2). The C-11 palmitic acid can be prepared for administration into experimental animals by the addition of a 4% bovine albumin solution to the ethanol (3,6). Filtration of the resulting cloudy white solution through a 0.22 $\mu$  Millipore filter affords a clear yellow solution containing the C-11 palmitic acid suitable for injection. It is also possible to prepare C-11 valproic acid by this same procedure.



- (1) Winstead, M.B., Lamb, J.F. and Winchell, H.S. *J. Nucl. Med.* **14**, 747 (1973).
- (2) Hoffman, E.J., Phelps, M.E., Weiss, E.S., Welch, M.J., Coleman, R.E., Sobel, B.E. and Ter-Pogossian, M.M. *J. Nucl. Med.* **18**, 57 (1977).
- (3) Weiss, E.S., Ahmed, S.A., Welch, M.J., Williamson, J.R., Ter-Pogossian, M.M. and Sobel, B.E. *Circulation* **55**, 66 (1977).
- (4) Sobel, B.E., Weiss, E.S., Welch, M.J., Siegel, B.A. and Ter-Pogossian, M.M. *Circulation* **55**, 853 (1977).
- (5) Goldstein, R.A., Klein, M.S., Welch, M.J. and Sobel, B.E. *J. Nucl. Med.* **21**, 342 (1980).
- (6) Lerch, R.A., Ambos, H.D., Bergmann, S.R., Welch, M.J., Ter-Pogossian, M.M. and Sobel, B.E. *Circulation* **64**, 689 (1981).
- (7) Livni, E., Elmaleh, D.R., Shlomo, L., Brownell, G.L. and Strauss, W.H. *J. Nucl. Med.* **23**, 169 (1982).
- (8) Winstead, M.B., Winchell, H.S. and Fawwaz, R. *Int. J. Appl. Rad. Isot.* **20**, 859 (1969).
- (9) Schmall, B. Conti, P.S., Bigler, R.E., Zanzonico, P.B., Reiman, R.E., Dahl, J.R., Jacobsen, J.K., Lee, R., and Winstead, M.B. 183rd National Meeting American Chemical Society, March, 1982, Las Vegas, Nevada.
- (10) Eadie, M.J. and Tyrer, J.H., "Neurological Clinical Pharmacology," ADIS Press, New York, 1980, p.210.
- (11) Nau, H., Rating, D., Koch, S., Hauser, I. and Helge H. *J. Pharmacol. Exp. Ther.* **219**, 768 (1981).

FIGURE 1

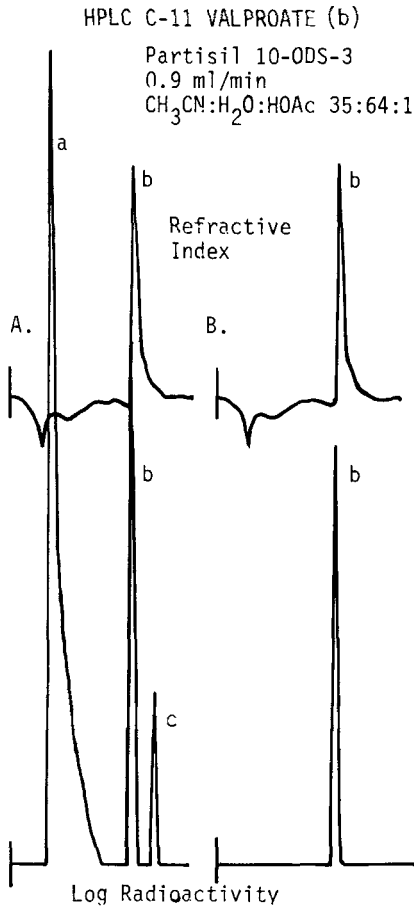
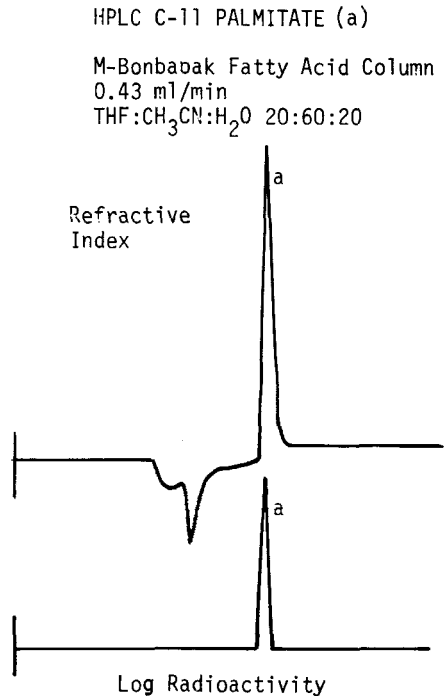


FIGURE 2

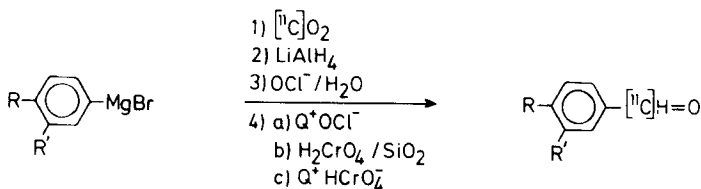


SYNTHESIS OF  $^{11}\text{C}$ -LABELLED AMINO ACIDS AND METHIONINE-CONTAINING PEPTIDES

B. Långström, G. Bergson, C. Halldin, H. Lundqvist, P. Malmberg, K. Någren, U. Ragnarsson, and H. Svärd.

Department of Organic Chemistry, Institute of Chemistry, University of Uppsala, Box 531, S-751 21 Uppsala, SWEDEN.

The synthesis of some amino acids, phenylalanine, tyrosine and DOPA labelled with  $^{11}\text{C}$  in the 2- and 3-position by two different synthetic routes will be discussed. In both routes the appropriate labelled aldehydes are key-substrates. (1) These aldehydes have been synthesized according to Scheme 1.



Scheme 1

The trapping of the  $^{11}\text{C}$ -carbon dioxide, produced in the gas-target by the  $^{14}\text{N}(p, \alpha)^{11}\text{C}$  reaction, in a solution of the appropriate Grignard reagent gave the salt of the corresponding acid which was directly reduced by lithium aluminium hydride. After hydrolysis, the liberated  $^{11}\text{C}$ -labelled alcohol was oxidized to corresponding aldehyde by several routes: chromic acid supported on silica gel, phase-transfer catalyzed oxidations using either hypochlorite or dichromate. The radiochemical yields varied and were in the order of 40-95 % with reaction times in the order of 15-20 min. (2)

The synthesis of some  $^{11}\text{C}$ -labelled methionine containing peptides using  $^{11}\text{C}$ -methyl iodide as the labelled precursor will also be discussed. In this synthesis the appropriate peptide precursor is generated from a protected peptide by the action of sodium in liquid ammonia in analogy with the synthesis of other peptides containing [ $^{11}\text{C}$ -methyl]-methionine. (3)

In the synthesis of amino acids labelled with short-lived radionuclides it is a problem to determine the enantiomeric purity of the product. A method suitable for determining the enantiomeric purity of naturally occurring amino acids labelled with short-lived radionuclides will be presented. The method (4) consists in the aminoacylation of the amino acid to tRNA, followed by a simple gel-filtration. By measuring the radioactivity of the low-molecular and high-molecular fractions, corrected for degree of incorporation, the enantiomeric purity can be determined. The method may be useful in the resolution of enantiomeric amino acids.

(1) Halldin, C., Bergson, G. and Långström, B. Manuscript in preparation.

(2) Halldin, C. and Långström, B. Manuscript to be submitted.

- (3) Långström, B. Sjöberg, S. and Ragnarsson, U. J. Lab. Comp. Radiopharmaceutical 18, 479 (1981)
- (4) Lundqvist, H., Långström, B. and Malmqvist, M., submitted to J. Radioanal. Chem.

EFFECT OF STRUCTURAL ALTERATIONS ON THE UPTAKE AND CLEARANCE OF PRIMARY ALIPHATIC AMINES IN RAT LUNG

L.C. Washburn, T.T. Sun, B.L. Byrd, and G.W. Kabalka\*

Medical and Health Sciences Division, Oak Ridge Associated Universities (ORAU), Oak Ridge, Tennessee 37830 and \*Department of Chemistry, University of Tennessee, Knoxville, Tennessee 37916.

$^{11}\text{C}$ -Labeled straight-chain primary aliphatic amines are sequestered selectively by lung endothelial cells (1) and, therefore, are potentially useful for positron tomographic pulmonary function studies. However, the rapid metabolic loss of these agents from the lung makes it difficult to accurately quantitate their pulmonary uptakes.  $^{11}\text{C}$ -Labeled primary aliphatic amines are oxidized by monoamine oxidase to aldehydes and then by aldehyde dehydrogenase to carboxylic acids. Beta-oxidation with subsequent metabolism to  $^{11}\text{CO}_2$  results in loss of the carbon-11 radiolabel from the lung (Fig. 1).

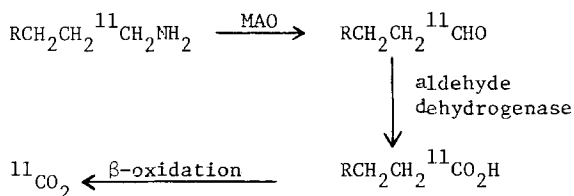


Fig. 1. Metabolism of  $^{11}\text{C}$ -labeled primary aliphatic amines.

We have previously studied the effect of chain branching at the carbon atom beta to the amine function on the lung uptake and clearance of aliphatic amines in the rat (2). Lung uptake of 2-methyloctylamine at early times was about twice that of octylamine itself, but significant metabolic loss from the lung still occurred. 2,2-Dimethyloctylamine, on the other hand, had much less lung uptake than 2-methyloctylamine or octylamine but showed virtually no metabolic loss of label, probably because steric hindrance inhibited enzymatic action.

Livni and co-workers (3) recently reported that  $^{11}\text{C}$ -labeled  $\beta$ -methylheptadecanoic acid may have potential as a myocardial metabolic tracer for positron tomography. They found that this agent is metabolically trapped in the myocardium, presumably because of inhibition of  $\beta$ -oxidation. We reasoned that a branched-chain amine which would be oxidized to a  $\beta$ -methylcarboxylic acid might be in effect similarly metabolically trapped in the lung, if the redistribution of this carboxylic acid was slow compared to the useful life of carbon-11 ( $\sim 1$  hr).

To test this hypothesis, we synthesized  $^{14}\text{C}$ -labeled 3-methyloctylamine and studied its short-term tissue distribution in rats. The synthetic route is shown in Fig. 2. 2-Methyl-1-heptene was converted in 80% yield to the anti-Markownikoff product, 1-bromo-2-methylheptane, by bromination of its trialkylborane derivative in water-tetrahydrofuran at  $0^\circ\text{C}$  (4). Nucleophilic displacement with  $\text{K}^{14}\text{CN}$  in dimethyl sulfoxide at  $70\text{--}80^\circ\text{C}$  for 2 hr followed by reduction using 1 M  $\text{LiAlH}_4$  in tetrahydrofuran gave  $^{14}\text{C}$ -labeled 3-methyloctylamine in 28% overall radiochemical yield.

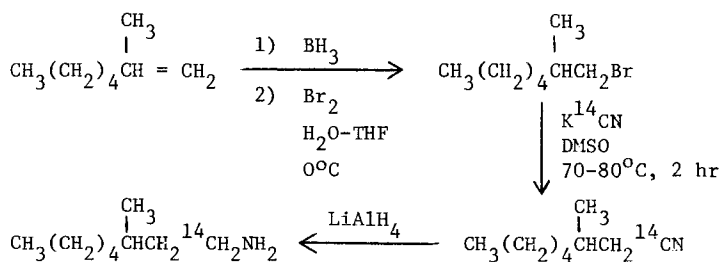


Fig. 2. Synthetic route for  $^{14}\text{C}$ -labeled 3-methyloctylamine.

$^{14}\text{C}$ -Labeled 3-methyloctylamine hydrochloride was dissolved in saline and injected via the tail vein into 4-month-old male Fischer rats. Each animal received 0.1 mg (5  $\mu\text{Ci}$ ) of the labeled amine per kg of body weight. At 1, 5, 15, and 30 min post-injection the rats were killed by exsanguination after light ether anesthesia. Each experimental group consisted of five animals. Weighed tissue samples were dissolved in NCS tissue solubilizer (Amersham/Searle Corp., Arlington Heights, Ill.) and assayed by liquid scintillation counting. Results were expressed as percent of the administered dose/g, normalized to a body weight of 250 g.

Figure 3 shows the lung uptake of  $^{14}\text{C}$ -labeled 3-methyloctylamine with time, along with the uptakes of the three amines previously studied. Identical 1-min lung uptakes were observed for 2- and 3-methyloctylamine, but the 3-methyl compound appeared to have a slightly slower rate of lung clearance, although the difference was not statistically significant. Contrary to our hypothesis,  $^{14}\text{C}$ -labeled 3-methyloctylamine was not metabolically trapped in the lung. The loss of radio-label from the lung appears to be predominantly due to redistribution of the  $\beta$ -blocked carboxylic acid, since an average of only 3% of the injected activity was exhaled as  $^{14}\text{CO}_2$  in 30 min. (This article is based on work supported by contract number DE-AC05-76OR00033 between the U. S. Department of Energy and ORAU.)

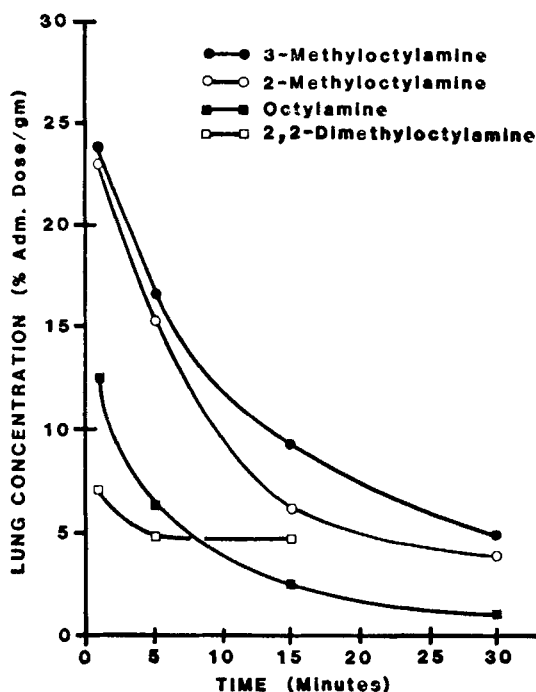


Fig. 3. Time course of the lung concentration of  $^{14}\text{C}$ -labeled primary aliphatic amines in the rat.

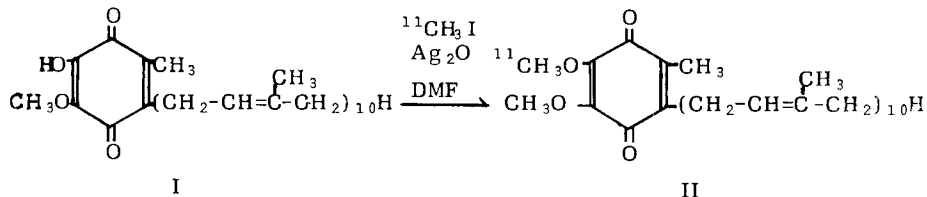
- (1) Fowler J.S., Gallagher B.M., MacGregor R.R. and Wolf A.P., *J. Pharmacol. Exp. Ther.* **198**, 133 (1976).
- (2) Washburn L.C., Sun T.T., Byrd B.L. and Hayes R.L., *J. Nucl. Med.* **21**, P13 (1980).
- (3) Livni E., Elmaleh D.R., Levy S., Brownell G.L. and Strauss W.H., *J. Nucl. Med.* **23**, 169 (1982).
- (4) Kabalka G.W., Sastry K.A.R., Hsu H.C. and Hylarides M.D., *J. Org. Chem.* **46**, 3113 (1981).

### SYNTHESIS OF ( $^{11}\text{C}$ )-COENZYME $\text{Q}_{10}$

T. Takahashi, R. Iwata, M. Shinohara, T. Ido, K. Hamamura, and H. Kogure.  
Cyclotron and Radioisotope Center, Tohoku University, Sendai, 980, Japan.

Coenzyme  $\text{Q}_{10}$  ( $\text{CoQ}_{10}$ ) was discovered as one component of the electron transfer sequence in mitochondrion, where the cellular energy was produced (1,2). It has been proved that  $\text{CoQ}_{10}$  not only performs the electron transfer by moving about freely in the mitochondrion membrane but acts as an antioxidant towards the superoxidative reactions in vivo. In these respects,  $\text{CoQ}_{10}$  is expected to be used as a therapeutic agent for various ischemia, which are mainly caused by the deficiency of oxygen owing to the blocking of electron transfer sequence. In practice,  $\text{CoQ}_{10}$  is used as a therapeutic agent for myocardial ischemia. We tried the  $^{11}\text{C}$ -labeling of  $\text{CoQ}_{10}$  for the application of scanning of ischemia in brain and heart.

We synthesized  $^{11}\text{C}$ - $\text{CoQ}_{10}$  (II) by the reaction of 3-demethyl  $\text{CoQ}_{10}$  (I) with  $^{11}\text{C}$ - $\text{CH}_3\text{I}$ .



The  $^{11}\text{C}$ - $\text{CH}_3\text{I}$  was produced from  $^{11}\text{C}$ - $\text{CO}_2$  with the automated synthesis system. The synthetic method of  $^{11}\text{C}$ - $\text{CoQ}_{10}$  (II) is shown in Fig.1.

The trapping effect of  $^{11}\text{C}$ - $\text{CH}_3\text{I}$  was greatly enhanced by the cooling of reaction vessel in dry ice - methanol.

The mixture of 3-demethyl  $\text{CoQ}_{10}$  (10  $\mu\text{mol}$ ) and  $\text{Ag}_2\text{O}$  (20  $\mu\text{mol}$ ) in DMF (100  $\mu\text{mol}$ ) was reacted with  $^{11}\text{C}$ - $\text{CH}_3\text{I}$  to give  $^{11}\text{C}$ - $\text{CoQ}_{10}$  (II) in 9-12 % of the radiochemical yield. In this synthesis, it has become apparent that the concentration of the starting material is important. The low concentration (1  $\mu\text{mol}$ ) of I resulted in the low radiochemical yield (1.5 %) of II.

$^{11}\text{C}$ - $\text{CoQ}_{10}$  (II) was isolated from the radioactive impurity (Fig.2; (A) and (B)) and the unreactive 3-demethyl  $\text{CoQ}_{10}$  (I) with a short silica gel column.

The time required for the synthesis was 50 min.

- (1) Crane F.L. and Widmer C., *Biochem. Biophys. Acta.*, 25, 220 (1957)
- (2) Green D.E., Hatefi Y. and Fechner W.F., *Biochem. Biophys. Res. Comm.*, 1, 45 (1959)

Fig. 1 Synthetic Method of  $^{11}\text{C}$ -Coenzyme  $\text{Q}_{10}$

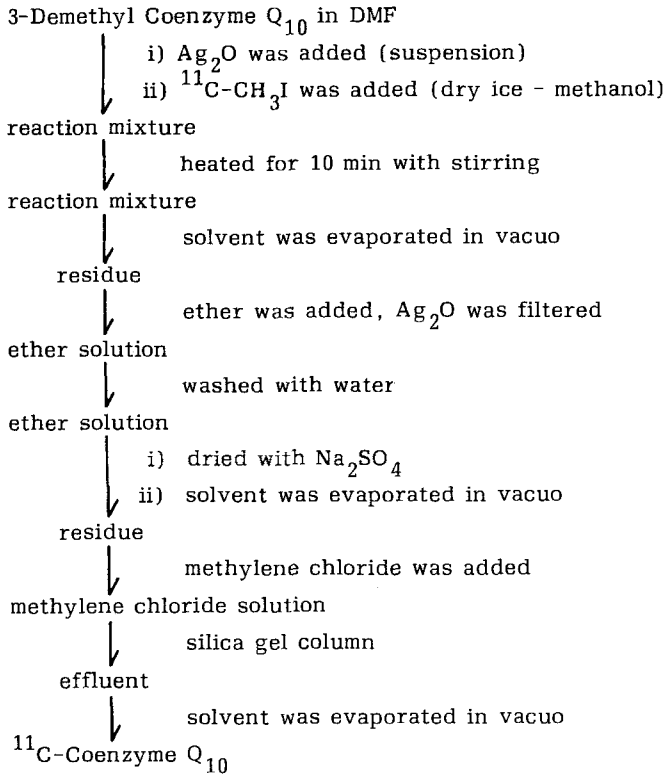
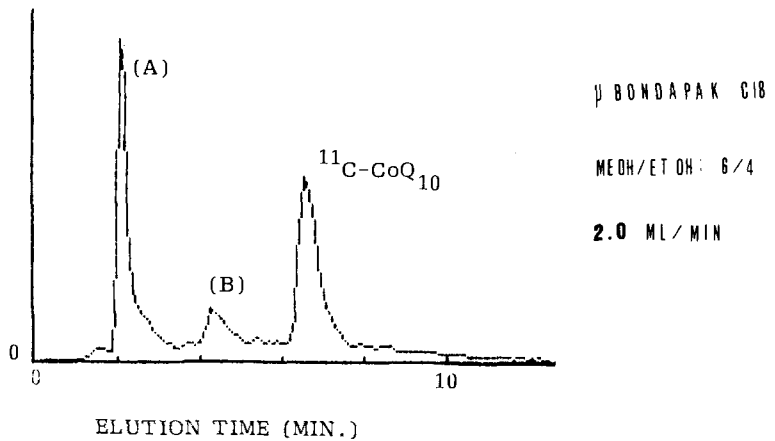


Fig. 2 Radiochromatogram of  $^{11}\text{C}$ -Coenzyme  $\text{Q}_{10}$  (before passing through a silica gel column)



ROUTINE PRODUCTION AND QUALITY CONTROL OF  $^{11}\text{C}$ -L-METHIONINE

G.-J. Meyer, A. Osterholz, and H. Hundeshagen.

Abteilung Nuklearmedizin und spezielle Biophysik, Medizinische Hochschule Hannover  
3000 Hannover-61, F. R. Germany.

$^{11}\text{C}$ -labeled amino acids belong to the small group of compounds labeled with short lived positron emitters which have gained some clinical importance already. So far two labeling methods have been used successfully for routine production. Labeling of the carboxyl group involves a reaction at the asymmetrical center of the amino acid and therefore results in D,L racemic mixtures which would make a final resolution of the optical antipodes desirable. On the other hand such a reaction can be used for all compounds with a similar chemical reactivity, i.e. a large variety of amino acids. Labeling in a different position enables the synthesis of pure D or L forms. However, it requires a specific procedure for each amino acid according to the chemical reactivity of the non-functional rest group.

The first method made use of a modified Strecker-Bücherer synthesis. It was developed and refined for routine production at Oak Ridge by Washburn and co-workers (1,2). Comar and co-workers from Orsay used the second method and prepared  $^{11}\text{C}$ -L-methionine by addition of  $^{11}\text{CH}_3\text{I}$  to L-homocystein (3). A routine production procedure was described subsequently (4). Because it seemed advantageous to us to use a pure L amino acid for positron emission tomography of the pancreas we adopted the method of Comar and co-workers and modified it slightly to our needs.

$^{11}\text{CO}_2$  is produced via the  $^{14}\text{N}(p, \gamma)^{11}\text{C}$  nuclear reaction in a  $\text{N}_2$  gas target, using 19 MeV protons at a current of 40  $\mu\text{A}$  from our MC-36 cyclotron. The gas is transferred to an automated vacuum system for processing of  $^{11}\text{C}$ -precursors (5).  $^{11}\text{CO}_2$  is obtained in a special reaction vessel within 6 min. after the end of bombardment (EOB). After addition of 0.1 mmol  $\text{LiAlH}_4$  in ethyl ether and 1 min. reaction time the ether is evaporated. Then the reaction vessel is attached to a reflux condenser fitted to a small receiver flask with 0.2 ml acetone which is cooled to  $-60^\circ\text{C}$  (see fig. 1). Through the septum 2 ml aq. HI (60%) are added and the reaction vessel is heated to  $150^\circ\text{C}$  by an electrical furnace. Subsequently the needle used for HI addition is changed to bubble a small stream of He (20 ml/min.) through the system. The  $^{11}\text{CH}_3\text{I}$  transfer is complete 6 min. after the attachment of the reaction vessel to the reflux condenser. The receiver flask is detached and 0.03 mmol of L-homocystein-thiolactone in 0.2 ml NaOH (0.4 M) are added. The reaction mixture is heated to  $70^\circ\text{C}$  for 5 min.. The major fraction of acetone is evaporated by a stream of  $\text{N}_2$  and the residual solution purified by HPLC, according to the conditions described by Comar and co-workers (4). After passing a 0.22  $\mu\text{m}$  filter the peak fraction of  $^{11}\text{C}$ -L-methionine (5 ml) is collected in a sterile, pyrogenfree flask.

Because the eluent used for the HPLC purification is an aqueous buffer solution (0.0025 M  $\text{NaH}_2\text{PO}_4$ ) it can be used for direct injection. Apyrogenicity is established bimonthly in test productions followed by conventional rabbit tests. The radiochemical purity is assayed routinely by analytical HPLC of a 5  $\mu\text{l}$  sample of the peak fraction. The overall yield of a typical production started with a 20 min. irradiation at 40  $\mu\text{A}$  beam current is 200 mCi of  $^{11}\text{C}$ -L-methionine, obtained ca 40 min. after EOB. The specific activity of the product was evaluated by comparison of its concentration with the lower threshold sensitivity of an IR-spectrometer. According to this determination the methionine content of the peak fraction was ca 0.02 mg.

- 1) Hayes, R.L., Washburn, L.C., Wieland, B.L., Sun, T.T., Turtle, R.R., and Butler, T.A., *J. Nucl. Med.*, 17, 748 (1976)
- 2) Washburn, L.C., Sun, T.T., Byrd, B.L., Hayes, R.L., Butler, T.A., and Callahan, A.P., in "Radiopharmaceuticals II", *Soc. Nucl. Med.*, New York 1979, p. 767-777.
- 3) Comar, D., Cartron, J.-C., Maziere, M., Marazano, C., *Eur. J. Nucl. Med.*, 1, 11 (1976)



- 4) Berger, G., Maziere, M., Knipper, R., Prenant, C., and Comar, D., *Int. J. Appl. Radiat. Isotopes*, 30, 393 (1979)
- 5) Meyer, G.-J., Harms, T., and Hundeshagen, H., see Proceedings of this symposium.

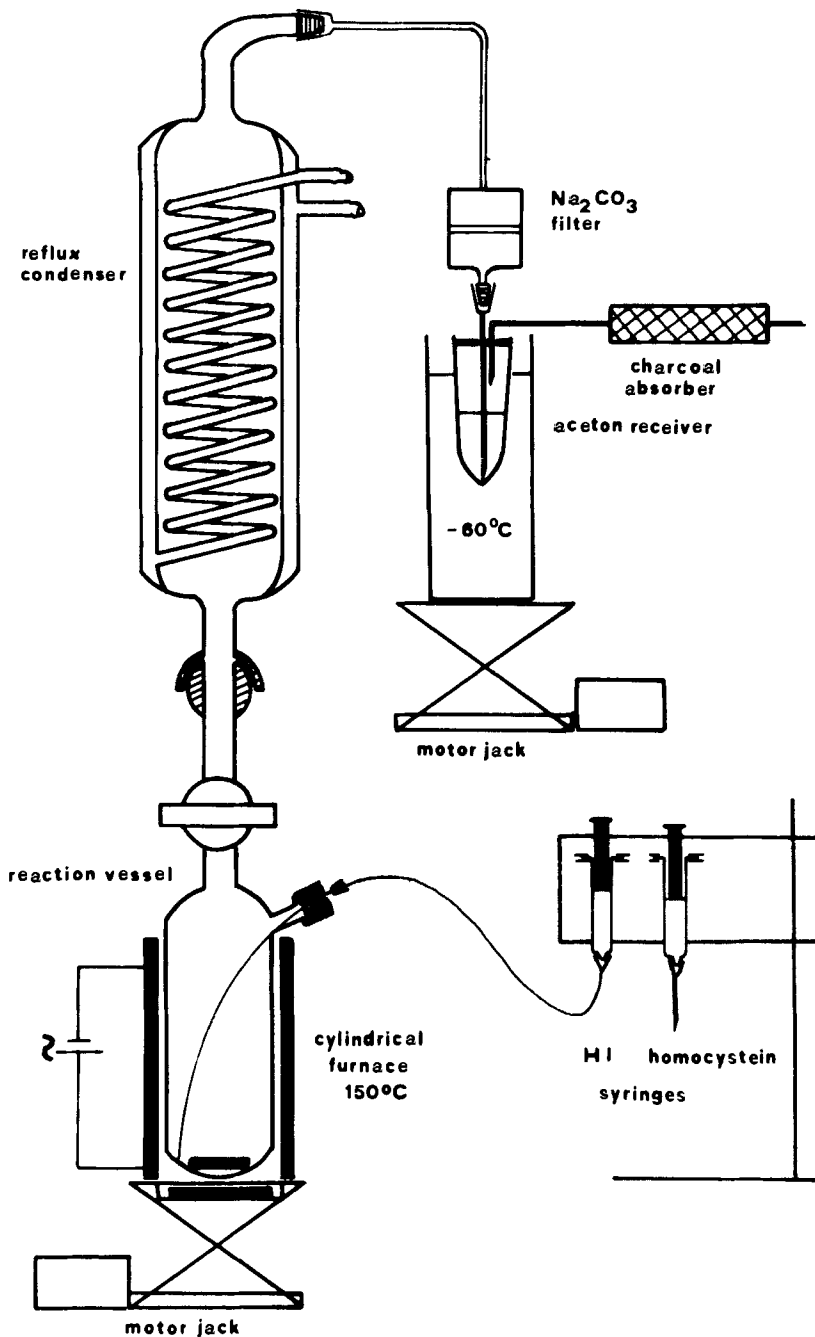


Fig. 1  $^{11}\text{CH}_3\text{I}$  production system

<sup>3</sup>H-LIGAND TO LABEL BRAIN RECEPTORS IN VIVO

P.M. Laduron.

Department of Biochemical Pharmacology, Janssen Pharmaceutica, Beerse, Belgium.

Presently, there is no explanation of why certain ligands, although successfully used in in vitro binding assays, are not appropriate for in vivo binding. <sup>3</sup>H-Spiperone, <sup>3</sup>H-ketanserin, <sup>3</sup>H-dexetimide and <sup>3</sup>H-lofentanil are certainly ligands of choice to identify brain dopamine, serotonin, muscarinic and opiate receptors. Moreover, <sup>3</sup>H-lofentanil was found to be useful to study axoplasmic transport of opiate receptors in the vagus nerve under in vivo conditions.

In order to ascertain that an in vivo binding is really specific for a given receptor, numerous criteria must be fulfilled: regional distribution, saturability, stereospecificity, drug displacement (the most important) and correlation between in vivo and in vitro binding. Such binding in vivo also seems appropriate to examine whether or not a drug is able to cross the blood brain barrier and for estimating the number of receptors which are really needed for a given agonist to elicit a physiological effect or for a drug to antagonize them.

IN VIVO DISPLACEMENT BY MUSCARINIC ACETYLCHOLINE RECEPTOR (m-AChR)  
BINDING LIGANDS

W.C. Eckelman, M. Grissom, J. Conklin, W.J. Rzeszotarski, R.E. Gibson,  
B. Francis, R. Eng, and R.C. Reba.  
Radiopharmaceutical Chemistry, George Washington University Medical Center,  
Washington, D.C. 20037.

We have attempted to develop an efficient strategy for the choice, synthesis, in vitro analysis and animal distribution studies of receptor binding radiotracers. Because of the special requirements for receptor binding radiotracers - high effective specific activity, high chemical and radiochemical purity, low nonreceptor binding - the choice is crucial. To the goal of preparing a gamma-emitting 3-quinuclidinyl benzilate (QNB) derivative we have synthesized a number of nonradioactive derivatives substituted with stable isotopes of the routinely-used radionuclides I-123, Br-77, Br-75, and F-18. These stable halogenated derivatives of QNB were used in in vivo displacement studies with H-3(-)QNB to determine their ability to compete with the parent structure QNB for m-AChR and thus give an indication of their own distribution. Because making each derivative with I-123, Br-77, Br-75 or F-18 would be an overwhelming task, we thought that this approach - in vivo displacement - would be an efficient strategy to determine which radiotracer to pursue. Fifty nmol of each halogen derivative of QNB was coinjected with H-3(-)QNB in rats. Meta- and para- fluorobenzilate of 3-quinuclidinol are the most potent, followed by the two bromo derivatives and finally the two iodo derivatives. These displacement values are in general agreement with the affinity constants determined by in vitro assay (Table, Fig.). Experimental values for the concentration of H-3(-)QNB in the organ with, (B), and without, (B<sub>0</sub>), coinjected displacer were plotted using a logit-log transformation. The equation for the heart is  $\text{logit } Y = 4.93 - 0.999 \ln \text{RBI}$  ( $r^2=0.77$ ) where  $\text{logit } Y = \log(B/B_0)/(1-B/B_0)$  and RBI is the relative binding affinity. More nonradioactive QNB is required to displace the same concentration of H-3(-)QNB from the midbrain than from the heart. This indicates higher concentration of receptor in the brain and/or less transfer across the blood-brain barrier.

The distribution of quinuclidinyl p-iodobenzilate (pIQNB) labeled with I-125 was studied to determine the correlation between the in vivo displacement study and radiolabeled distribution studies. I-125 labeled p-IQNB gives reasonable heart to blood ratios but high lung concentration is also evident. The radioactivity is displaceable by 50 nmol of QNB from the heart, the cerebellum and the midbrain indicating that pIQNB is binding to m-AChR at least in part in these organs. Using I-123 labeled pIQNB we were able to visualize the heart and the cerebrum of dog. The major route of excretion is by the hepatobiliary system.

In the case of these m-AChR binding ligands, the in vivo displacement studies correlate with the in vitro affinity constants indicating that transport to the receptor is not a major factor in determining the distribution but the affinity constant to the receptor is. In general, the in vivo displacement study using nonradioactive halogenated derivatives is an important screening test for receptor binding radiotracers.

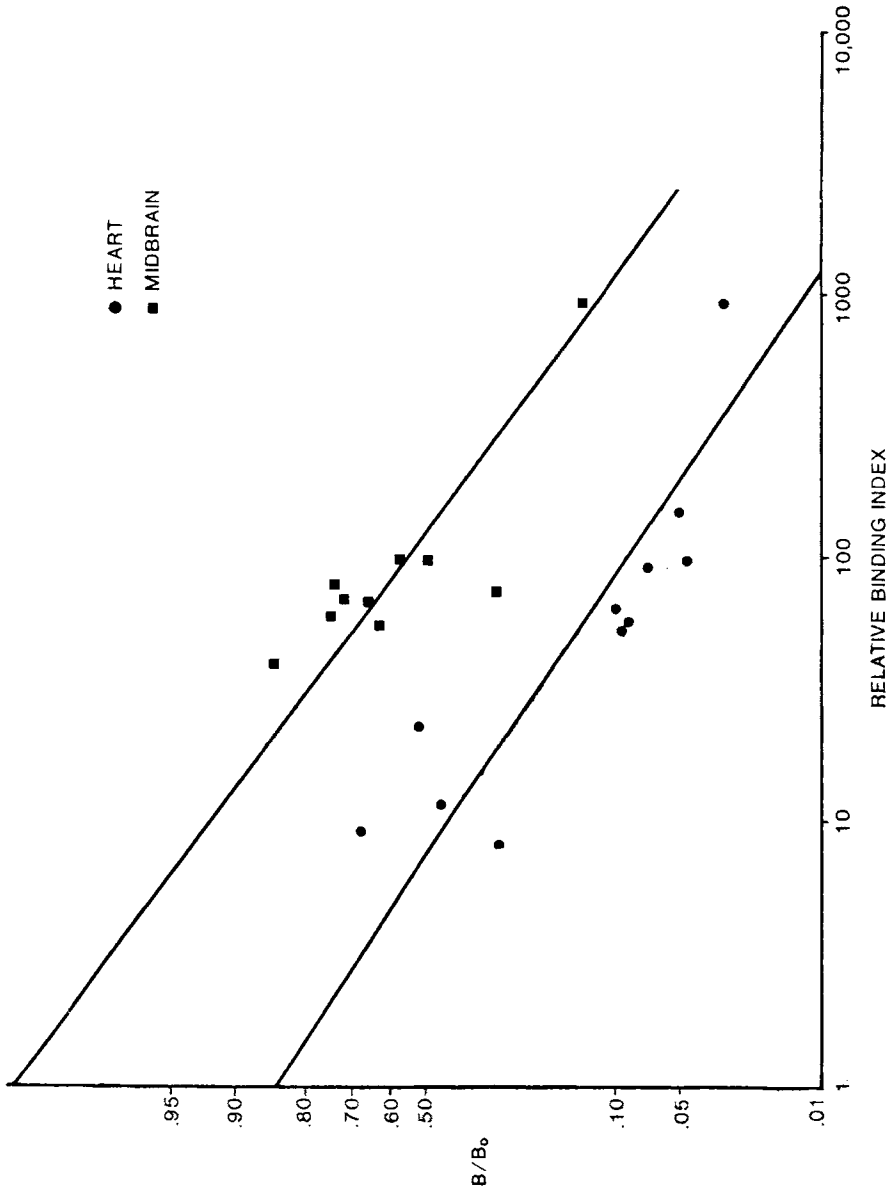
Relative Binding Index (RBI) of QNB Derivatives Obtained from In Vitro Studies Using Rat Heart and Rat Brain and In Vivo Distribution of H-3(-)QNB and Coinjected Derivative.

R	<u>RBI(Heart)</u>	<u>%Dose/g Heart*</u>	<u>RBI(Midbrain)</u>	<u>%Dose/g Midbrain*</u>
C <sub>6</sub> H <sub>5</sub> (QNB)	100	.092±.013	100	.389±.064
C <sub>5</sub> H <sub>9</sub>	155	.206±.019	76	.210±.021
C <sub>6</sub> H <sub>11</sub>	66	.446±.043	60	.460±.079
C <sub>4</sub> H <sub>9</sub>	55	.378±.093	--	.336±.055
4-FC <sub>6</sub> H <sub>4</sub>	55	.363±.053	71	.454±.031
3-FC <sub>6</sub> H <sub>4</sub>	95	.284±.020	83	.508±.086
4-BrC <sub>6</sub> H <sub>4</sub>	11	1.88±.173	71	.491±.102
3-BrC <sub>6</sub> H <sub>4</sub>	8	1.23±.133	62	.515±.067
4-IC <sub>6</sub> H <sub>4</sub>	23	2.12±.067	67	.722±.134
3-IC <sub>6</sub> H <sub>4</sub>	9	2.78±.385	40	.627±.086

\* dose/g in organ 2 hr after injection of H-3(-)QNB and 50 nmol of derivative. B/B<sub>0</sub> is calculated by dividing the %Dose/g in the presence of derivative by the %Dose/g in the presence of saline.

Distribution of I-125 pIQNB at 1/4 and 2 hr in Rat

Displacer	Time	<u>% Dose/g ± SD</u>				
		Blood	Lung	Heart	Cerebellum	Midbrain
Saline	1/2 hr	.118±.009	5.57±.811	1.03±.235	.180±.042	.222±.047
50nmol QNB	1/2 hr	.056±.018	4.92±1.94	.45±.134	.139±.047	.178±.068
Saline	2 hr	.049±.009	1.43±.405	.274±.016	.080±.024	.333±.093
50nmol QNB	2 hr	.038±.003	.961±.174	.124±.013	.030±.002	.069±.005



PREPARATION AND PROPERTIES OF HALOGENATED ESTROGENS AS IMAGING AGENTS FOR BREAST TUMORS

---

S.W. Landvatter, M.K. Mao, J.A. Katzenellenbogen, K.D. McElvany, and M.J. Welch. Department of Chemistry, University of Illinois, Urbana, IL 61801 USA.

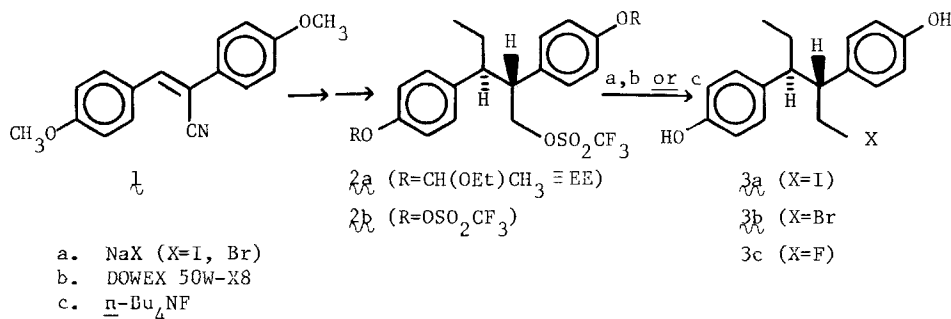
An ideally-behaved estrogen receptor-based breast tumor imaging agent would have: (1) high affinity for the estrogen receptor, (2) low non-receptor binding, (3) high specific activity, (4) high chemical and metabolic stability, and (5) an efficient clearance that proceeds at a rate commensurate with the half-life of the label and the observation time. We have investigated two series of halogenated estrogens with respect to the above criteria, 1-halopentestrols (3; norhexestrols), and 16 $\alpha$ -halomethylestradiols (6).

The norhexestrols 3 were prepared from the  $\alpha$ -cyanostilbene 1 (1, see Scheme I); all three members have high affinity for the receptor and are expected to have low non-specific binding (2) (see Table 1). The I-125 and Br-77 derivatives (3a and 3b) were obtained by halide displacement on the unstable bis(ethoxyethyl) triflate 2a, followed by phenol deprotection in acid. Treatment of 2a or 2b with base, results in rapid loss of halogen by spirocyclization of the p-hydroxyphenethyl system. These two agents show selective, receptor-mediated uptake by estrogen target tissues in the immature rat, and 3b has been used to image a DMBA-induced mammary tumor in an adult rat; however, the uptake selectivity of these compounds is compromised by a dehalogenation process that is rapid both *in vivo* and *in vitro*. The lability of these compounds at neutral pH was confirmed by solvolysis studies (see Table 1) in which they were found to be two to three orders of magnitude less stable than other related primary and secondary halides. In contrast to 3a and 3b, 1-fluoropentestrol 3c is stable in base and resistant to solvolysis. It can be synthesized efficiently by fluoride displacement on the tristriflate (2b), in a reaction that is efficient in fluoride.

The 16 $\alpha$ -bromomethyl- and 16 $\alpha$ -iodomethylestradiols (6a and 6b) are prepared from estrone in an 8 or 9-step sequence (see Scheme II); they also have high affinity for the estrogen receptor and are expected to have low non-receptor binding (see Table 1). Solvolytically, they are much more stable than the halopentestrols, being comparable to 16 $\alpha$ -bromoestradiol (3) in their reactivity (see Table 1). The bromo and iodo compounds can be prepared easily by halogen ion displacement on 16 $\alpha$ -methyl sulfonate derivatives.

- (1) Niederl, J. B. and Ziering, A., J. Am. Chem. Soc., 64, 885 (1942).
- (2) Katzenellenbogen, J. A., Heiman, D. F., Carlson, K. E. and Lloyd, J. E., *In Vivo and In Vitro Steroid Receptor Assays in the Design of Estrogen Pharmaceuticals* in "Receptor Binding Radiotracers", Eckelman, W. C., Ed.; Vol. X in the Uniscience Series "Radiotracers in Biology and Medicine"; Colombetti, L. G., Series Ed.; Chemical Rubber Company: Cleveland, 1982.
- (3) Katzenellenbogen, J. A., Senderoff, S. G., McElvany, K. D., O'Brien, H. A., Jr. and Welch, M. J., J. Nucl. Med., 22, 42 (1981).

Scheme I



Scheme II

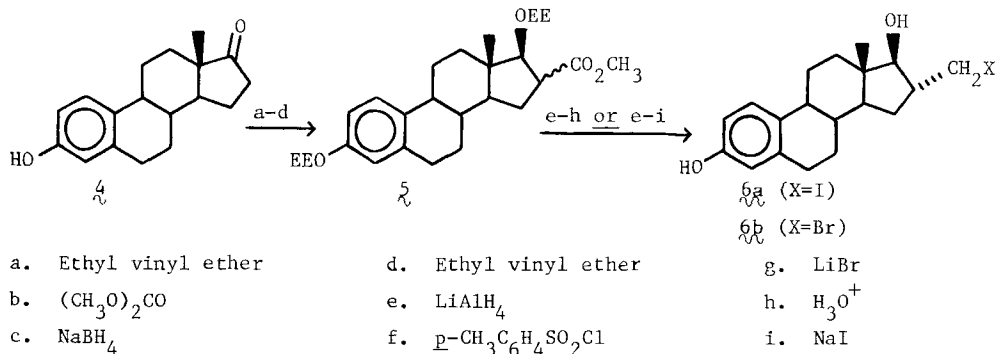


Table 1. Binding and Solvolytic Behavior of Halogenated Estrogens

	RAC <sup>a</sup>	NSB <sup>b</sup>	BSI <sup>c</sup>	Relative Solvolytic Stability <sup>d</sup>
Estradiol ( $E_2$ )	100	1	100	--
3a	127	2.58	49	0.71
3b	150	1.80	83	1.2
3c	129	0.83	155	-- <sup>e</sup>
1-bromohexestrol	65	3.10	21	230
6a	74	3.66	20	450
6b	93	2.54	37	-- <sup>e</sup>
16 $\alpha$ -Bromo $E_2$	139	1.52	91	1280

<sup>a</sup>RAC = ratio of association constants for estrogen receptor binding.

<sup>b</sup>NSB = non-specific binding (2)

<sup>c</sup>BSI = binding selectivity index = RAC/NSB (2)

<sup>d</sup>Solvolytic rate at 50° in 40% EtOH-H<sub>2</sub>O pH 7, relative to 2(4-hydroxyphenyl)ethyl bromide (HPEBr):  $k_{\text{HPEBr}}/k_{\text{compound}}$ .

<sup>e</sup>not determined.

A POTENTIAL BENZODIAZEPINE RECEPTOR-BINDING RADIOPHARMACEUTICAL FOR POSITRON EMISSION TOMOGRAPHY: [ $^{75}\text{Br}$ ]-7-BROMO-1,3-DIHYDRO-5-(2'-FLUOROPHENYL)-1-METHYL-2H-1,4-BENZODIAZEPINE-2-ONE ([ $^{75}\text{Br}$ ]-BFB)

H. Scholl, P. Laufer, G. Kloster, and G. Stöcklin.

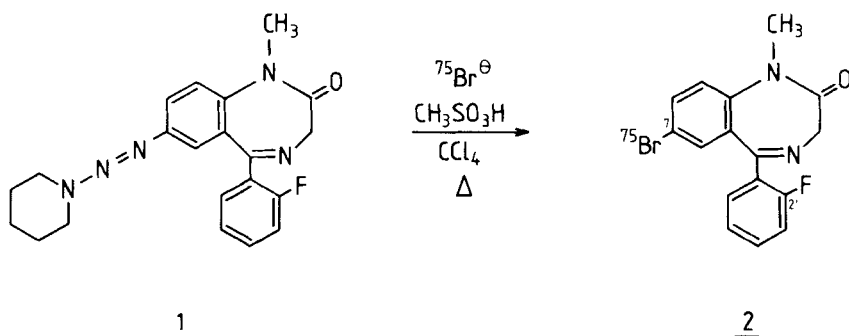
Institut für Chemie 1 (Nuklearchemie), Kernforschungsanlage Jülich GmbH, D-5170 Jülich, FRG.

Visualisation of benzodiazepine receptor sites in intact organisms requires a radioligand with high receptor affinity, high specific activity and a radionuclide suitable for positron emission computed tomography (PECT).

Recently a synthesis of [ $^{11}\text{C}$ ]-flunitrazepam has been reported (1). Since  $^{11}\text{C}$  has a short half-life of only 20 min, the time available for synthesis and application with PECT is limited. In addition, it is difficult to obtain ultra-high specific  $^{11}\text{C}$ -activities. These difficulties can be bypassed to some extent by using the halogen analogue approach with the positron emitter bromine-75 ( $T_{1/2}=98$  min). Bromine-75 can be produced via the  $^{75}\text{As}(^3\text{He},3n)^{75}\text{Br}$  reaction (2) in high specific activities and yields. A routine production method has recently been described by our laboratory (2,3).

In view of the fact that receptor affinity is increased by electron-withdrawing groups and halogens at C-2' and C-7 and decreased by halogen substitution at other aromatic positions (4,5), we chose the benzodiazepine 2 for radiobromination (see formula below). 2 has a low in vitro inhibition constant of 1.7 nmol, determined by competitive displacement of clonazepam by the inactive compound (6).

Because labelling at C-7 must be performed with high regioselectivity, we synthesized [ $^{75}\text{Br}$ ]-BFB 2 and [ $^{77}\text{Br}$ ]-BFB using the triazene method (7). The triazene 1, which was produced by reaction of the



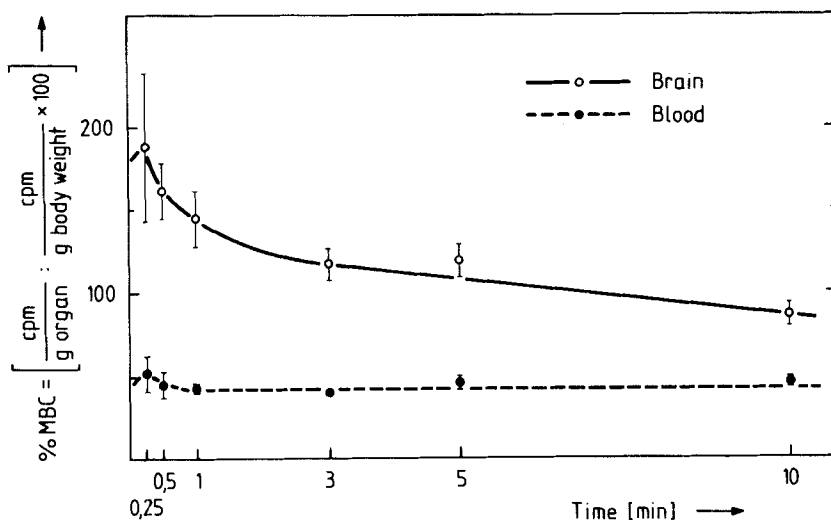
corresponding diazotised 7-amino-compound with piperidine, and the added aqueous radiobromide solution were dried by azeotropic evaporation with acetonitrile. The triazene was then decomposed using a threefold excess of  $\text{CH}_3\text{SO}_3\text{H}$  in refluxing  $\text{CCl}_4$  at a concentration of 35  $\mu\text{mol}$  of 1 per ml  $\text{CCl}_4$ . After subsequent hplc-purification (LiChroSorb RP-18, 7  $\mu\text{m}$ , methanol: $\text{H}_2\text{O}$  = 3:2) and sterile filtration, the eluted bromo compound ( $K'$ =11) was obtained in a NaCl solution ready for injection at an average overall radiochemical yield of 17.9±2% and a specific activity of  $\geq 2 \cdot 10^4$  Ci/mmol. The procedure was completed within 55 min, and the maximum amount prepared up to now was 14 mCi of 2 in a single run. Identification of the product was carried



out by comparative hplc and tlc with the authentic inactive compound, which was synthesized by the Sandmeyer reaction from 1.

The radiochemical yield is dependent on the concentration of triazene and of acid and the amount of carrier bromide present. Addition of  $5 \cdot 10^{-7}$  mol/ml Br<sup>-</sup>-carrier increases the reaction yield to 67%. Dimerisation, dediazonisation and chlorination products from the main side reactions at C-7 were also identified.

The tissue distribution of [<sup>77</sup>Br]-BFB in mice showed a 188% MBC in brain 0.25 min after injection, followed by a decrease to about 100% after 10 min (see Fig.). Over this period the relatively low blood level of 45% is nearly constant. Similar to earlier observations (8), a rapid uptake into lung (maximum: 550% MBC), kidney (maximum: 560% MBC) and liver can be observed. While the course of lung and kidney activity parallels that of brain enrichment, liver uptake increases slowly during 10 min to 310%.



In conclusion, 2 seems to be a compound useful for delineation of benzodiazepine receptor areas using PECT.

- (1) Comar D., Maziere M., Godot J.M., Berger G., Soussaline F., Menini C., Arfel G., Naquet R, *Nature* 280, 329 (1979).
- (2) Weinreich R., Alfassi Z.B., Blessing G., Stöcklin G., *Proc. 17th Int. Annual Meeting of Soc. Nucl. Medicine, Innsbruck 1979*, p. 209
- (3) Blessing G., Weinreich R., Qaim S.M., Stöcklin G., *Int. J. appl. Radiat. Isotopes*, 33, 333 (1982).
- (4) Braestrup C., Squires R.F., *Europ. J. Pharmacol.* 48, 263 (1978).
- (5) Borea P.A., Gilli G., Bertolasi V., *Il farmaco*, Ed. Sc. 34, 1073 (1979).
- (6) Möhler, H., Okada, T., *Science* 198, 849 (1977).
- (7) Tewson, T.J., Welch, M., *J. Chem. Soc. Chem. Comm.* 1149 (1979).
- (8) Tallman J.F., Paul S.M., Skolnik P., Gallagher D.W., *Science* 207, 274 (1980).

IN VIVO DETECTION OF CENTRAL DOPAMINERGIC PROCESSES: STUDIES WITH 1-C-11-DOPA AND C-11-LABELLED N-ALKYLATED ADTN DERIVATIVES

J.F. van der Werf, H.D. Beerling-Van der Molen, A.M.J. Paans, T. Wiegman, J. Korff, and W. Vaalburg.

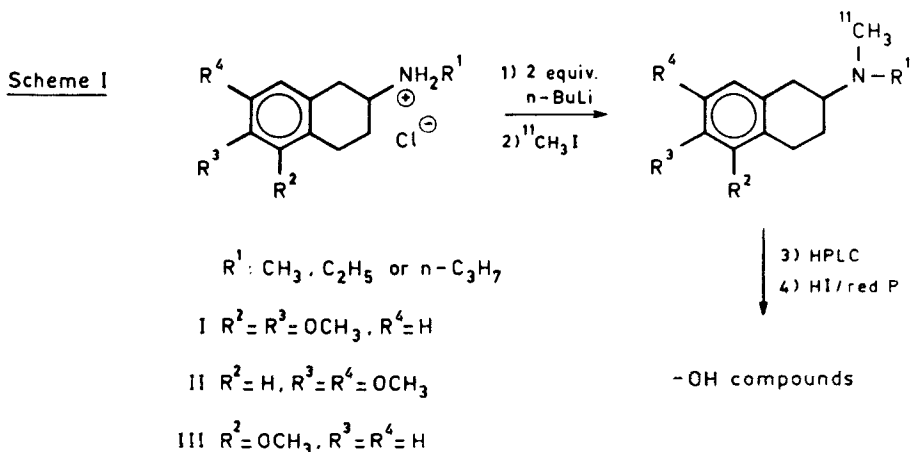
Depts. of Nucl. Med. and Biol. Psychiat., University Hospital, Oostersingel 59, 9713 EZ Groningen, The Netherlands.

Central dopaminergic processes are involved in Parkinson's and Huntington's disease and in the action of many psychotropic drugs. Application of Positron-Emission Tomography (PET) makes it possible to study neuronal processes in a non-invasive way and can provide information about the molecular events underlying the normal and anomalous in vivo situation.

Two principal research lines on the in vivo detection of the dopaminergic system can be distinguished. One is focussed on the detection of dopamine(DA) receptors. Accordingly the labelling of a number of DA antagonists e.g. haloperidol, spiroperidol and pimozide with positron-emitting isotopes has been reported. Along the second line compounds labelled with positron-emitting nuclides were synthesized to study metabolic events. Thus syntheses of F-18-DOPA (1) and 1-C-11-DOPA (2) were reported.

Previously we have shown (3) that 1-C-11-DOPA has potentials for the specific in vivo detection of dopaminergic processes. In these studies, after injection of C-11-DOPA i.v. in rats, significantly less label was found in the striatum, as a consequence of decarboxylation and subsequent elimination of the label. From PET studies with 1-C-11-DOPA in the cat and dog we were not able to detect DA-rich areas specifically, although "cold spots" could be localized in the brain. This prompted us to start research to visualize dopaminergic processes by "hot spot" detection.

ADTN(2-amino-6,7-dihydroxy-1,2,3,4-tetrahydronaphthalene), a DA agonist, has been shown to bind with high affinity to DA receptors in vitro (4) and in vivo (after intra-cerebral application) (5), and to interfere with neuronal DA uptake systems (6) in vitro. Moreover a number of N-alkylated derivatives of ADTN, iso-ADTN and the 5-monohydroxy analogue, in particular the N,N-dipropyl compounds, were shown to have high affinity for DA receptors in vivo (7,8,9). This is of interest because these compounds can pass the blood-brain-barrier, while ADTN itself does not have this property.



N-alkyl derivatives of ADTN were labelled with carbon-11 by N-methylation with C-11 methyl iodide. Starting with the HCl-salt of the N-monoalkyl derivative

(catechol/phenol-protected methoxy compound) the lithium salt of the secondary amine was prepared in THF with 2 equivalents of n-BuLi under a helium-atmosphere at  $-30^{\circ}\text{C}$  (Scheme I). Carbon-11 methyl iodide was introduced by a helium flow. The reaction mixture was stirred during 5 min at  $0^{\circ}\text{C}$ . After acid-base separation the C-11-labelled product was purified by HPLC(alumina). The catechol/phenol moiety was restored by boiling in HI/red P (3 min,  $140^{\circ}\text{C}$ ). The synthesis was completed in one hour and the yield was 15%. By varying the alkyl function (methyl, ethyl, or n-propyl group) and the position of the hydroxyl function(s) (5,6-diOH, 6,7-diOH, or 5-OH), a variety of C-11-labelled compounds can be prepared with this method.

The investigations were supported by the Foundation for Medical Research FUNGO which is subsidized by the Netherlands Organization for the Advancement of Pure Research (ZWO).

- (1) Firnau G., Nahmias C. and Garnett S., *Int. J. Appl. Radiat. Isotop.* 24, 182 (1973).
- (2) Reiffers S., Beerling-van der Molen H.D., Vaalburg W., Hoeve W. ten, Paans A.M.J., Korf J., Woldring M.G. and Wijnberg H., *Int. J. Appl. Radiat. Isotop.* 28, 955 (1977)
- (3) Korf J., Reiffers S., Beerling-van der Molen H.D., Lakke J.P.W.F., Paans A.M.J., Vaalburg W. and Woldring M.G., *Brain Res.* 145, 59 (1978)
- (4) Davis A., Poat J.A. and Woodruff G.N., *Eur. J. Pharmacol.* 63, 237 (1975)
- (5) Clement-Cormier Y. and Smith C.E., *Neurochem. Res.* 5, 641 (1980)
- (6) Mulder A.H., Braakhuis B., Regt V. de, Dijkstra D. and Horn A.S., *Eur. J. Pharmacol.* 64, 349 (1980)
- (7) McDermed J., McKenzie G.M. and Philips A.P., *J. Med. Chem.* 18, 362 (1975)
- (8) Cannon J.G., Lee T., Goldman H.D., Costall B. and Naylor R.J., *J. Med. Chem.* 20, 1111 (1977)
- (9) Hacksell U., Svensson U., Nilsson J.L.G., Hjorth S., Carlsson A., Wikström H., Lindberg P. and Sanchez D., *J. Med. Chem.* 22, 1469 (1979)

RADIOLABELED ANTIBREAST CARCINOMA MONOCLONAL ANTIBODIES FOR DETECTION OF BREAST CANCER

M.R. Zalutsky, D. Colcher, D.W. Kufe, and J. Schlom.

Department of Radiology, Harvard Medical School, Boston, MA 02115.

This work investigated the ability of  $^{125}\text{I}$ -labeled monoclonal antibodies (MCA) and antibody fragments directed against human breast carcinoma associated antigens to selectively identify human breast tumor xenografts in nude mice. Of particular interest was whether sufficient contrast between tumor and other tissues could be achieved within a time frame compatible with the half life of a clinically useful isotope such as  $^{99\text{m}}\text{Tc}$  or  $^{125}\text{I}$ .

A series of antibreast carcinoma monoclonal antibodies has been produced (1) from hybridomas resulting from the fusion of murine mouse myelomas with splenic lymphocytes of mice immunized with the cell extract of a human breast metastasis to the liver. One of these MCA, BC(1), was chosen for the following reasons (2): a) BC(1) is reactive with more than 80% of primary breast carcinomas but is unreactive with a variety of normal tissues and other tumor lines; b) the BC(1) antigen is not shed into the circulation; c) the antigen-antibody complex is stable on the tumor cell membrane in the presence or in the absence of an excess of unbound antibody; d) the variability in BC(1) antigen expression within the tumor cell cycle has been determined; and e) the absence of factors present in the sera of patients with breast cancer which can block binding of BC(1) antibody to breast carcinomas has been demonstrated.

Monoclonal antibody BC(1) and its  $\text{F(ab')}_2$  and  $\text{Fab}'$  fragments were labeled with  $^{125}\text{I}$  using the stationary phase chloramide 1,3,4,6-tetrachloro-3 $\alpha$ -6 $\alpha$ -diphenylglycouril (Iodogen) (3). The effects of reaction time, protein concentration and Iodogen concentration on iodination yield were investigated. Labeling efficiencies of about 60% were obtained using as little as 5 $\mu\text{g}$  of Iodogen and 100 $\mu\text{g}$  of antibody. The rate of dehalogenation of  $^{125}\text{I}$ -BC(1) in vitro determined by serial dialysis was about 1% per day.

The binding of  $^{125}\text{I}$ -BC(1) and its  $^{125}\text{I}$ -labeled  $\text{F(ab')}_2$  and  $\text{Fab}'$  fragments to cell extracts of both a breast metastasis to the liver and normal liver tissue were investigated using solid phase radioimmunoassay. At a specific activity of about 1  $^{125}\text{I}$  atom per molecule and a protein concentration of 1nM, the ratio of tumor to normal liver tissue binding was about 50 to 1 for the three labeled proteins.

The biodistribution of  $^{125}\text{I}$ -BC(1) and its labeled  $\text{F(ab')}_2$  and  $\text{Fab}'$  fragments was studied in two groups of nude mice, one implanted with human breast tumors (Clouser) and the other bearing tumors derived from the A375 melanoma cell line. The tissue distribution results at doses of about 25 pmole protein per mouse (Tables 1 and 2) indicate that the uptake of  $^{125}\text{I}$ -BC(1) and  $^{125}\text{I}$ - $\text{F(ab')}_2$  in Clouser tumors is considerable and much greater than in other tissues. In the A375 mice less tumor uptake is observed, and the target to nontarget ratios are less favorable. Preliminary results suggest that improved tumor to tissue ratios can be obtained at lower doses of antibody. In a series of imaging studies at 25 pmole antibody per mouse, tumors could generally be delineated in the Clouser mice but not in the A375 mice.

The blood clearance of  $^{125}\text{I}$  activity following injection of  $^{125}\text{I}$ -BC(1) and  $^{125}\text{I}$ -labeled  $\text{F(ab')}_2$  and  $\text{Fab}'$  fragments was studied in nude mice bearing

Clouser tumors. Although extrapolation from animals is often misleading, the blood clearance data (Table 3) suggest that with F(ab')<sub>2</sub> or Fab' fragments it may be possible to achieve acceptable tumor to blood ratios at times compatible with the half lives of <sup>99m</sup>Tc and <sup>123</sup>I.

- (1) Colcher, D., Horan, P., Hand, M., Nuti, M and Schlom, J., Proc. Nat. Acad. Sci. U.S.A., 78, 3199 (1981).
- (2) Kufe, D., Nadler, L., Sargent, L., Shapiro, H., Colcher, D. and Schlom, J. (submitted).
- (3) Fraker, P.J. and Speck, J.D., Biochem. Biophys. Res. Comm., 80, 849 (1978).

Table 1. Tissue distribution of <sup>125</sup>I antibreast carcinoma MCA in nude mice with breast carcinomas and melanomas (n = 4)

	Clouser	A375	Clouser	A375
	24 Hr	24 Hr	72 Hr	72 Hr
tumor uptake (% I.D./gm)	11.6	3.8	10.1	3.2
tumor/blood	1.0	0.3	2.1	0.3
tumor/liver	4.2	1.5	7.0	1.3
tumor/lungs	1.6	0.5	4.2	0.4
tumor/muscle	7.8	1.4	14.2	1.4
tumor/bone	7.6	2.2	26.4	2.2

Table 2. Tissue distribution of <sup>125</sup>I antibreast carcinoma MCA F(ab')<sub>2</sub> fragment in nude mice with breast carcinomas and melanomas (n = 2)

	Clouser	A375	Clouser	A375
	24 Hr	24 Hr	72 Hr	72 Hr
tumor uptake (% I.D./gm)	8.4	2.2	2.7	1.2
tumor/blood	1.4	0.4	5.2	1.2
tumor/liver	5.7	1.8	10.7	4.0
tumor/lungs	2.3	0.7	4.0	1.8
tumor/muscle	12.7	2.0	15.8	3.8
tumor/bone	10.6	3.1	18.0	6.5

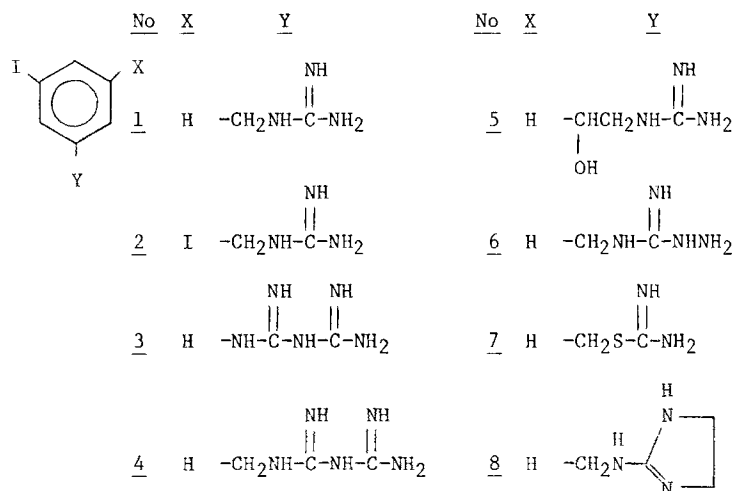
Table 3. Blood clearance of <sup>125</sup>I activity following injection of <sup>125</sup>I-labeled BC(1), F(ab')<sub>2</sub> and Fab' in nude mice bearing Clouser tumors (n = 3)

IgG	1	1.9 hr	70
	2	41 hr	30
F(ab') <sub>2</sub>	1	0.5 hr	66
	2	14 hr	34
Fab'	1	<15 min	91
	2	1.9 hr	7
	3	8.6 hr	2

**SYNTHESIS AND STRUCTURE-DISTRIBUTION STUDY OF RADIOIODINATED NOREPINEPHRINE STORAGE ANALOGS**

D.M. Wieland, M. Inbasekaran, L.E. Brown, D.D. Marsh, and W.H. Beierwaltes.  
University of Michigan Medical Center, Ann Arbor, Michigan 48109.

Iodine-123-meta-iodobenzylguanidine (MIBG), an analog of the neuron blocker guanethidine, has been used to image the human heart (1). However, use of MIBG (1) to determine norepinephrine (NE) turnover in the heart is hampered by its relatively low (~60%) neuronal specificity (2). Compounds 2-8 have been synthesized in an attempt to develop an agent with heart uptake and neuronal specificity greater than MIBG. The syntheses of unlabeled compounds



1-8 were based on literature procedures for similar analogs. Compounds 1-8 were radiolabeled by electrophilic, solid-phase exchange with NaI-125 using  $(\text{NH}_4)_2\text{SO}_4$  facilitation (3,4). The labeling procedure was modified with compounds 4, 6 and 8 either because of their low melting points or hydrolysis under the usual reaction conditions (i.e., initial dissolution in water; 140°; 1-4 HR). In these cases the reactants were dissolved in  $\text{CH}_3\text{OH}$  and the solvent removed by a stream of argon at ambient temperature. The exchange reactions were then conducted at approximately 10° below the melting point of the organic substrate or at 140° in the case of compound 4. Radiochemical yields (isolated) were 45-92%. Specific activities ranged from 0.5-2.0 mCi/mg. Radiochemical purity (>95%) was determined by radio-TLC (two systems) and in select cases confirmed by radio-HPLC. Most of the functional groups in analogs 2-8 are found in drugs known to either block or deplete NE in adrenergic nerves. In the dog, 4 and 5 show heart concentrations similar to MIBG 30 min after i.v. injection but heart-to-blood concentration ratios are lower. The neuronal specificity of 4 and 5 are being evaluated in the rat heart by pretreatment with 6-hydroxydopamine.

- (1) Kline R.C., Swanson D.P., Wieland D.M., Thrall J.H., Gross M.D., Pitt B. and Beierwaltes W.H., *J. Nucl. Med.* **22**, 129 (1981).
- (2) Wieland D.M., Brown L.E., Marsh D.D., Mangner T.J. and Beierwaltes W.H., *J. Nucl. Med.* **22**, P20 (1981).
- (3) Mangner T.J., Wu J.L. and Wieland D.M., *J. Org. Chem.*, In press (1982).
- (4) Mangner T.J., Wu J.L., Wieland D.M. and Beierwaltes W.H., *J. Nucl. Med.* **22**, P12 (1981).

## Biological and Synthetic Data

## 1. Methods

Animal Evaluation:

Our screening protocol entailed whole body tissue distribution studies of compounds 2-7 in mongrel dogs (15-25 kg) by i.v. injection of 100  $\mu$ Ci of the I-125 test compound. The dogs were killed at 0.5 and 2.0 hours post-injection by i.v. injection of sodium pentobarbital. Two animals were sacrificed per time interval. The concentration of radioactivity in 18 different tissues was determined and expressed as % kg dose/g (wet weight). Data for 4 major tissues at 0.5 HR are compiled below.

Synthesis of Cold Compounds:

Compound 2 was synthesized by a 4-step sequence from p-aminobenzonitrile. Analog 5 was made from the respective amine obtained by borane reduction of the cyanohydrin of m-iodobenzaldehyde. Other analogs were synthesized by modification of literature procedures.

Radiosynthesis:

Radiolabeling of all compounds was achieved by solid-state exchange with NaI-125/(NH<sub>4</sub>)<sub>2</sub>SO<sub>4</sub> at 110-140°C for 0.5-4.0 hours. Specific activities ranged from 0.5-2.0 mCi/mg. All radiocompounds were formulated in 0.9% saline. Radiochemical purity was >95% for all compounds as determined on 203 TLC systems.

## 2. Results

CONCENTRATION\* OF I-125 NOREPI STORAGE ANALOGS IN SELECTED  
DOG TISSUES AT 0.5 HR

<u>Cmpd. NO.</u>	<u>HEART**</u>	<u>BLOOD</u>	<u>LIVER</u>	<u>LUNG</u>	<u>H/B</u>
<u>1</u>	0.47 +0.02	0.02 +0.00	0.34 +0.03	0.22 +0.06	24
<u>2</u>	0.27 +0.01	0.09 +0.01	1.57 +2.21	0.16 +0.01	3
<u>3</u>	0.35 +0.01	0.08 +0.00	0.63 +0.02	0.26 +0.03	4
<u>4</u>	0.57 +0.1	0.06 +0.01	0.82 +0.06	0.19 +0.01	10
<u>5</u>	0.49 +0.02	0.03 +0.00	1.01 +0.03	0.14 +0.05	16
<u>6</u>	0.26 +0.01	0.04 +0.00	0.36 +0.01	0.30 +0.01	6
<u>7</u>	0.07 +0.00	0.19 +0.01	0.08 +0.01	0.07 +0.01	0.4

\* % kg dose/g (wet weight)

\*\* Left ventricle

### 3. Work in Progress

The neuronal specificity of compounds 4 and 5 in various regions of the rat heart are presently being determined. Rats (5) are being treated with 6-hydroxydopamine (100 mg/kg) 5 days prior to injection of either compound 4 or 5. Controls as well as analogous studies with H-3-norepinephrine will provide an estimate of the neuronal uptake.

The tissue distribution of compound 8 is presently being evaluated.



RADIOIODINATED 1-SUBSTITUTED-4-PHENYLPYPERAZINES: POTENTIAL MYOCARDIAL IMAGING AGENTS

R.N. Hanson.

Department of Medicinal Chemistry, College of Pharmacy, Northeastern University, and Joint Program in Nuclear Medicine, Department of Radiology, Harvard Medical School, Boston, MA 02115.

One approach to the development of new myocardial imaging agents is the use of analogs of drugs that exert a cardioselective pharmacologic action and which can readily be labeled. Two classes of drugs of current interest are the antiarrhythmic quaternary aralkyl amines, similar to bretylium (1) and pranolinium (2), and the catecholamine depleting aralkyl guanidines, such as bethanidine (3) and 1-carboxamidino-4-phenylpiperazine (4). In this study the 4-phenylpiperazine moiety is used both as the aralkyl group and as the site for facile electrophilic radioiodination (5).

Two series of 4-phenylpiperazines were synthesized as analogs of each class of drugs. In the first group, the 4-phenylpiperazine was dialkylated in two or three steps, then labeled with iodine-125 to give the target compounds I-IV. The 1-carboxamidino-4-phenylpiperazines, V-VIII, were synthesized by two methods and also radioiodinated with iodine-125 and chloramine-T.

The tissue distributions and heart to nontarget tissue ratios as a function of time were determined for I-V in normal rats. As the results in Table I indicate, most of the radiochemicals demonstrate high uptake and selectivity for the heart. The primary differences are in the uptake of nontarget organs and the rate of clearance from the blood. Clearly III and V show the highest heart to blood and heart to lung ratios over the first 4 hours. This is due partially to the retention of activity in the heart and partially to the continued decline in blood levels. For compounds I and II, although the activity in the heart remains high, levels in the lung are also high, and the concentration of activity in the blood increases with time. The addition of the phenyl group in IV results in lower myocardial uptake and a significant shift of activity to the liver.

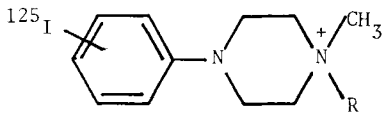
Compounds III and V have been labeled with iodine-131 and are being evaluated in dogs.

- (1) Boura, A.L.A., Copp, F.C., Duncombe, W.G., Green, A.F. and McCoubrey, A., *Brit. J. Pharmacol.*, 15, 265 (1960).
- (2) Patterson, E., Stetson, P. and Lucchesi, B.R., *J. Pharmacol. Exp. Ther.*, 214, 449 (1980).
- (3) Boura, A.L.A., Duncombe, W.G., Robson, R.D. and McCoubrey, A., *J. Pharm. Pharmacol.*, 14, 722 (1962).
- (4) Ozawa, H. and Iwatsuki, K., *Chem. Pharm. Bull.*, 16, 2482 (1968).
- (5) Stock, L.M., "Aromatic Substitution Reactions", Prentice-Hall, Inc., Englewood Cliffs, N.J., 1968, p.52.

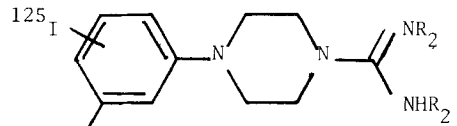
Table 1. Biodistribution of compounds in normal rats.

Compound	Time	Heart	Lung	Blood	Heart Blood	Heart Lung
I	0.08 h	0.68*	0.43	0.04	17.0	1.4
	0.25 h	0.69	0.56	0.07	10.0	1.5
	1 h	0.35	0.49	0.12	2.9	0.7
	4 h	0.18	0.62	0.17	1.0	0.5
	24 h	0.07	0.35	0.13	0.5	0.2
II	0.25 h	1.06	0.64	0.07	14.3	1.6
	1 h	0.62	0.38	0.06	10.8	1.7
	4 h	0.24	0.29	0.06	3.9	0.9
	24 h	0.23	0.06	0.04	6.4	0.6
III	0.25 h	0.90	0.23	0.04	22.5	4.0
	1 h	0.56	0.19	0.03	17.0	3.0
	4 h	0.23	0.09	0.02	11.5	2.5
	24 h	0.01	0.01	<0.01	2.0	1.0
IV	0.25 h	0.04	0.18	0.05	0.8	0.2
	1 h	0.04	0.11	0.04	1.0	0.4
	4 h	0.02	0.05	0.03	0.7	0.4
	24 h	<0.01	0.03	<0.01	1.0	0.4
V	0.08 h	0.62	0.43	0.03	20.7	1.4
	0.25 h	0.54	0.36	0.03	18.0	1.5
	1 h	0.54	0.32	0.04	13.5	1.6
	4 h	0.12	0.11	0.02	6.0	1.1
	24 h	0.04	0.07	0.03	1.3	0.5

\*concentration (%ID - kg/g)



I	R	CH <sub>3</sub>
II		CH <sub>2</sub> CH <sub>3</sub>
III		CH <sub>2</sub> CH <sub>2</sub> OH
IV		CH <sub>2</sub> CH(OH)C <sub>6</sub> H <sub>5</sub>



V	R <sub>1</sub>	H	R <sub>2</sub>	H
VI		CF <sub>3</sub>		H
VII		H		CH <sub>3</sub>
VIII		CF <sub>3</sub>		CH <sub>3</sub>

SYNTHESIS AND BRAIN UPTAKE OF ISOMERIC  $^{123}\text{I}$ -IODOAMPHETAMINE  
DERIVATIVES

R.M. Baldwin, T.H. Lin, and J.L. Wu.  
Medi-Physics, Inc., Emeryville, California 94608 USA.

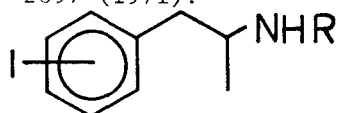
Radiiodinated amines have been reported recently to localize in the brain (1-3), and  $^{123}\text{I}$ -p-iodoamphetamine was found to have higher retention in rat brain than other simple aromatic or aliphatic amines (2). The purpose of this study was to examine in greater detail the effect of structural modifications to the iodoamphetamine moiety on its brain uptake and retention. In particular, the factors examined were the optical configuration of the asymmetric center, N-alkylation, and the iodine substitution pattern on the aromatic ring.

The iodinated amphetamine derivatives were synthesized (figure) from d-, l- or dl-amphetamine. Electrophilic iodination (4) of the N-acetyl protected amphetamine yielded a mixture of ortho, meta, and para substituted products in the ratio 30:5:65, respectively; treatment with  $\text{I}_2$  for several days gave N-acetyl-3,4-diiodoamphetamine as the only significant poly-iodinated product. After acid hydrolysis, the mixture of iodinated amines (I) was converted to a mixture of the corresponding N-isopropyl derivatives (II) by reductive alkylation with acetone and  $\text{NaBH}_3\text{CN}$  (5). The isomeric iodo- and the 3,4-diiodo derivatives were then separated by preparative gas chromatography (10% Carbowax 20M containing 0.2% KOH on 100/120 mesh Chromosorb W, 200-300°). Due to incomplete resolution of the meta isomer, this product could only be obtained in an enriched state (Table 2). The pure para isomer (Ip,IIp) could be obtained in good yield by fractional recrystallization of p-iodoamphetamine hydrochloride. Exchange labeling with  $^{123}\text{I}$  was carried out by heating 5-20mg of the amine with 10-100mCi  $^{123}\text{I}$ -NaI (no-carrier-added) in 50  $\mu\text{l}$  ethanol at 121° for 45-90 minutes. The product was purified by sequential partitioning between ether and aqueous HCl or NaOH; radiochemical yields (not corrected for decay) ranged from 36 to 51%, with radiochemical purities of 93-99%, determined by thin layer chromatography on silica gel 60 using  $\text{CH}_3\text{OH}/\text{CHCl}_3/\text{acetic acid}$  (15:85:1) as developing solvent. For bioassay, the labeled amine was converted to the HCl salt with aqueous HCl, and administered intravenously in normal saline (adjusted to pH 4-7 with NaOH) to female Sprague-Dawley rats. Animals were sacrificed at 5 min and 60 min after injection and selected organs were removed, counted with a NaI scintillation detector, and weighed.

From the results of a number of experiments, summarized in Table I, no preferential brain uptake or retention by either R or S enantiomer could be demonstrated, either for p-iodoamphetamine or for N-isopropyl-p-iodoamphetamine. Neither did N-alkylation have much effect: although a slightly higher initial uptake might be seen with the N-isopropyl compound (about 1.6 versus 1.3%/g at 5 min), longer term retention was similar for both compounds. The position of the iodine on the aromatic ring, however, did influence the distribution (Table 2). With the compounds bearing iodine in the para position (IIp,III), brain activity increased between 5 min and 60 min, whereas with the compounds having iodine in the ortho or meta position (IIo,IIm), the brain activity decreased with time.

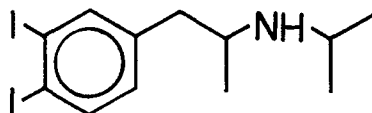
Taken with previous results (2), it appears that in simple phenyl alkyl amines para-substitution and  $\alpha$ -branching in the aralkyl chain are important for brain retention, whereas N-alkylation and optical configuration have little effect on gross brain localization.

- (1) Sargent T., Budinger T.F., Braun G., Shulgin A.T., and Braun U., J. Nucl. Med. 19, 17 (1978).
- (2) Winchell H.S., Baldwin R.M., and Lin T.H., J. Nucl. Med. 22, 940 (1980).
- (3) Tramosch K.M., Kung H.F., and Blau M., J. Nucl. Med., 22, P12 (1981).
- (4) Blaschke G. and Donow F., Chem. Ber. 108, 2792 (1975).
- (5) Borch R.F., Bernstein M.D., and Durst H.D., J. Am. Chem. Soc. 93 2897 (1971).



(o, m, p)

I, R = H

II, R = CH(CH<sub>3</sub>)<sub>2</sub>

III

Table 1. Enantiomers of <sup>123</sup>I-p-iodoamphetamine and N-isopropyl-p-iodoamphetamine: uptake in rat brain (mean ± 1 standard deviation)

Compound	Config-uration	%Dose/g Brain		Brain/Blood		# rats
		5 min	60min	5 min	60min	
p-Iodoamphetamine (Ip)	R	1.4±0.1	2.1±0.8	10.6±2.0	18.5±2.8	4
	S	1.2±0.2	1.9±0.3	7.0±1.0	11.3±2.4	6
N-Isopropyl-p-iodoamphetamine (IIp)	R(-)	1.7±0.3	1.9±0.4	15.8±6.6	20.0±4.8	24
	S(+)	1.5±0.2	2.1±0.2	11.4±1.2	16.1±3.0	6
	RS(+)	1.5±0.3	1.9±3.1	10.3±3.1	12.2±3.3	18

Table 2. Effect of Iodine Substitution pattern on brain uptake of <sup>123</sup>I-iodoamphetamine derivatives

Substitution Pattern	Isomeric Purity %	%Dose/g Brain		Brain / Blood	
		5 min	60 min	5 min	60 min
ortho(IIo)	92	1.0	0.6	8.2	7.0
meta(II <sub>m</sub> )	44*	1.1	0.9	3.1	6.5
para(II <sub>p</sub> )	>98	1.5	1.9	10.3	12.2
3,4-diiodo(III)	>99	1.1	1.2	8.7	11.0

\*Composition: 27% o, 44% m, 29% p

NEW IODINATED AMPHETAMINES BY RAPID SYNTHESIS FOR USE AS BRAIN BLOOD FLOW INDICATORS

T. Sargent, III, A.T. Shulgin, and C.A. Mathis.

Rm. 312, Donner Laboratory, Lawrence Berkeley Laboratory, University of California, Berkeley, California 94720 U.S.A.

Our initial observations of the first-pass brain uptake of III (4-<sup>123</sup>I-2,5-dimethoxyamphetamine)(1,2,3) have led to development by others of iodoamphetamines having different ring and nitrogen substitution patterns (4). Although <sup>123</sup>I is an ideal isotope for single photon tomographic imaging, a positron emitting isotope is required for Positron Emission Tomography (PET). The preferred isotope for this latter purpose is 3.6 min <sup>122</sup>I, a daughter of 20 hr <sup>122</sup>Xe; a generator system for the production of <sup>122</sup>I has been described (5). The iodoamphetamine derivatives described in (4) were radiolabelled, without exception, by exchange reactions which are inherently too slow for the short-lived <sup>122</sup>I. We have thus reinvestigated compounds that maintain the 2,5-dimethoxy ring pattern, as it allows the possibility of rapid iodination by direct substitution.

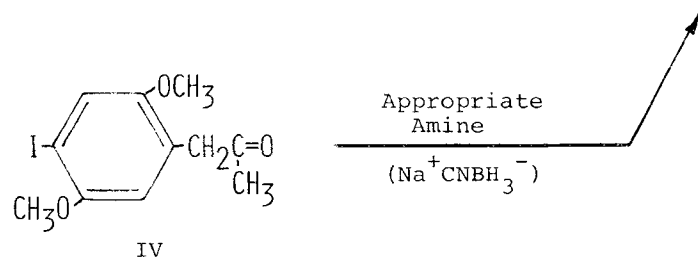
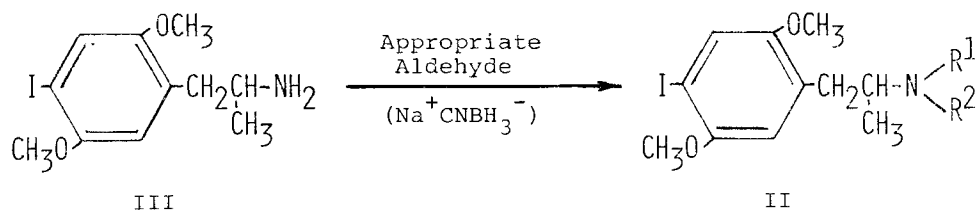
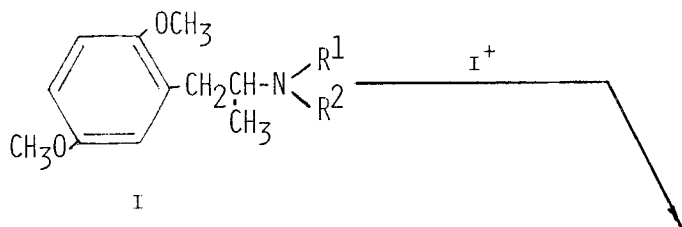
We have found that tertiary amines of the general formula I can be iodinated directly without attack on the basic nitrogen. In the preliminary biological investigations of various R<sup>1</sup> and R<sup>2</sup> nitrogen substituents in II, iodine isotopes with more conventional half lives were used (usually <sup>131</sup>I). Two labelled precursors, III and IV, allowed a broad versatility of nitrogen substitution. 4-Iodo-2,5-dimethoxyamphetamine (III) reacted readily with an appropriate aldehyde in the presence of NaCNBH<sub>3</sub> to yield II in which R<sup>1</sup> = R<sup>2</sup>. Similarly, 4-iodo-2,5-dimethoxyphenylacetone (IV) was reacted with amines in the presence of NaCNBH<sub>3</sub>. Primary amines (R<sup>1</sup>NH<sub>2</sub>) were the more effective, yielding II, with R<sup>2</sup> being hydrogen.

We have found that the direct labelling reaction of I → II (R<sup>1</sup> = R<sup>2</sup> = CH<sub>3</sub>) provided maximum incorporation of radioiodine within one minute, and hence represents a practical procedure for synthesis with <sup>122</sup>I.

Using II labelled with <sup>131</sup>I and R<sup>1</sup> = R<sup>2</sup> = CH<sub>3</sub> (IIa) and R<sup>1</sup> = R<sup>2</sup> = CH<sub>2</sub>CH<sub>3</sub> (IIb), we have measured brain, blood and other organ uptake in the rat. Compound IIa was studied in the dog by whole body scanning; brain uptake was 3.6 % at 5 min, and the maximum brain/blood ratio of 8.7 occurred at 8 min.

This type of compound thus appears to provide an excellent basis for radiopharmaceuticals which can provide a measure of regional brain blood flow with PET. The short T<sub>1/2</sub> of <sup>122</sup>I will result in a low patient radiation dose and the possibility of sequential measurements at short intervals. The <sup>122</sup>Xe → <sup>122</sup>I generator system can provide the isotope to institutions some distance from a production cyclotron.

- (1) Braun G., Shulgin A.T. and Sargent III T., J. Labelled Compds. Radiopharmaceut., 14, 767 (1978).
- (2) Sargent III T., Braun G., Braun U., Budinger T.F. and Shulgin A.T., Commun. Psychopharm., 2, 1 (1978).
- (3) Sargent III T., Budinger T.F., Braun G., Shulgin A.T. and Braun U., J. Nucl. Med., 19, 71 (1978).
- (4) Winchell H.S., Baldwin R.M. and Lim T.H., J. Nucl. Med., 21, 940 (1980).
- (5) Richards P. and Lim T.H., Int. J. Appl. Radiat. Isotop., 30, 250 (1979).



BIOMEDICAL APPLICATIONS OF NMR SPECTROSCOPY

J. Feeney.

Biomedical NMR Centre, National Institute for Medical Research,  
Mill Hill, London.

Over the last 20 years nuclear magnetic resonance (nmr) spectroscopy has become established as one of the foremost techniques for determining the molecular structures and conformations of complex molecules in solution. Such conventional applications to determine structures of drug molecules and to study interactions in drug-receptor complexes have made important contributions to understanding problems in molecular pharmacology. More recently two new areas of application have emerged which have attracted the attention of clinicians interested in using nmr as a safe, non-invasive diagnostic tool in medicine. In the first, high resolution nmr techniques have been used to study metabolic processes within localised intact living tissues and organs (Radda, Wilkie and Gadian). By observing nmr signals from  $^{31}\text{P}$  nuclei (100% naturally occurring isotope) in phosphorus containing metabolites such as phosphocreatine, ATP, inorganic phosphate and sugar phosphate, in intact cells or organs one can continuously monitor their levels and thus assess the energetic state of living tissues or organs. Clinical applications related to diagnosing muscle disorders, monitoring the viability of transplant organs and for following the effects of drug therapy have already been reported. The second area of diagnostic application is the use of nmr to provide proton density maps (spin-imaging) of intact biological specimens. Instruments for providing nmr 'head-scan' images are already in clinical use in several hospitals.

Examples of the applications of nmr to problems in molecular pharmacology and the use of nmr as a diagnostic tool for studying metabolism and spin-imaging of intact organs will be discussed.

pH SHIFT BRAIN IMAGING AGENTS

---

M. Blau and H. F. Kung.

Dept of Nuclear Medicine, State University of New York at Buffalo, Buffalo, New York 14215.

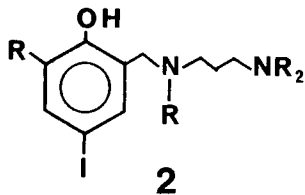
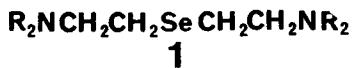
Intracellular pH is significantly lower than blood pH. For the brain this shift is about 0.4 pH units (blood pH = 7.4; brain pH = 7.0). Labeled diamines with suitable pK's and lipid solubility can be designed to function as brain perfusion indicators based on the concentration gradient established by this pH differential. At high pH these compounds are neutral and lipid soluble and can cross the blood-brain barrier into brain. At the lower intracellular pH they become charged and cannot readily diffuse out.

The dominant factor in the structure - localization relationships for these agents is the partition coefficient - pH profile. In the region of P.C.=0.1 to 10, increasing lipid solubility at blood pH increases brain uptake. First pass extraction efficiency can be as high as 90%. The upper limitation on lipid solubility is binding to blood proteins (which also increases with lipid solubility). High protein binding in blood prevents entry into brain.

The slope of the partition coefficient - pH profile determines the rate of washout from brain. The sharper the drop in lipid solubility with pH in the region pH 7.0 - 7.4, the longer the brain retention. Washout half-times are up to 24 hours.

Using the Henderson-Hasselbalch equation, the expected concentration ratios can be calculated from the pK's and the inherent lipid solubility (P.C. at pH = 11.5) for each compound. Using buffered red cells as a model system, the measured intracellular-extracellular ratios were very close to the predicted values except at high pH differentials ( $\Delta$  pH > 0.3) where the measured concentration gradient was higher than expected. A similar phenomenon is observed in animal studies where brain-to-blood concentration ratios can be as high as 20 although the calculated ratio would be expected to be about 6. This may be due to non-specific binding to intracellular components or localization in low pH regions in cells.

Two series of compounds have been studied.





The Se-75 series (R= -morpholino,-piperidino,-Me etc.) was prepared by reducing Se-75 selenious acid with sodium borohydride and reacting the intermediate with active aminoalkyl chlorides. Because of the long Se-75 half-life and the chemical stability of the compounds, most of the structure-localization relationships and biodistribution studies were carried out with these compounds. The radioiodine labeled phenolic diamines (series 2) are analogs of the Se compounds where one of the N-alkyl groups is replaced with an aromatic system to accommodate the iodine label. Since aromatic iodides are more stable than their aliphatic counterparts, this feature minimizes in vivo deiodination. The aromatic ring is activated by an OH group and radiolabeling can be achieved by a simple exchange reaction which is adaptable to a kit for routine use with I-123.

By changing the groups bonded to N and through other modifications one can design agents with any desired partition coefficient-pH profile. Since this profile plays an important role in determining the brain uptake it is possible to design brain imaging agents with optimal physical and biological properties.

RADIOIODINATED BRANCHED-CHAIN FATTY ACIDS: SUBSTRATES FOR BETA OXIDATION?

C.A. Otto, L.E. Brown, and W.H. Beierwaltes.  
University of Michigan-Dearborn, Dearborn, Michigan 48128.

Terminally iodinated fatty acids have been evaluated for use as metabolic probes of the myocardium. Their use is complicated by short myocardial T 1/2 and high blood activity levels. One approach to limit these complications is to manipulate the carbon skeleton of the fatty acid in order to trap the radiolabeled fatty acid in the myocardium. This approach was initially evaluated by the synthesis and tissue distribution study of beta methyl-13-<sup>125</sup>I-iodotridecanoic acid (I) (1). This compound would theoretically not be a substrate for  $\beta$ -hydroxyacyl dehydrogenase. The data (Table I) show reduced uptake relative to 13-<sup>125</sup>I-iodotridecanoic acid (II) and high thyroid and blood levels suggestive of extensive deiodination. The validity of this approach has been recently demonstrated by E. Livni, et al (2) using beta methyl [1-<sup>11</sup>C]heptadecanoic acid. Recent work by G. Kloster and G. Stöcklin (3) coupled with Livni's is further evidence for hydrolysis of the primary carbon-iodine bond of the iodo beta methyl compound.

We report a continued exploration of iodinated beta methyl compounds as potential imaging agents as iodinated compounds do not require close proximity to cyclotron produced <sup>11</sup>C and <sup>18</sup>F.

Beta methyl-16-<sup>125</sup>I-iodohexadecanoic acid was synthesized in order to evaluate a more natural length, even carbon fatty acid. The synthesis was achieved via a copper (I) iodide catalyzed condensation of 11-bromomagnesium undecene with the acid chloride of monomethyl 3-methylglutarate followed by carbonyl reduction, HBr addition and radioiodide displacement with Na<sup>125</sup>I in methylethyl ketone. Data in female rats shows comparable myocardial uptake with 16-<sup>125</sup>I-iodohexadecanoic acid (the straight chain analog) and comparable loss of activity again suggesting possible hydrolytic loss of radiolabel.

A dimethyl analog has been synthesized by a condensation of 11-bromomagnesium undecene with isopropylidene diethylmalonate. Saponification, decarboxylation and HBr addition yield 14-bromo-3,3-dimethyltetradecanoic acid. Exchange labelling and biological evaluation are in progress.

Stabilization of the carbon iodine bond has been demonstrated by using a phenyl carbon iodine bond rather than a primary carbon iodine bond (4). We report the synthesis of a beta methyl fatty acid containing a phenyl iodide. Condensation of the Grignard of 3-bromophenyl propane with the acid chloride of monomethyl 3-methylglutarate in the presence of copper (I) iodide followed by reduction of the carbonyl yields 8-phenyl-3-methyloctanoic acid. Esterification, iodination with bis (trifluoroacetoxy)iodobenzene and iodine and saponification yield 8-(p-iodophenyl)-3-methyloctanoic acid. Exchange labelling and biological evaluation are in progress.

- (1) Otto C.A., Brown L.E., Wieland D.M. and Beierwaltes W.H., Presented at the Third International Symposium on Radiopharmaceutical Chemistry, St. Louis, Missouri, June, 1978.
- (2) Livni E., Elmaleh D.R., Levy S., Brownell G.L. and Strauss W.H., J. Nucl. Med., 23, 169 (1982).
- (3) Kloster G. and Stöcklin G., Radioaktive Isotope in Klinik und Forschung 15, 235 (1982).
- (4) Machulla H.-J., Marsmann M. and Dutschka K., Eur. J. Nucl. Med., 5, 171 (1980).

TABLE I

HEART (M), BLOOD (B) AND THYROID (T) CONCENTRATIONS\* FOR  
BETA METHYL-13-IODOTRIDECAHOIC (I) ACID AND 13-IODOTRIDECAHOIC ACID (II)

Compound	5 min			10 min			20 min		
	M	B	T	M	B	T	M	B	T
I	0.14	0.30	3.12	0.09	0.21	4.46	0.07	0.18	11.26
II	0.30	0.18	2.07	0.26	0.14	2.85	0.21	0.17	4.23

\*concentrations expressed as % kg dose/g.

MYOCARDIAL UPTAKE AND IN VIVO DISTRIBUTION OF I-123 LABELED LONG-CHAIN FATTY ACID DERIVATIVES IN RATS

T.H. Lin, G.E. Harris, R.M. Baldwin, J.L. Wu, and J.F. Lamb.  
Medi-Physics, Inc., Emeryville, California 94608.

Radioiodinated  $\omega$ -iodo-9-hexadecenoic acid,  $\omega$ -iodoheptadecanoic acid and  $\omega$ -iodohexadecanoic acid have been intensively studied for use as myocardial metabolic indicators. These fatty acids, however, are rapidly metabolized and deiodinated in vivo. (1,2,3) The resulting fast clearance of activity from the heart and high level of blood activity render these compounds unsuitable for practical clinical use. Considerable research effort has been directed toward the derivatization of fatty acids which suffer a lower rate of metabolism and/or lead to metabolites that are stable toward deiodination. (4,5,6,7)

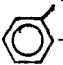
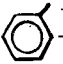
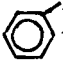
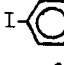
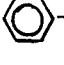
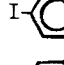
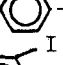
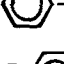
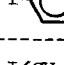
We have prepared fatty acids containing the iodophenoxy-, iodophenylthio-, iodoanilino-, iodobenzamido-, iodobenzoyloxy-, and iodobenzene-sulfamido groups at the  $\omega$  position. These compounds were I-123 labeled by exchange reaction. The in vivo distribution in rats indicated that;

- 1) Most of these compounds localized as well in myocardium as  $\omega$ -iodohexadecanoic acid. The clearance rates were also similar except for the o-iodophenoxy derivatives which showed longer retention of activity in heart.
- 2) The in vivo deiodination was negligible.
- 3) High levels of blood activity, however, were observed for all of the compounds.

The usefulness of these iodine-containing moieties in derivatization and radioiodination is thus demonstrated. Such derivatives show promise for more sophisticated structure-activity relationship studies due to the stability of the carbon-iodine bond and the variety of functional groups represented.

1. Robinson, G.D., Int. J. Appl. Rad. Isotop. 28, 149 (1977).
2. Machulla, H.J., Stöcklin G., Kupfernagel, C.H., Höck, A., Vyska, K., and Feinendegen, L.E., J. Nucl. Med., 19, 298 (1978).
3. Vyska, K., Höck, A., Freundlieb, C., Profant, M., Feinendegen, L.E., Machulla, H.J., Stöcklin, G., J. Nucl. Med., 20, 650 (1979).
4. Wieland, D.M., and Beierwaltes, W.H., J. Labeled Comp. & Radiopharm, 16, 171 (1979).
5. Knapp, F.F., Ambrose, K.R., Callahan, A.P., Grigshy, R.A., and Irgolic, K.J., Proceedings of the 2nd Intl. Symp. on Radiopharmaceuticals, Seattle, Washington, p.101, (1979).
6. Machulla, H.J., Marsmann, M., and Dutschka, K., Eur. J. Nucl. Med., 5, 171 (1980).
7. Livni, E., Elmaleh, D.R., Levy, S., Brownell, G.L. and Strauss, W.H., J. Nucl. Med., (in press).

IN VIVO DISTRIBUTION OF RADIOIODINATED LONG-CHAIN FATTY ACID  
DERIVATIVES IN PATS

FATTY ACIDS	In Vivo Time (min)	% Dose / Gram				% Dose in Stomach
		Blood	Heart	Heart Blood	Heart Lung	
 -O-(CH <sub>2</sub> ) <sub>9</sub> COOH	5	2.5	3.4	1.4	2.6	0.9
	60	2.1	2.1	1.0	2.1	0.9
 -O-(CH <sub>2</sub> ) <sub>6</sub> CH=CH(CH <sub>2</sub> ) <sub>7</sub> COOH	5	2.1	4.9	2.3	3.2	0.8
	60	1.8	2.2	1.2	2.2	0.8
 -O(CH <sub>2</sub> ) <sub>15</sub> COOH	5	1.3	2.8	2.2	3.2	0.6
	30	1.3	2.4	1.9	2.4	0.8
 -O(CH <sub>2</sub> ) <sub>6</sub> CH=CH(CH <sub>2</sub> ) <sub>7</sub> COOH	5	3.1	2.7	0.9	1.1	0.7
	60	2.7	1.8	0.7	1.0	0.9
 -S-(CH <sub>2</sub> ) <sub>6</sub> CH=CH(CH <sub>2</sub> ) <sub>7</sub> COOH	5	1.6	2.8	1.8	1.8	0.9
	60	1.2	1.0	0.9	1.0	4.0
 -NH(CH <sub>2</sub> ) <sub>6</sub> CH=CH(CH <sub>2</sub> ) <sub>7</sub> COOH	5	1.6	3.0	1.9	1.6	0.6
	60	1.2	0.8	0.7	0.6	2.0
 -C(=O)NH(CH <sub>2</sub> ) <sub>6</sub> CH=CH(CH <sub>2</sub> ) <sub>7</sub> COOH	5	0.5	1.3	2.5	2.5	0.4
	60	0.2	0.4	2.2	1.8	0.8
 -C(=O)-O-(CH <sub>2</sub> ) <sub>15</sub> COOH	5	2.2	3.5	1.6	2.3	0.8
	30	1.3	1.8	1.4	1.8	2.1
 -SO <sub>2</sub> NH(CH <sub>2</sub> ) <sub>6</sub> CH=CH(CH <sub>2</sub> ) <sub>7</sub> COOH	5	1.3	0.3	0.2	0.4	1.7
	60	2.1	1.1	0.6	0.9	0.5
I(CH <sub>2</sub> ) <sub>15</sub> COOH	5	0.5	3.4	7.7	2.4	1.6
	60	0.6	0.8	1.1	0.8	10.2
I(CH <sub>2</sub> ) <sub>6</sub> CH=CH(CH <sub>2</sub> ) <sub>7</sub> COOH	5	0.9	2.5	2.9	2.0	2.0
	60	0.9	0.8	1.0	0.8	14.9
I(CH <sub>2</sub> ) <sub>16</sub> COOH	5	1.0	3.1	3.1	2.3	1.4
	60	0.6	1.1	2.0	1.2	5.4

SYNTHESIS OF RADIOIODINATED  $\omega$ -p-(IODOPHENYL)-SUBSTITUTED METHYL BRANCHED LONG-CHAIN FATTY ACIDS

M. M. Goodman, G. Kirsch and F. F. Knapp, Jr., Nuclear Medicine Technology Group, Health and Safety Research Division, Oak Ridge National Laboratory, Oak Ridge, TN 37830, U.S.A.

We have developed a new class of long-chain fatty acids in which methyl branching has been introduced in the alkyl chain as a means of inhibiting  $\beta$ -oxidation and thus lead to increased myocardial retention. Radioiodinated terminal p-(iodophenyl)-substituted alkanolic fatty acids containing methyl branching in the  $\alpha$ - and  $\beta$ -positions have now been prepared. These studies have been prompted by a recent report of the pronounced uptake and prolonged myocardial retention of  $\beta$ -methyl-[1- $^{11}\text{C}$ ]heptadecanoic acid (1). This agent is rapidly extracted by the myocardium and exhibits a high heart:blood ratio (10:1) after 1 hour. The mechanism resulting in the prolonged retention appears to involve inhibition of a crucial metabolic transformation. The presence of the methyl group may sterically or chemically inhibit the metabolism of fatty acids analogous to the inhibition of glucose metabolism observed with 2-fluoro-2-deoxyglucose in the heart and brain. Because of the attractive 13.2 hour physical half-life and emission of a single gamma photon with an energy of 159 keV in 83% abundance, p-[ $^{123}\text{I}$ ]iodophenyl methyl-branched fatty acids can be available for distribution to a large patient population for evaluation of heart disease. The present study has focused on the preparation of 14-(p-[ $^{125}\text{I}$ ]iodophenyl)-2-(R,S)-methyltetradecanoic acid and 15-(p-[ $^{125}\text{I}$ ]iodophenyl)-3-(R,S)-methylpentadecanoic acid. The unlabeled model agents have been prepared by the new methods outlined in Schemes 2, 3, and 4.

The phenyl-dodecyl iodide substrate (VIII) was prepared as described in Scheme 1. The pivotal step in this synthesis of the branched fatty acids (Scheme 2) involved introduction of the methyl branching via alkylation of the anion of 2-ethyl-4,4-dimethyl-2-oxazoline (IX), to give the substituted oxazoline (X). The oxazoline derivative (X) was treated with ethanolic- $\text{H}_2\text{SO}_4$  to afford ethyl-14-phenyl-2-(R,S)-methyltetradecanoate (XI), which was then converted to methyl-15-phenyl-3-(R,S)-methylpentadecanoate (XII) as outlined in Scheme 3. Regiospecific para-*bis*-(trifluoroacetyl)thallation of (XI) and (XII) gave the substituted products (XIV) and (XVI) which were treated with excess K-I followed by NaOH hydrolysis to give 3-(R,S)-methyl-15-(p-iodophenyl)pentadecanoic acid (XV; oil;  $\text{M}^+$ , m/z 458), and 2-(R,S)-methyl-14-(p-iodophenyl)tetradecanoic acid (XVII; mp 59-60°C;  $\text{M}^+$ , m/z 444), respectively. The 3-(R,S)-methyl-15-p-(iodophenyl)pentadecanoic acid (XV) was also prepared by the thiophene route outlined in Scheme 4 (n=6), which involved Raney nickel reduction of the 2,5-disubstituted thiophene (XX), prepared by treatment of the monosubstituted thiophene (XIX) with 3-methylglutaric anhydride followed by Wolf-Kishner reduction. Compounds (I)-(XX) exhibited elemental analyses, and chromatographic, mass spectral and  $^1\text{H}$ -nuclear magnetic resonance properties which were consistent with the proposed structures. Both 3-(R,S)-methyl-15-(p-[ $^{125}\text{I}$ ]iodophenyl)pentadecanoic acid ( $^{125}\text{I}$ -XV) and 2-(R,S)-methyl-14-(p-[ $^{125}\text{I}$ ]iodophenyl)tetradecanoic acid ( $^{125}\text{I}$ -XVII) have been prepared by treatment of (XIV) and (XVI), respectively, with K- $^{125}\text{I}$ .

Tissue distribution studies of  $^{125}\text{I}$ -labeled (XV) and (XVII) were performed in Fischer rats and compared with data for the unbranched analogs, 14-(p-[ $^{125}\text{I}$ ]tetradecanoic acid (XXI) and 15-(p-[ $^{125}\text{I}$ ]iodophenyl)pentadecanoic acid (XXII). The four agents showed significant heart uptake (Table 1). Although the blood levels were high in these preliminary studies, the low thyroid uptake demonstrated minimal in vivo deiodination. Over the first 60 minute period, all four compounds showed myocardial retention and the branched analogs (XV) and (XVII) appeared to show greater myocardial uptake than the straight-chain compounds. Studies are now in progress to resolve the racemic mixtures and evaluate the R and S isomers of the methyl-branched fatty acids.

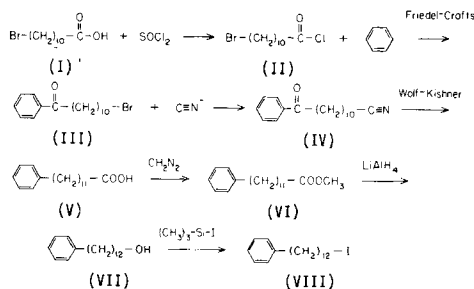
Table 1. Tissue distribution of  $^{125}\text{I}$ -labeled p-(iodophenyl)-substituted fatty acids in tissues of Fischer female rats\*

$^{125}\text{I}$ -labeled fatty acid, minutes after injection	Range % dose/g values for four rats					
	Heart	Blood	Lung	Liver	Thyroid	
(XXII)	5	1.47-2.41	0.75-1.44	1.12-1.55	9.50-10.06	2.35-5.07
	60	1.65-2.95	1.34-1.59	0.98-1.27	2.13-3.10	7.74-9.80
(XV)	5	2.34-3.47	0.67-1.18	0.81-1.72	4.40-8.10	5.64-9.54
	60	2.20-2.47	1.17-1.41	1.22-1.39	3.25-4.01	7.19-7.63
(XXI)	5	1.22-2.26	0.83-1.30	1.29-1.49	5.89-8.19	1.32-1.70
	60	1.03-2.40	1.29-1.51	0.99-1.42	2.11-2.69	2.04-4.23
(XVII)	5	2.42-3.10	1.37-1.79	1.41-1.82	4.66-5.02	0.90-1.97
	60	1.32-2.01	1.43-1.62	1.23-1.58	1.73-2.22	1.89-3.99

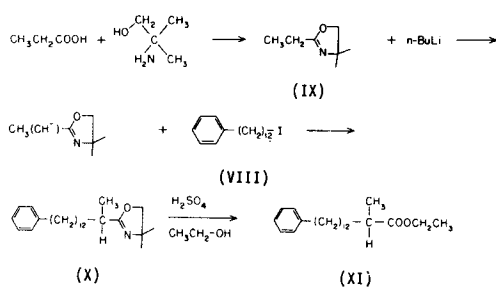
\*The radioiodinated fatty acids had specific activities from 25-30 mCi/mole. Each rat received 5-10  $\mu\text{Ci}$  of the agent.

(1) Livni, E., Elmaleh, D. R., Levy, S., Brownell, G. L. and Strauss, H. W. J. Nucl. Med., 23, 169 (1982).

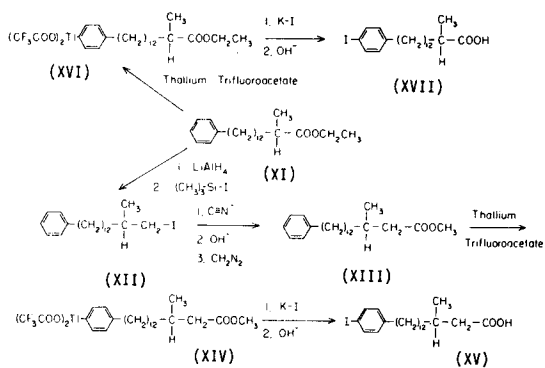
Research sponsored by the Office of Health and Environmental Research, U.S. Department of Energy under contract W-7405-eng-26 with the Union Carbide Corporation.



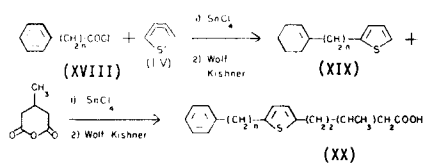
Scheme 1



Scheme 2



Scheme 3



Scheme 4



**RADIOIODINATION OF PHENYL PENTADECANOIC ACID VIA AN ORGANTHALLIUM INTER-MEDIATE**

P.V. Kulkarni and R.W. Parkey. Department of Radiology, The University of Texas Health Science Center at Dallas, Texas 75235.

Fatty acids labeled with various radionuclides are of great interest in myocardial imaging because of their potential applications as metabolic markers. Long chain aliphatic fatty acids labeled with I-123 at the terminal position have been in clinical use for some time (1). Recently Machulla et al. proposed radiolabeled  $\omega$ -phenyl fatty acid for myocardial imaging (2). They showed that  $\omega$ -(p-iodo)phenyl pentadecanoic acid (IPPA) has better *in vivo* stability compared to  $\omega$ -iodo aliphatic fatty acids which rapidly release free iodine following  $\beta$ -oxidation. The direct iodination of PPA by electrophilic aromatic substitution reaction as proposed by Machulla et al. gave poor yields (<25%) with NaI-125 and the yields were poorer and not reproducible with expensive NaI-123. A method for the preparation of radioiodinated phenyl fatty acids utilizing an organothallium intermediate is presented. Radiochemical yields of I-PPA by this method are found to be consistently high (70-75%). The animal distribution studies indicated that the product prepared by this method was comparable to that produced by direct iodination of PPA.

Direct electrophilic iodination. Method A. Radioiodination of PPA with I-125 was performed according to the method proposed by Machulla et al. with minor modifications (2,3). PPA (0.5 mg), 1-2 mCi (37-74 MBq) of I-125 or I-123 in 1-50  $\mu$ l of 0.1 N NaOH were used. The product was eluted from the C<sub>18</sub> column with methanol:water:acetic acid (96:3:1) solvent system using Beckman HPLC system. The labeled fatty acid peak pooled and solvent evaporated. The residue was dissolved in 100  $\mu$ l of ethanol and 3 ml of 6% human serum albumin was added with stirring. The product was sonicated in an ultrasonic bath for 5 minutes and passed through a small anion exchange (DOWEX 1x8) column to remove any free iodine. The final product was passed through 0.22  $\mu$  membrane filter to remove any aggregate particles.

Radioiodination via an organothallium intermediate. Method B. Thallium complex of PPA was first prepared by incubating PPA with thallium trifluoroacetate (TTFa) in trifluoroacetic acid at room temperature. The incubation times varied from 1 hr to 24 hrs. In these reactions the ratio of the amount of TTFa to PPA was held constant (2.2 mg TTFa/mg PPA).

The second reaction involved the treatment of the *in situ* formed PPA-Tl complex with radioiodine (I-125, I-123). Radioiodine 0.1-1.0 mCi (3.7-37 MBq) in 0.1N NaOH (5-50  $\mu$ l) was added to the PPA-Tl complex and incubated either at a) room temperature or b) 50°C. The kinetics of formation of I-PPA was studied by determining the extraction efficiency of the radioactivity (the labeled product) in hexane. In our preliminary studies we evaluated the effect of the following factors on the radiochemical yield: a) the amount of PPA (0.1 mg-4 mg), b) the time of incubation, c) the temperature (room temperature vs. 50°C). The labeled product was first extracted in hexane and then the solvent was evaporated. The residue was dissolved in methanol and the product purified on a reversed phase (C<sub>18</sub>) column. The elution and further treatment of the product was performed according to the procedure described above.

Results and Discussion. The PPA, labeled by the new proposed method utilizing an organothallium intermediate, gave a single radioactivity peak on an HPLC C<sub>18</sub> column. This was presumed to be the para-iodinated compound. We do not have spectroscopic (NMR) data at present to confirm the structure. Further studies are being planned to elucidate the structure.

The radiochemical yields were very much dependent upon the temperature of the iodination reaction (Fig. 1). The reaction reached equilibrium within 30 minutes at 50°C, however, it took about 3 hours at room temperature. The

radiochemical yields were sufficiently high (>60%) as early as 5 minutes at 50°C (Fig. 1). Reasonable yields (>60%) could be obtained by using as little as 0.2 mg of PPA. The radiochemical yields did not significantly increase by increasing the amount of PPA up to 4 mg of PPA. Our preliminary data indicate that 0.5 mg PPA may be used for carrying out the iodination reaction at 50°C for 15 minutes with good yields (~75%).

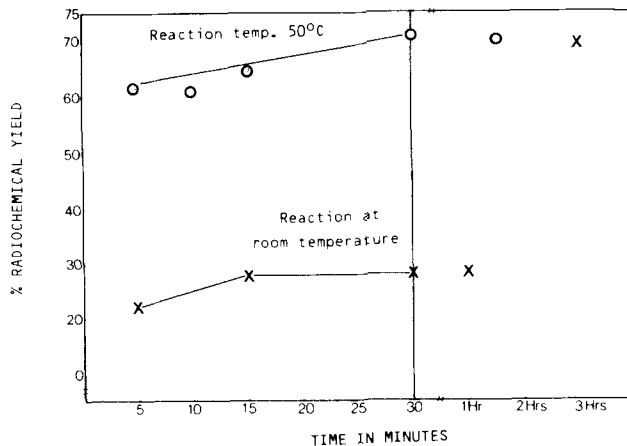


Figure 1. Radioiodination of phenylpentadecanoic acid (PPA) by using PPA-thallium intermediate. Percent labeling determined by extraction of radioactivity into the hexane layer. Reactions were carried out at room temperature: x-x and at 50°C: o-o.

The biological distribution of I-PPA prepared by the thallation method (B) was very similar to that prepared by the direct iodination method (A). The heart to blood ratios in rats (cpm/g heart : cpm/g blood) at 1 minute after i.v. administration were:  $5.41 \pm 0.6$  for method A and  $6.10 \pm 1.5$  (mean  $\pm$  SEM) for method B. These values are lower than those reported by Machulla et al. for the heart to blood ratios in mice. The discrepancy may be due either to species difference or to the presence of impurities in our preparation. This is being further evaluated.

It has been proposed that thallation of phenyl ring occurs in aromatic compounds (4). In compounds such as phenyl pentadecanoic acid, overwhelming preference may be for *para* substitution due to steric factors, the bulkiness of thallium. Organothallium intermediates might be useful in radioiodination of compounds containing a phenyl ring.

Our preliminary data suggest that radioiodination of phenyl fatty acid suitable for myocardial imaging is feasible using thallium trifluoro acetate reagent. This method is simple, convenient, and provides reproducible good yields. This method may have applications in preparation of other important radioiodinated radiopharmaceuticals.

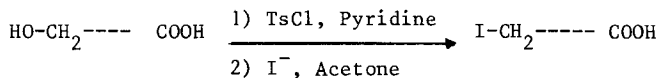
#### References:

- (1) Poe, N.D., Robinson G.D. Jr., Zielinski, F.W., et al. *Radiology*, 124, 419 (1977).
- (2) Machulla H.J., Marsmann, M., and Dutschka K., *Europ J Nucl Med* 5, 171, (1980).
- (3) Angelberger, P., Wagner-Loffler, M., Dudczak, R., et al., "Progress in Radiopharmacology", Vol. 2, 1981, p. 61.
- (4) McKillop A., Fowler, J.S., Zelesko, M.J., and Hunt, J. D., *Tetrahedron Letters*, 29, 2423 (1969).

FATTY ACIDS LABELLED WITH IODINE  $^{123}\text{I}$  OR  $^{131}\text{I}$  IN  $\omega$  POSITION; MYOCARDIAL EVOLUTIONF. Riche<sup>1</sup>, J.P. Mathieu<sup>3</sup>, S. Coornaert<sup>2</sup>, A. Bardy<sup>2</sup>, G. Busquet<sup>3</sup>, J. Godart<sup>4</sup>, M. Comet<sup>3</sup>, and M. Vidal<sup>1</sup>.<sup>1</sup>Laboratoire d'Etudes Dynamiques et Structurales de la Sélectivité, U.S.M. de Grenoble, Domaine Universitaire; B.P. 53 X, 38041 Grenoble Cedex, France.

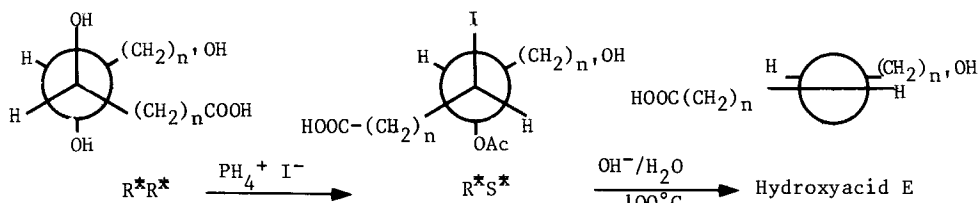
The labelling of a fatty acid with an atom of radioactive iodine  $^{123}\text{I}$  or  $^{131}\text{I}$  causes no perceptible modification of its myocardial behaviour (1 and 2), which depends on the physiopathological state of the cardiac muscle. In order to examine the relationship between the structure of the fatty acids and their myocardial uptake, and thereby to determine the molecule most suitable for a study by external means of myocardial metabolism in man, we have synthesized a number of saturated, acetylenic, and Z or E ethylenic acids labelled in  $\omega$  position with a radioactive iodine atom. In the course of this work, we have developed a simple and rapid labelling method requiring no product purification (3,4,5), which should therefore be routinely useful in nuclear medicine laboratories.

- The synthesis of long-chain fatty acids iodinated in  $\omega$  position is performed by tosylation of the  $\omega$ -hydroxyacids followed by a  $\text{TsO}^- - \text{I}^-$  exchange reaction:



The  $\omega$ -hydroxyacids are prepared through the following methods:

The Z and E ethylenic derivatives are obtained by trans-elimination of vicinal iodoacetates (with determined relative structures) in basic medium.



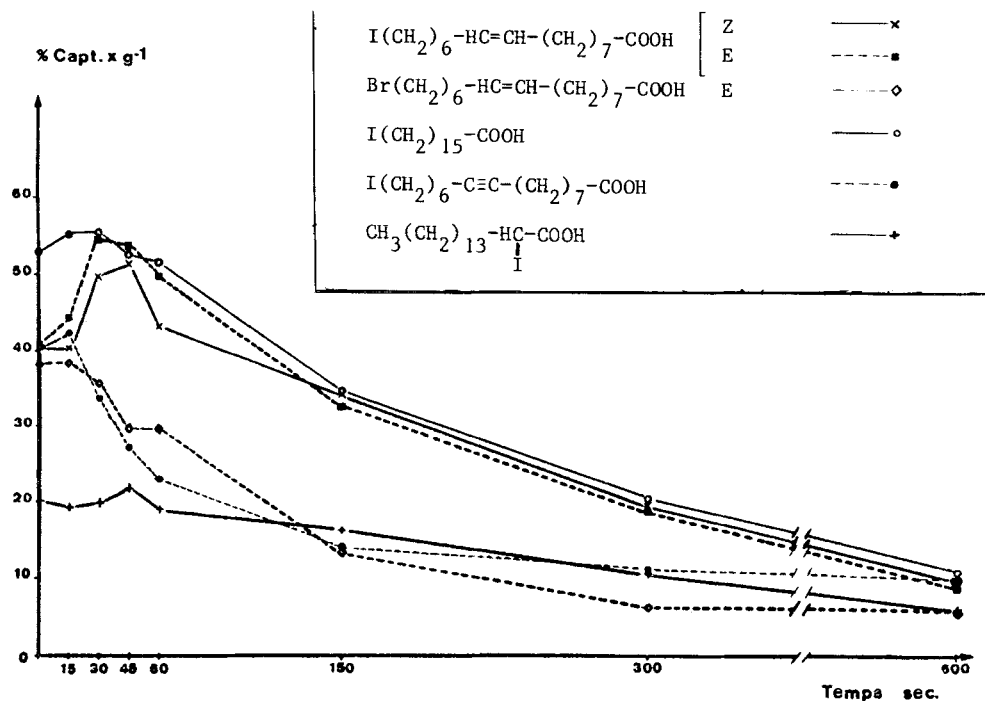
The action of phosphonium iodide on vicinal diols followed by basic treatment shows a high stereoselectivity but is not stereospecific; on the other hand, the yields of the elimination reaction are low.

The synthesis of the acetylenic  $\omega$ -hydroxyacids is effected by coupling an acetylenic alcohol with a  $\omega$ -bromo acid in liquid ammonia. The reduction of these acetylenic derivatives leads to the Z ( $\text{H}_2$ , Pd Lindlar), E ( $\text{Na}$ ,  $\text{NH}_3$ ) and saturated ( $\text{H}_2$ , Pt Adams) derivatives. The stereoselectivity of the triple bond reduction, evaluated by  $^{13}\text{C}$  NMR, is higher than 95% for all the cases studied. This method offers the possibility of synthesizing numerous derivatives having different chain lengths and positions of the  $\pi$  bond; it has afforded, by tosylation and iodination, the acetylenic, ethylenic Z and E, and saturated  $\omega$ -iodinated fatty acids for following n and n' values (5,5- $\text{C}_{13}$ ), (5,6- $\text{C}_{14}$ ), (7,5- $\text{C}_{15}$ ), (7,6- $\text{C}_{16}$ ), (7,8- $\text{C}_{18}$ ), (10,7- $\text{C}_{20}$ ).

- The labelling by  $^{123}\text{I}$  or  $^{131}\text{I}$  fatty acids iodinated in  $\omega$  position is performed by  $\text{I}^-$ ,  $^*\text{I}^-$  exchange ( $\text{Na}^+ ^*\text{I}^-$  solution) in acetone at about  $100^\circ\text{C}$ . The influence of carrier quantity, pH and water concentration has been studied. The exchange performed at  $100^\circ\text{C}$  on  $10^{-5}$  mole of iodinated fatty acid and 1 mCi of ( $\text{Na}^+$ ,  $^{123}\text{I}^-$ ) in acetone gives labelling yields from 95 to 97% for reaction times less than 10'. The labelled products obtained by this method are homogeneous and may be used without purification. The quality of this product has been studied by HPLC ( $\text{SiO}_2$  or  $\text{C}_{18}$  column) and by  $^{13}\text{C}$  and  $^1\text{H}$  NMR. Labelling yields are determined by

electrophoresis, anionic resin chromatography, TLC (cellulose - heptane: 380, ether: 80, AcOH : 1) and HPLC ( $\text{SiO}_2$ , 10  $\mu\text{m}$ ; 50 cm; heptane: 981; ether: 15; AcOH: 4).

- Some  $\text{C}_{16}$  fatty acids were injected in mice. The existence of a double bond and the character Z or E have no influence on myocardial fixation. The existence of a triple bond decreases the fixation and induces a modification in the intramyocardial metabolism including perhaps a stop in the course of  $\beta$  oxidation at the triple bond level.



- (1) Machulla H.J., Stöcklin G., Kupfernagel Ch., Freundlieb Ch., Höck A., Vyska K., Feinendegen L.E., J. Nucl. Med., 19, 298 (1978).
- (2) Poe N.D., Robinson G.D., Graham L.S., Mac Donald N.S., J. Nucl. Med., 17, 1077 (1976).
- (3) Machulla H.J., Dutschka K., Astfalk C., Radiochem. Radioanal. Letters, 47, 189 (1981).
- (4) Kabalka G.W., Gooch E.E., Sastry K.A., J. Nucl. Med., 22, 908 (1981).
- (5) Otto C.A., Brown L.E., Wieland D.M., Beierwaltes W.H., J. Nucl. Med., 22, 613 (1981).

<sup>2</sup> Office des Rayonnements Ionisants, C.E.A., B.P. N° 21, 91190 Gif/Yvette, France.

<sup>3</sup> Laboratoire de Biophysique, U.S.M. de Grenoble, Domaine de la Merci, Place du Commandant Nal, 38700 La Tronche, France.

<sup>4</sup> Institut des Sciences Nucléaires, 53, Avenue des Martyrs, 38000 Grenoble, France.

RADIOIODINATION OF 15-(p-iodophenyl)-6-tellurapentadecanoic acid BY TRIAZENE DECOMPOSITION WITH RADIOIODIDE

F. F. Knapp, Jr., M. M. Goodman, and A. P. Callahan, Nuclear Medicine Technology Group, Health and Safety Research Division, Oak Ridge National Laboratory, Oak Ridge, TN 37830, U.S.A.

Radiolabeled long-chain fatty acids have important applications in nuclear medicine for the diagnosis of heart disease and can be used to delineate regions of abnormal fatty acid metabolism within the myocardium. The most extensively investigated agents of this type are terminal  $^{123}\text{I}$ -labeled long-chain fatty acids (1). The results of tissue distribution studies with 9-[ $^{123m}\text{Te}$ ]tellurapentadecanoic acid (9-[ $^{123m}\text{Te}$ ]THDA) have shown pronounced heart uptake and prolonged myocardial retention in rats and dogs (2-5). If such unique "trapping" reflects the metabolic integrity of the myocardium, these molecules may be useful for the heart in the same manner as 2-fluoro-2-deoxyglucose has been used in the brain. Because of the more attractive physical properties of iodine-123 ( $t_{1/2} = 13.2$  h), we recently described the preparation and evaluation of a model  $^{125}\text{I}$ -labeled terminal iodoalkyl-substituted long-chain fatty acid containing non-radioactive tellurium; 17-iodo-9-tellurapentadecanoic acid [ $^{125}\text{I}$ -CH<sub>2</sub>-(CH<sub>2</sub>)<sub>7</sub>-Te-(CH<sub>2</sub>)<sub>7</sub>-COOH; 17- $^{125}\text{I}$ -9-THDA]. Tissue distribution studies with 17-[ $^{125}\text{I}$ ]-9-THDA indicated high myocardial uptake but also demonstrated significant *in vivo* deiodination (6). Because of high blood levels and pronounced thyroid uptake of radioactivity, these agents have not been investigated further.

Several strategies have now been explored to chemically stabilize radioiodine on tellurium fatty acids. The approach described here involves chemical stabilization of the iodide by attachment of the *p*-(iodophenyl) moiety to tellurium fatty acids. Studies by other workers have demonstrated the pronounced heart uptake and *in vivo* stability of radioiodinated 15-(*p*-iodophenyl)pentadecanoic acid (7-9). Because of the potential clinical importance of using the trapping phenomenon of radioiodinated tellurium fatty acids to diagnose heart disease, we have developed a general synthetic method for the preparation of radioiodinated *para*-iodophenyl tellurium fatty acids. In the present investigation we report the synthesis (Schemes 1 and 2) and tissue distribution in rats (Table 1) of 15-(*p*-[ $^{125}\text{I}$ ]iodophenyl)-6-tellurapentadecanoic acid (X) as a model agent.

The route chosen for introduction of iodine into the *para*-position of (X) involved the decomposition of the aryltriazene intermediate (V). This method was chosen because the decomposition reaction can generally be performed rapidly (<5 min) on a very small scale and the *para*-iodophenyl products are obtained in high yield. These characteristics are particularly attractive for the preparation of high specific activity products labeled with the short-lived iodine-123 ( $t_{1/2} = 13$  h). Treatment of 1-chloro-9-(*p*-aminophenyl)nonane (IV) at 0°C with nitrous acid followed by aqueous piperidine, and subsequent purification by adsorption chromatography, gave 1-[4-(1-chloro-9-phenylnonyl)-3,3-(1,5-pentanediy)]triazene (V) in 40% yield. Compound (V) was then treated with sodium iodide and trifluoroacetic acid. After purification by column chromatography 1-chloro-9-(*p*-iodophenyl)nonane (VI) was obtained in 60% yield. The *p*-iodophenylalkyl chloride (VI) was then coupled with sodium (methylvaleryl)-telluride (VIII) to afford methyl-15-(*p*-iodophenyl)-6-tellurapentadecanoate (IX) in 90% yield (Scheme 2). Hydrolysis of compound (IX) gave the desired 15-(*p*-iodophenyl)-6-tellurapentadecanoic acid (X; mp 72-73°C;  $M^+$  =  $m/z$  560) in 65% yield. The spectral properties, elemental analyses and chromatographic properties substantiated the structures of compounds (I)-(X).

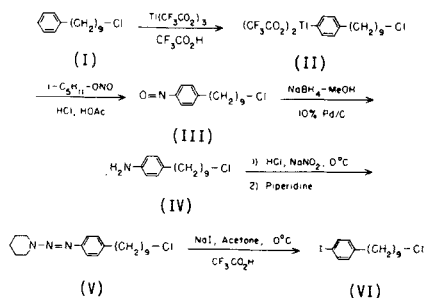
The  $^{125}\text{I}$ -labeled analog was prepared by the same method outlined in Schemes 1 and 2 by employing Na[ $^{125}\text{I}$ ]. Tissue distribution studies were performed in

rats at various time periods from 5 min to 5 days (Table 1). This agent shows rapid and pronounced myocardial uptake analogous to that reported earlier for 9-[ $^{123}\text{mTe}$ ]THDA. These studies illustrate that the terminal p-iodophenyl moiety does not interfere with the myocardial specificity observed with similar agents. After 6 hours the heart retained 80% of the maximum uptake observed after 5 min, which decreased to only 55% after 24 hours. The mean heart:blood ratios were 22:1 at 5 min and 17:1 at 2 hours. Only marginal radioactivity accumulated in the thyroid tissue; 1.52% dose/g after 5 min and 5.89% dose/g after 6 h. The minimal thyroid radioactivity and low blood levels demonstrate that attachment of the radioiodine to the phenyl ring is an effective means of stabilizing the iodine and overcoming facile *in vivo* cleavage. Similar results have also been obtained with the  $^{131}\text{I}$ -labeled fatty acid (X).

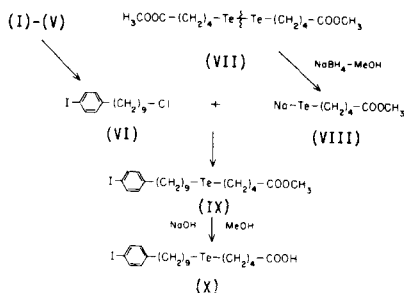
Since triazene derivatives such as (V) are generally stable substances that can be stored indefinitely, this regiospecific route for the introduction of the iodine in the para-position may be more useful than methods that give isomeric mixtures requiring subsequent separation. An additional advantage of this route is the potential consumption of all of the radioiodide during this step. The excess triazene is easily removed from the iodophenyl product by simple chromatography. We have also used the triazene route to prepare 15-(p-[ $^{125}\text{I}$ ]-iodophenyl)pentadecanoic acid. We have recently prepared high-specific activity p-[ $^{123}\text{I}$ ]iodophenylnonylchloride by decomposition of (V) with carrier-free  $^{123}\text{I}$  (10). The unique properties described for 15-(p-iodophenyl)-6-tellurapentadecanoic acid indicate that the  $^{123}\text{I}$ -labeled analog is an attractive agent for potential clinical use.

- (1) Feinendegen, L. E., Vyska, K., Freundlieb, Chr., Hock, A., Machulla, H-J., Kloster, G. and Stöcklin, G. *Eur. J. Nucl. Med.*, 6, 191 (1981).
- (2) Knapp, F. F., Jr., Ambrose, K. R., Callahan, A. P., Grigsby, R. A., and Irgolic, K. J. *Radiopharmaceuticals II*, 101 (1979).
- (3) Knapp, F. F., Jr., Ambrose, K. R., Callahan, A. P., Ferren, L. A., Grigsby, R. A. and Irgolic, K. J. *J. Nucl. Med.* 22, 988 (1981).
- (4) Elmaleh, D. R., Knapp, F. F., Jr., Yasuda, T., Coffey, J. L., Kapiwoda, S., Okada, R. D. and Strauss, H. W. *J. Nucl. Med.*, 22, 994 (1981).
- (5) Okada, R. D., Knapp, F. F., Jr., Elmaleh, D. R., Yasuda, T., Boucher, C. A. and Strauss, H. W. *Circul.*, 65, 305 (1982).
- (6) Goodman, M. M. and Knapp, F. F., Jr. *J. Med. Chem.*, in press.
- (7) Machulla, H-J., Marsmann, M. and Dutschka, K. *J. Radioanal. Chem.*, 56, 253 (1980a).
- (8) Machulla, H-J., Marsmann, M., Dutschka, K., and Van Beuningen, D. *Radiochem. Radioanal. Lett.*, 42, 243 (1980).
- (9) Machulla, H-J., Marsmann, M. and Dutschka, K. *Eur. J. Nucl. Med.*, 5, 171 (1980).
- (10) Knapp, F. F., Jr., Goodman, M. M., and Richards, P., unpublished experiments.

Research sponsored by the Office of Health and Environmental Research, U.S. Department of Energy under contract W-7405-eng-26 with the Union Carbide Corporation.



Scheme 1



Scheme 2

Table 1. Distribution of radioactivity in tissues of Fischer 344 female rats after intravenous administration of 15-(p-[<sup>125</sup>I]iodophenyl)-6-tellurapentadecanoic acid<sup>a</sup>

Tissue	Mean percent injected dose/g (range)						
	Time after injection						
	5 min	30 min	60 min	2 h	6 h	24 h	5 d
Heart	5.87 (5.30-6.45)	6.43 (4.35-8.98)	5.55 (4.01-7.27)	5.85 (4.01-7.56)	4.78 (3.89-5.33)	3.25 (3.02-3.41)	0.94 (0.77-1.13)
Blood	0.26 (0.24-0.27)	0.45 (0.38-0.50)	0.34 (0.28-0.40)	0.42 (0.32-0.57)	0.31 (0.29-0.32)	0.20 (0.18-0.21)	0.03 (0.03-0.034)
Lungs	1.14 (0.86-1.52)	1.25 (1.14-1.40)	1.48 (1.10-1.95)	1.57 (1.29-2.05)	1.10 (0.97-1.17)	0.89 (0.77-1.05)	0.33 (0.30-0.36)
Liver	9.57 (8.97-10.28)	7.78 (6.73-8.86)	7.69 (6.68-8.28)	8.38 (7.32-9.90)	8.37 (7.86-9.08)	6.24 (5.53-6.73)	1.28 (1.23-1.36)
Kidneys	1.02 (0.79-1.15)	1.25 (1.09-1.39)	1.41 (1.23-1.55)	1.37 (1.20-1.69)	1.12 (0.95-1.20)	0.70 (0.64-0.80)	0.20 (0.18-0.22)
Thyroids	1.52 (1.41-1.63)	1.51 (0.83-2.21)	1.48 (0.95-1.94)	3.51 (1.91-4.42)	5.89 (5.33-7.08)	22.78 (18.15-27.13)	30.25 (25.36-34.81)

<sup>a</sup>Mean and range values for four female Fischer rats. Other tissues that were analyzed include the spleen, lungs and intestines.

IMINO-BIS-(METHYL PHOSPHONATE) (IBMP): A NEW BIFUNCTIONAL CHELATE FOR Tc-99m. EFFECT OF FATTY ACID SUBSTITUTION ON BIODISTRIBUTION IN RATS

R. F. Schneider, G. Subramanian, J. G. McAfee, C. Zapf-Longo, E. Palladino T. Feld, and F. D. Thomas.

S.U.N.Y., Upstate Medical Center, 750 E. Adams Street, Syracuse, NY 13210.

A new bifunctional chelating group, iminobis (methyl phosphonate) was incorporated into a series of fatty acids and compounds of the general formulae.

$\text{HOOC}-(\text{CH}_2)_n - \text{N} (\text{CH}_2\text{PO}_3\text{H}_2)_2$ ;  $n = 1, 3, 5, 7, 11, 15, 17$  were synthesized.

Terminal amino fatty acids up to chain length  $n=11$  were obtained from commercial sources.\* The 16-amino hexadecanoic acid ( $n = 15$ ) was prepared by treating the 16-hydroxy fatty acid with HBr to obtain 16 Br-hexa-decanoic acid derivative. Reaction with excess ammonium hydroxide yielded the required amino acid. The 18-amino octadecanoic acid ( $n = 17$ ) was prepared by a multistep synthesis similar to that described by DeVries(1). The terminal amino fatty acids were reacted with formaldehyde and phosphorous acid in acidic media to obtain the required IBMP's (Mannich type reaction, see Moedritzer(2)).

The structure of the above compounds were verified using IR, NMR and other standard analytical techniques. These agents were then labeled quantitatively with Tc-99m using stannous tin reduction technique (kit method) and their biodistribution was studied in male Sprague-Dawley rats.

None of these agents localized well in the myocardium (0.3-0.5%). As the chain length increased beyond  $n=7$ , there was considerable activity present in the blood. The bone (including marrow) concentration increased to about 35% of injected dose for the compound  $n = 7$  and decreased to a low level of 5% at for  $n = 17$ . The hexadecanoic acid derivative concentrated well in the kidneys 20-25% at 15'-30'. The short chain derivatives were excreted predominantly in the urine (44-57% @ 1 hr.) compared to 7-8% for the longest one.

Thus for the short chain length ( $n = 1-7$ ) fatty acid compounds, the methyl phosphonate moiety strongly influenced the biodistribution. However for the longer derivatives the fatty acid group dictated the organ localization.

\*Aldrich Chemicals

(1) DeVries, V.G., Moran, D.B., Allen, G.R. et al J. Med. Chem. 19,946(1976)

(2) Moedritzer, K., Irani, R.R. J. Amer. Chem. Soc. 31,1603(1966)





DEVELOPMENT OF A RELIABLE  $^{195m}\text{Hg}$ - $^{195m}\text{Au}$  GENERATOR

C. Brihaye, M. Guillaume, N. Lavi, and M. Cogneau.

Centre de Recherches du Cyclotron, Université de Liège  
Sart Tilman - 4000 LIEGE - Belgium.

A mercury- $^{195m}$  — gold- $^{195m}$  generator has been developed which allows the elution of 30.6 sec-gold- $^{195m}$  from its 41h-mercury- $^{195m}$  parent with an injectable solution of glucose, buffered at pH 7.7 with Tris (hydroxy) methylaminomethane. The exchanger is the chelating resin chelex 100.

The mercury- $^{195m}$  is obtained by bombardment of gold with 35 MeV protons and the separation of the mercury from the gold target (1, 2) is carried out by complete volatilisation of the mercury isotopes at 950° C. The carrier-free mercury is swept by an argon stream into concentrated nitric acid.

The resulting solution is neutralized to pH 7.7 (25°C) with a 2 M Tris solution. After the addition of 70 g of gold carrier and 0.5 mg of mercury carrier, the solution is slowly passed through a chelex 100 column previously equilibrated with a  $10^{-2}$  M Tris solution at pH 7.7. After washing,  $\text{Au}^{195m}$  is eluted with a 5% glucose solution buffered with  $5.10^{-2}$  M Tris at pH 7.7 (25°C).

The variation of the distribution coefficients of Hg and Au on chelex 100 in nitrate solution as a function of pH shows that both ions (Hg and Au) are strongly fixed on chelex at pH 7.7, but the kinetics of gold fixation is slow, allowing the elution of this ion. The yield of  $^{195m}\text{Au}$  eluted expressed as percentage of the theoretical maximum is 40 % at a flow rate of 12 ml/min and the mercury breakthrough defined as the percentage of parent activity detected in one ml of the eluate is  $8.10^{-4}\%$ /ml at the same flow rate. These parameters remain constant for eluent volume of up to 3 liters. The study of the biodistribution of gold in rats was performed by means of  $^{193}\text{Au}$  (17.6h) eluted from a similar generator  $^{193m}\text{Hg}$  —  $^{193}\text{Au}$ . This study showed that the (11.1h) eluted gold is vascular for a period of 1 hour.

(1) Crouzel C., Petitjean F., Comar D. et al., Radiochem. Radioanal. Letters, 27, 185 (1976).

(2) Parker W., Nucl. Inst. Meth., 8, 354 (1960).

CROSS SECTIONS FOR PHOTON INDUCED NUCLEAR REACTIONS

C.N.M. Bakker, G.A. Brinkman, B.W. van Halteren, D. de Jong, and J. Visser. Chemistry Department, National Institute for Nuclear Physics and High Energy Physics (NIKHEF, section K (former IKO)), P.O. Box 4395, 1009 AJ Amsterdam/The Netherlands.

Cross sections per equivalent quantum ( $\sigma_q$ ) have been determined for the formation of a series of isotopes which are of interest for hot atom chemistry research and for application in organic chemistry, biochemistry and nuclear medicine.

- a) relative  $\sigma_q$  values were measured for composite targets of C, N, O and of C, F, Cl for ( $\gamma, n$ ) reactions leading to  $^{11}\text{C}$ ,  $^{13}\text{N}$ ,  $^{15}\text{O}$ ,  $^{18}\text{F}$  and  $^{34\text{m}}\text{Cl}$  with initial electron energies between 25 and 70 MeV. The data are in good agreement with measurements from Lund (1,2).
- b) absolute  $\sigma_q$  values were measured for the production of halogen and rare gas isotopes for  $\gamma(xp, yn)$  reactions on several targets with initial electron energies around 100 MeV. These data are in good agreement with relative measurements from Kato *et al.* (3) and with calculated values.

- (1) Hyltén, G., Nucl. Phys. A158, 225 (1970).
- (2) Friberg, B., Anderson, G., Fortman, B., Nucl. Phys. A171, 551 (1971).
- (3) Kato, T., Masumoto, K., Sato, N., Suzuki, N., J. Radioanal. Chem. 32, 51 (1976).

201-Tl PRODUCTION STUDIES BY 203-Tl(p,3n)201-Pb and 202-Hg(p,2n) NUCLEAR REACTIONS

C. Birattari, M. Bonardi, and A. Salomone.

Istituto di Fisica, Cyclotron Laboratory, via Celoria 16, 20133 Milano, Italy.

The Milan University AVF Cyclotron accelerates proton beams with variable energy up to 45 MeV. In the available proton energy range, 201-Tl can be produced either by 203-Tl(p,3n)201-Pb  $\rightarrow$  201-Tl (1,2,3) or by Hg(p,xn) nuclear reactions (2,4,5). Thin-target excitation functions for 201-Tl production by nat-Tl and 81% enriched 203-Tl targets have been measured in the 5 - 42 MeV proton energy range obtaining results in accordance with those found in the literature, within the experimental errors (6,7). With this method, the calculated yields for 201-Tl are 4.9 GBq/C and 14.3 GBq/C respectively for natural and 81% 203-Tl enriched targets, employing a target thickness of 8 MeV, at a bombarding proton energy of 27 MeV, if the first chemical separation (Tl/201-Pb) is performed at the end of an instantaneous bombardment (EOIB) and the second one (201-Pb/201-Tl) is performed 32 hours later. The contamination by 200-Tl and 202-Tl at this time is about 0.28% in both cases.

Thin-target excitation functions have been measured in the 10 - 36 MeV proton energy range for nat-Hg(p,xn) (5) and 98.6% enriched 202-Hg(p,xn) nuclear reactions. The results are shown in Figs. 1 and 2. According to these figures, using a Hg target of natural isotopic composition the minimum contamination level for 201-Tl is very high, anyway more than 15%. In case of 98.6% enriched 202-Hg target, 201-Tl calculated yield is, for example 24.9 GBq/C at the EOIB, for a 6 MeV target thickness at a bombarding proton energy of 19 MeV. This is the optimal situation from the point of view of the contamination, which is reduced to 3.4%, about 60 hours after the EOIB, with a residual yield of 14.2 GBq/C. In Table 1 are reported the yields for 201-Tl production from a 202-Hg enriched target of different thickness, evaluated at time tw(h) from the EOIB, when the contamination from other Tl radioisotopes (199,200, 202-Tl) is minimum, at the optimal 19 MeV incident proton energy.

TABLE 1 - Yields and contaminations for the production of 201-Tl from 202-Hg enriched targets of various thicknesses, evaluated at time tw from EOIB when the contamination from 199,200,202-Tl is minimum, for 19 MeV incident proton energy, with total proton energy absorption.

Target thickness (MeV)	tw(h)	201-Tl (GBq/C)	Contamination (%)
9	50	17.6	4.5
6	60	14.2	3.4
3	90	7.1	2.3

The behaviour of the total contamination level (%) obtainable with different incident proton energies is shown in Fig. 3 as a function of waiting time from the EOIB.

Radiochemical separations and quality controls

For the first production method, a radiochemical separation based on the precipitation of monovalent thallium target as thallos iodide in acetate buffer (pH 4.6) after complexation of lead by EDTA has been adopted (3). The second step (32 hours later) was carried out in accordance to a well known chromatographic method (8) with small modifications. The enriched thallium target recovery is quantitative (98%) and 203-Pb contamination in the final product is about 0.1% at the end of target processing (EOP). The total thallium carrier content is about 5 - 10  $\mu$ g.

For the second production method a very simple separation has been adopted, based on the washing by warm 3M HCl of the metallic mercury target and of the tantalum target holder, on which about 40% of radio-thallium adheres (5). After addition of NaOH 3M and dilution by water, a physiological solution with a pH value around 4 - 6 is obtained, with a specific activity in no-carrier-added form (NCA), greater than 1.5 GBq/ $\mu$ g of thallium, probably close to the theoretical carrier-free (CF) value of

7.8 GBq/ $\mu$ g(4,5).

Radiochemical quality controls have been carried out for both methods by paper radiochromatography in acetone/phosphate and n-butanol/HBr media, ensuring that 99.8 % of thallium is in the desired monovalent state (3,8).

In particular, high-specific-activity radio-thallium obtained by the Hg(p,xn) method self-reduces to the monovalent state in some ten hours from the EOP, even without the addition of reducing agents. In Fig. 4 the behaviour of the areas (%) of the three chromatographic peaks are shown as a function of waiting time from the EOP. Tl(I) peak percentage ( $R_f = 0.00$ ) increases sharply during storage of NCA radio-thallium in plastic vials in 3M HCl, while Tl(III) peak percentages ( $R_f = 0.62$ , 0.96) decrease to a value lower than 1 % after about 30 hours from the EOP. Tl(III) peak at  $R_f = 0.62$ , being probably a chlorocomplex, is destroyed if radio-thallium is spotted on the paper strip at a pH value around neutrality.

The chromatographic test mentioned above is quick, easy and reliable and ensures that  $^{201}\text{Tl}$  radiopharmaceutical obtained with this method is stable for a long time from the EOP, as thalious chloride.

- (1) Girardi F. et al., *Int. J. Appl. Radiat. Isotopes*, 26, 267 (1975).
- (2) Acerbi E. et al., Status report on the program of radioisotope production at the Milan AVF Cyclotron, Report of the Istituto Nazionale di Fisica Nucleare, INFN /TC-77/9, Frascati, Rome, Italy, 1977.
- (3) Bonardi M., *Radiochem. Radioanal. Letters*, 42, 35 (1980).
- (4) Sabbioni E., Goetz L., Birattari C. and Bonardi M., *Sci. Total Environ.*, 17, 257 (1981).
- (5) Goetz L., Sabbioni E., Marafante E., Edel-Rade J., Birattari C. and Bonardi M., *J. Radioanal. Chem.*, 67, 183 (1981).
- (6) Lagunas-Solar M. C., Jungerman J. A., Peek N.F. and Theus R. M., *Int. J. Appl. Radiat. Isotopes*, 29, 159 (1978).
- (7) Qaim S. M., Weinreich R. and Ollig H., *Int. J. Appl. Radiat. Isotopes*, 30, 85 (1979).
- (8) Lebowitz E. et al., *J. Nucl. Med.*, 16, 151 (1975).

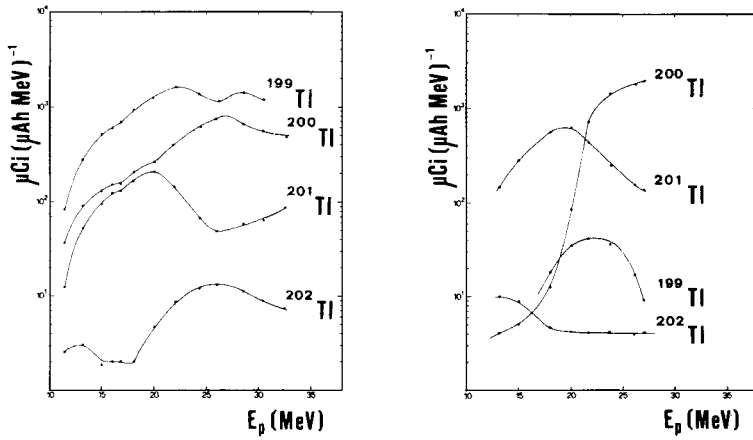


Fig. 1,2 - Excitation functions for (p,xn) nuclear reactions on natural and 98.6 % enriched  $^{202}\text{Hg}$  targets.

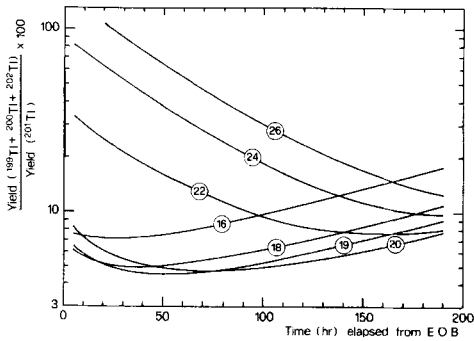
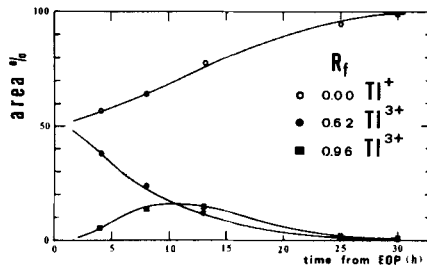


Fig. 4 - Behaviour of the three chromatographic peak areas (%) obtained after spotting the NCA radio-thallium from 3 M HCl solution, as a function of the waiting time from the EOP. Eluent: Acetone / Phosphate Radioscanning of Whatman n. 1 paper strips ( 14.5 cm ).

Fig. 3 - Behaviour of the contamination level (%) for  $^{201}\text{Tl}$  production from 98.6 % enriched  $^{202}\text{Hg}$  targets, as a function of incident proton energy with total proton energy absorption.



A COMPUTER-CONTROLLED AUTOMATIC APPARATUS FOR RADIOCHEMICAL SEPARATION OF  $^{75}\text{Br}$  AND SYNTHESIS OF  $^{75}\text{Br}$ -LABELLED RADIOPHARMACEUTICALS

---

G. Blessing, H.H. Coenen, M. Hennes, and H. Lipperts.  
 Institut für Chemie 1 (Nuklearchemie), Kernforschungsanlage Jülich GmbH, D-5170 Jülich, FRG.

The increasing significance of positron emission computed tomography (PECT) in diagnostic nuclear medicine calls upon large scale production of suitable  $\beta^+$ -emitters and preparation of biomolecules labelled with those radioisotopes. This, in general, demands:

- Routine production of the radioisotope (targetry) with high availability.
- Fast processing of the irradiated material, followed by synthesis of the radiopharmaceutical.
- Adaptability of the apparatus to various types of syntheses.
- Remote control of the apparatus to be able to cope with the high-level of starting radioactivity, preferably within a small lead cell.
- Reliable and automatic methods of production and synthesis to obtain good reproducibility.

In order to meet these requirements in connection with the production of  $^{75}\text{Br}$  ( $T_{1/2}$ : 1.6 h), an important  $\beta^+$ -emitter whose large-scale production has been developed at Jülich (1,2) using the  $^{75}\text{As}(^3\text{He},n)^{75}\text{Br}$  reaction, and which has found applications in PECT (cf. 3,4), we decided to automatise the production as well as the labelling procedure and to control the entire process with the help of a microcomputer. A flow-sheet of the process is shown in Fig. 1. The computer system consists of a KONTRON<sup>®</sup> microcomputer Model PS $\psi$ 80. The hardware as well as software were developed in the Institute. The software is stored on disks and the programs have been written in BASIC. The time-critical parts of the program have been written in ASSEMBLER. It uses the interrupt technique. In case of failure of a program manual service is always possible. The computer system is connected to the various components of the apparatus which are placed in the lead cell (an oven for  $^{75}\text{Br}$  separation, a carousel for the synthesis of the radiopharmaceutical, an HPLC system for quality control, etc.) via integrated interface technique. Fig. 2 shows schematically the control panels for the various stages involved in the complete preparation of a radiopharmaceutical. These are:

a) Separation of  $^{75}\text{Br}$

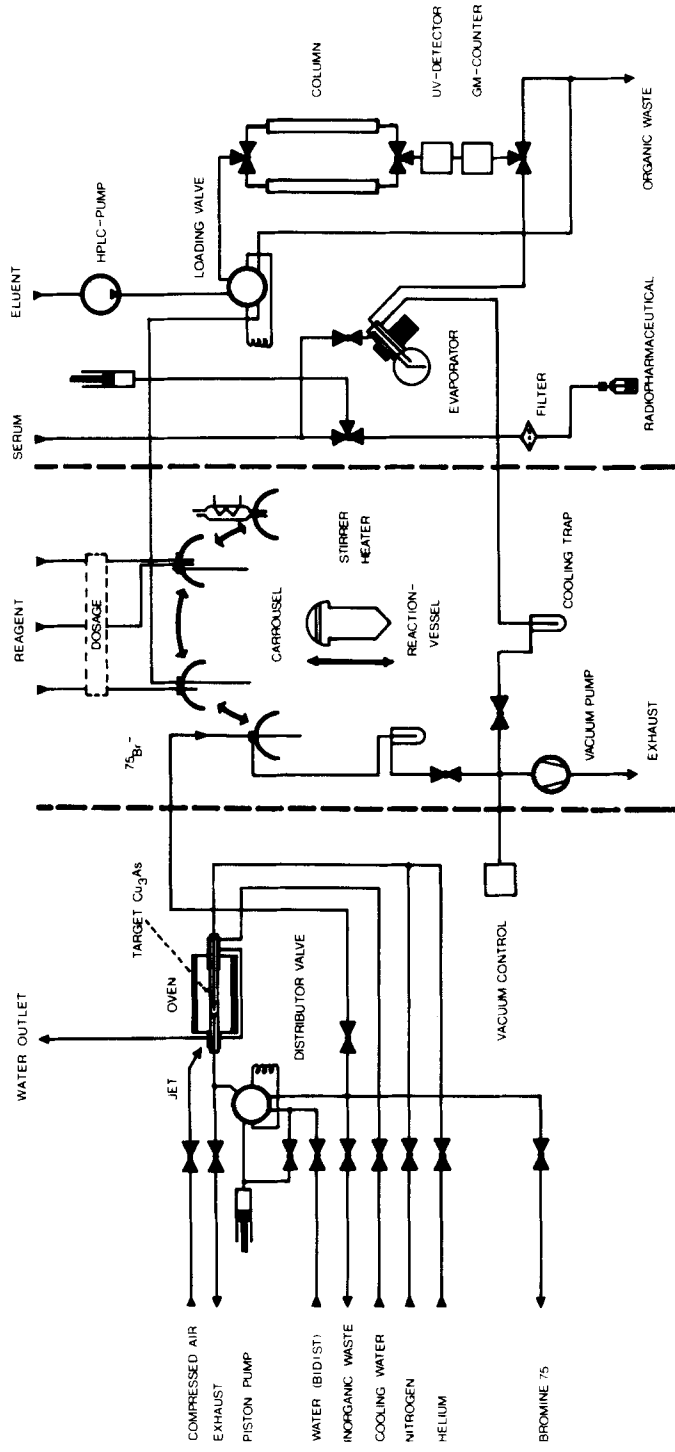
The irradiated  $\text{Cu}_3\text{As}$ -target is heated in an oven at  $800^\circ\text{C}$  in an inert gas flow atmosphere. Radiobromine is separated by thermochromatography and dissolved in water. Through the use of a specially-designed dosage pump the volume of the water is limited to  $500\ \mu\text{l}$ .

b) Synthesis of radiopharmaceutical

Following the initial separation of radiobromine, the various steps involved in the chemical synthesis of a radiopharmaceutical (such as addition of reagents, refluxing, aliquoting, etc.) are carried out using a carousel system. The reaction vessels can be moved both horizontally and vertically. The vacuum tight connections are achieved using pneumatically-controlled lifts. The carousel system avoids the use of valves and long connecting tubes, thereby reducing the dead volumes drastically.

# FLOW-SHEET OF THE COMPUTER CONTROLLED <sup>75</sup>Br-SEPARATION AND LABELING DEVICE

Fig. 1



ISOLATION OF BROMINE-75

SYNTHESIS

QUALITY CONTROL



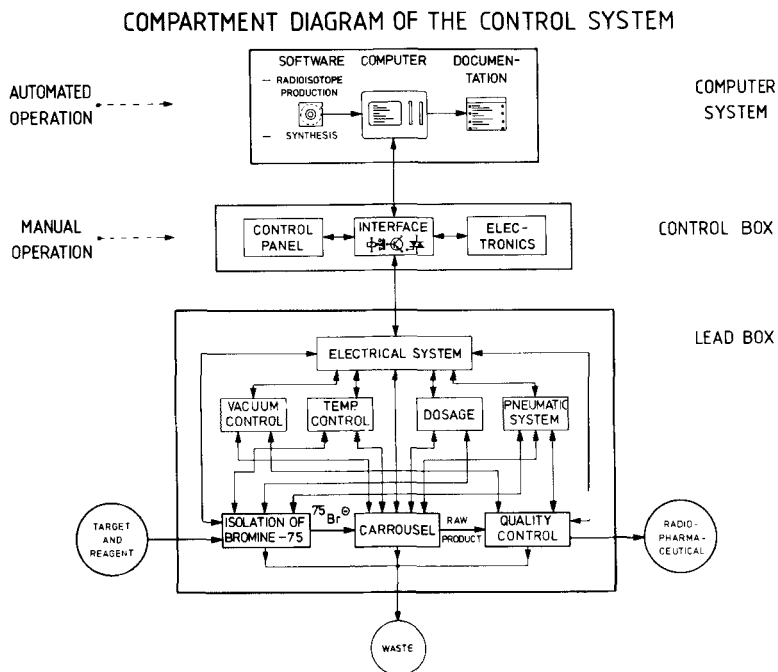


Fig. 2 Compartment diagram of the control system for complete synthesis of a  $^{75}\text{Br}$ -labelled radiopharmaceutical.

### c) Quality control

After the synthesis the reaction mixture is pressed into the injection block of a high-pressure liquid chromatograph (HPLC). After separation the active peak is cut off and the liquid collected in an evaporator. The subsequent dissolution of the radiopharmaceutical in blood serum as well as filtration for achieving sterility is carried out in a special apparatus.

The separation of radiobromine from the irradiated target presently requires about 30 min but it may be further reduced. The time needed for synthesis depends on the type of the radiopharmaceutical. For  $^{75}\text{Br}$ -labelled phenyl fatty acid, for example, it was about 2 h and the yield of the end product was about 3 mCi.

We thank Prof. G. Stöcklin and Dr. S.M. Qaim for their active support of this work and for fruitful discussions.

- (1) Weinreich R., Alfassi Z.B., Blessing G. and Stöcklin G., Proc. 17th Int. Annual Meeting of Soc. Nucl. Medicine, Innsbruck, 1979, p. 209.
- (2) Blessing G., Weinreich R., Qaim S.M. and Stöcklin G., Int. J. appl. Radiat. Isotopes, 33, 333-339 (1982).
- (3) Coenen H.H., Harmand M.F., Kloster G. and Stöcklin G., J. nucl. Med., 22, 891-896 (1981).
- (4) Friedman A.M., Huang C.C., Kulmala H., Dinerstein R. and Brunsten B., J. nucl. Med., 22, P73 (1981).

PRODUCTION YIELDS OF  $^{11}\text{C}$ ,  $^{13}\text{N}$ ,  $^{15}\text{O}$  AND  $^{18}\text{F}$ , ESPECIALLY WITH SMALLER ACCELERATORS

M. Anwar Chaudhri.

Department of Medical Physics, Austin Hospital, Heidelberg, Victoria 3084, Australia and Department of Medicine at Austin, University of Melbourne.

From experimentally measured excitation functions, and tabulated range-energy data, thick target yields at saturation for production of  $^{11}\text{C}$ ,  $^{13}\text{N}$ ,  $^{15}\text{O}$  and  $^{18}\text{F}$  through different nuclear reactions, have been computed over a wide range of incident energies. Yield curves have been plotted from which the production rate of any one of these isotopes can be directly read for given bombarding conditions (incident energy and intensity) and the target thickness.

The reactions and the corresponding energy ranges included in this work are :

(A) Carbon-11

$^9\text{Be}$	$(^3\text{He}, n)$	2-30 MeV
$^9\text{Be}$	$(\alpha, 2n)$	2-17 MeV
$^{10}\text{B}$	$(d, n)$	1-12 MeV
$^{10}\text{B}$	$(^3\text{He}, d) + ^{10}\text{B} (^3\text{He}, pn)$	5-27 MeV
$^{11}\text{B}$	$(p, n)$	3-12 MeV
$^{11}\text{B}$	$(d, 2n)$	7-20 MeV
$^{11}\text{B}$	$(^3\text{He}, t)$	5-30 MeV
$^{12}\text{C}$	$(d, t)$	16-21 MeV
$^{12}\text{C}$	$(^3\text{He}, \alpha)$	3-30 MeV

(B) Nitrogen-13

$^{11}\text{B}$	$(^3\text{He}, n)$	7-18 MeV
$^{12}\text{C}$	$(d, n)$	1.5-20 MeV
$^{12}\text{C}$	$(^3\text{He}, d) + (^3\text{He}, pn)$	6-30 MeV
$^{14}\text{N}$	$(^3\text{He}, \alpha)$	3-30 MeV

(C) Oxygen-15

$^{12}\text{C}$	$(\alpha, n)$	12-22 MeV
$^{14}\text{N}$	$(d, n)$	0.6-6 MeV
$^{14}\text{N}$	$(^3\text{He}, d)$	7-17 MeV
$^{16}\text{O}$	$(^3\text{He}, \alpha)$	4-9 MeV

(D) Fluorine-18

$^{16}\text{O}$	$(^3\text{He}, p)$	3-10 MeV
$^{19}\text{F}$	$(^3\text{He}, \alpha)$	4-30 MeV
$^{20}\text{Ne}$	$(d, \alpha)$	2-20 MeV
$^{20}\text{Ne}$	$(^3\text{He}, p)$	4-30 MeV

The calculated yields have been compared to experimental yields (where available).

This comprehensive data would help in selecting the most suitable reaction and the bombarding conditions for producing a particular isotope, and to check the efficiency of the production facility. Moreover, it would also provide information regarding the extent of any possible undesirable activity being produced simultaneously along with the isotope of interest, and help in reducing this unwanted isotope by manipulation of the bombarding conditions.

**THEMAL CHARACTERISTICS OF THE RELEASE OF FLUORINE-18 FROM AN INCONEL-600 GAS TARGET****J.C.Clark and F.Oberdorfer.**

Medical Research Council, Cyclotron Unit, Hammersmith Hospital, London W12.

Several publications dealing with no carrier added syntheses of radiopharmaceuticals containing fluorine have made only brief mention of the methods by which the "anhydrous no-carrier-added HF-18" was prepared(1,2). A patent(3) refers to the recovery of F-18 in an unspecified chemical form after deuteron irradiation of a neon-filled nickel target is followed by a hydrogen purge whilst heating to 900 C. Inconel(4), Monel(5) and copper(6) have also been proposed as constructional materials for neon targets to be operated in the anhydrous no-carrier-added mode. The target (internal dimensions 162x50mm) used in this study was fabricated from Inconel-600 using the tungsten-arc inert gas welding process (T.I.G.) and Inconel filler metal 82(7). The walls were polished using silicon carbide paper and water as a lubricant. Heating was achieved using a 1.25KW ceramic knuckle band heater on the target barrel and a 0.35KW annular ring heater on the window flange. With the ceramic fibre lagging (as shown in Fig.1) conditions of minimal temperature gradients were demonstrated on the inner surface of the target by thermocouple scanning. A 25mm diameter 0.050mm thick Inconel-625 entry window was sealed to the target vessel using a 3mm square section soft copper ring. Before filling with target gas mixtures the target was treated in two alternative ways.

a) Target heated to 500 °C under a neon flow of 100ml/min and allowed to cool isobarically.

b) Target heated to 500 °C under a hydrogen flow of 100ml/min and allowed to cool isobarically.

Hydrogen concentrations were varied between 10 and 20 volumes % in neon and target filling pressures were typically 200psig. Irradiations were carried out with 16MeV deuterons for approximately 1µamp.h. at 2 to 3µamp. After irradiation the target was removed from the cyclotron to a hot cell where the target gas was released through a potassium carbonate trap with no observed loss of F-18. Valve V4 Fig.1 was removed and a 1/8 inch PTFE tube together with a PTFE coil trap were connected to the target outlet. Dry oxygen-free hydrogen was then passed through the target at a flow rate of 250ml/min whilst the target was heated to a preselected maximum temperature of 700 °C. The PTFE outlet connection was held at below 150 °C by forced air cooling and the PTFE coil cooled to -78 °C. As shown in Fig.2 the release of F-18 starts between 80 °C and 140 °C when the target was pretreated with hydrogen and between 200 °C and 400 °C when the target was pretreated with neon. The recovery profile also strongly depends on the neon to hydrogen ratio in the irradiated mixture; the starting temperature decreases with increasing amounts of hydrogen. This is possibly due to direct formation of HF-18 during the irradiation. The decrease in the recovery temperature observed after hydrogen pretreatment is probably the result of HF-18 formation at the hydrogen-saturated Inconel wall. Another important observation, which may lead to a better understanding of the chemical processes and kinetics of F-18 removal from a target wall, refers to the situation of low hydrogen concentration in the target gas and the pretreatment with neon (run 5 Fig2b). Here temperatures in excess of 500 °C were reached before any F-18 was recovered. Thus the temperature must be related to the activation temperature for the thermal desorption of the fluorine atoms from the target wall; these reactive fluorine atoms then combine with the hydrogen purge gas to form HF-18.

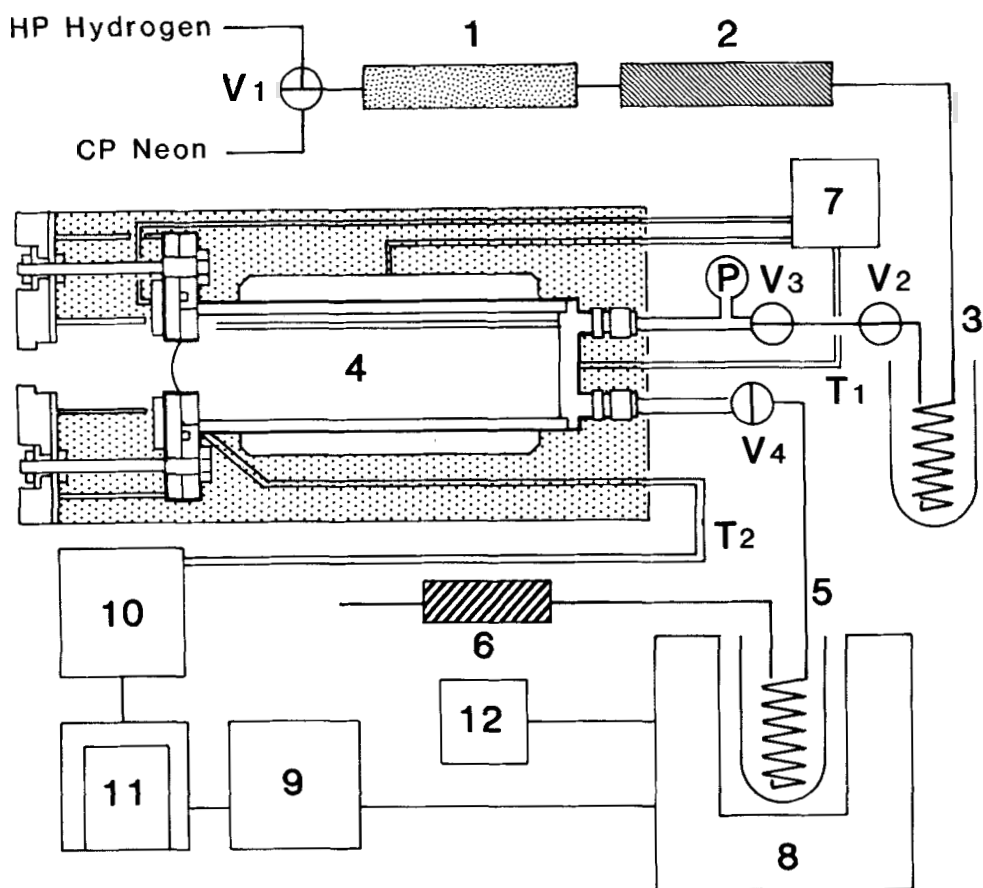


Figure 1

(1) Palladium catalyst (Engelhard "Deoxo Model-D") 150x25mm. (2) Magnesium perchlorate 150x25mm. (3) Copper trap  $-196^{\circ}\text{C}$ . (4) Inconel target vessel with heaters and thermocouples T1 and T2 for temperature control and monitoring. (5) PTFE trap 400x3mm OD coil  $-78^{\circ}\text{C}$ . (6) Potassium carbonate trap (for checks on the efficiency of trap 5). (7) Temperature controller. (8) Shielded re-entrant ionisation chamber. (9) DC Amplifier. (10) Thermocouple conditioning amplifier. (11) Dual channel recorder. (12) Ionisation chamber polarising supply.

These preliminary results from extraction studies of F-18 from the target system described could be interpreted in terms of model calculations for heterogenous fluorine atom reactions on metal surfaces(8). Further problems relating to the kinetics of adsorption and desorption processes of fluorine atoms highly diluted in an inert medium are presently under investigation at The German Cancer Research Center using a model based on the Langmuir-Rideal mechanism(9). This model agrees very well with our observations on the removal of F-18 from the target walls. We suggest that the following reactions give rise to observations described here.

- (I)  $F-18 + HH = HF-18 + H$ .
- (II) ADSORBED F-18 + DISSOLVED HH = DESORBED HF-18.
- (III) ADSORBED F-18 + (T>400 C) = DESORBED F-18 + HH = HF-18 + H.

- (1) Tewson T.J., Welch M.J. and Raichle M.E., J. Nucl. Med., 19, 1339 (1978).
- (2) Tewson T.J., Maeda M. and Welch M.J., J. Label. Compds. Radiopharm. 18, 21 (1981).
- (3) Winchell H.S. et al., U.S. Patent 3981769 (1976).
- (4) Wolf A.P., Personal communication.
- (5) Welch M.J., Personal communication.
- (6) Dahl J.R. et al., J. Label. Compds. Radiopharm., 18, 34 (1981).
- (7) "Wiggin welding products". Publications 3489 (1973) and 3591 (1978), Henry Wiggin and Co.Ltd.
- (8) Jumper E.J., Ultee C.J. and Dorko E.A., J. Phys. Chem. 84, 41 (1980).
- (9) "Chemical Kinetics" Laidler K.J. 2nd.ed. Chapter 6. McGraw Hill, New York (1965).

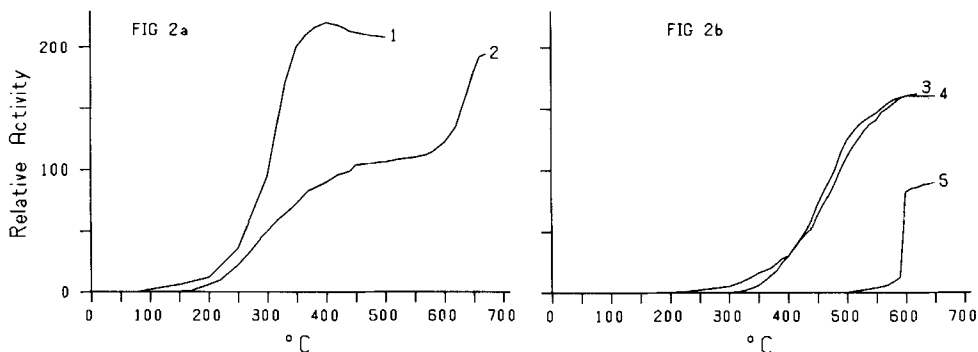


Figure 2a. Target pretreated with hydrogen at 500°C. Runs 1 and 2 15 volumes % hydrogen in neon.

Figure 2b. Target pretreated with neon at 500°C. Runs 3 and 4 15 volumes % hydrogen in neon. Run 5 <10 volumes % hydrogen in neon.

CONSIDERATIONS IN THE REUSE OF ENRICHED STABLE TARGET MATERIALS

R. D. Finn, J. P. Dwyer, K. K. Koh, A. Rodon, Y. Sheh, J. S. Sinnreich, and P. M. Smith.

Cyclotron Facility, Mount Sinai Medical Center, Miami Beach, Florida 33140.

The application of compounds incorporating various short-lived radionuclides to the diagnosis of human diseases is a rapidly growing modality. The biomedical investigations, as a result of various technological improvements, constantly places stringent demands on cyclotron-produced radionuclides. Although pharmaceutical quality control has often been emphasized (1), the measurement and compliance to strict radionuclidic purity is of prime importance.

The need for using large quantities of enriched stable nuclides has placed additional responsibilities on the cyclotron physicists and chemists, not only for the preparation of a chemically pure radiochemical, but also for the quantitative recovery of the scarce and expensive target material.

As an illustrative example of the subtleties encountered in this facet of synthesis, the results of our several years of experience in the preparation of gallium-67 from enriched zinc-68 metallic targets will be presented. The losses of enriched materials throughout the production cycle, and the apparent decrease in enrichment (Table 1) will be discussed. Thick target yields and cross sectional data from various research groups will be compared.

- (1) K. A. Krohn and A.-L. Jansholt, *Int. J. Appl. Radiat. Isotopes*, 28, 213-227(1977).

T A B L E 1

	Natural	Original Composition (1/78)	Final Composition* (2/82)	Difference	Estimated Incorporated Natural Zinc
Zn-64	48.9	0.42 ± 0.2	2.70 ± 0.1	2.3 ± 0.3	4.3 ± 0.6
66	27.8	0.35 ± 0.15	1.53 ± 0.1	1.16 ± 0.25	4.2 ± 0.9
67	4.1	0.20 ± 0.05	0.32 ± 0.05	0.12 ± 0.1	3.0 ± 3
68	18.6	98.8 ± 0.2	95.39 ± 0.2	3.4 ± 0.4	3.4 ± 0.4
70	0.6	0.02 ± 0.02	0.06 ± 0.01	0.04 ± 0.03	6.5 ± 4.7

\*The analyzed solution was mixed with new material (> 99%) and the actual old material might have been lower in purity than the above table indicates.

FLUORINE-18 LABELLED XENON DIFLUORIDE

G. Firnau, R. Chirakal, G. Schrobilgen, and E.S. Garnett.

Departments of Nuclear Medicine and Chemistry, McMaster University, Hamilton, Ontario, Canada. L8N 3Z5.

A convenient procedure for the rapid synthesis of F-18 labelled XeF<sub>2</sub> was developed. Neon gas with 0.5 to 5% carrier fluorine was irradiated with deuterons to produce [<sup>18</sup>F]F<sub>2</sub> (17 mCi/uA h,EOB), which was, in turn, reacted with molar excess of xenon in a specially constructed nickel reactor(1). The reactor was heated to 400°C for half an hour. The isolated reaction product was shown to be XeF<sub>2</sub> exclusively. The table shows the production yields and the specific activities. The production yield is independent of carrier fluorine between 1 and 5%.

[<sup>18</sup>F]Xenon difluoride will be a versatile intermediate for the synthesis of F-18 labelled radiopharmaceuticals: for example, 2-fluoro-2-deoxy-glucose (2) and aromatic compounds (3,4,5). [<sup>18</sup>F]2-Fluoro-2-deoxy-glucose was obtained in 20% yield (with respect to [<sup>18</sup>F]XeF<sub>2</sub>, corrected for decay).

Table of Yields (F-18 decay corrected to EOB)

Run	[ <sup>18</sup> F]F <sub>2</sub> started		[ <sup>18</sup> F]XeF <sub>2</sub> isolated			
	% F <sub>2</sub> in Ne	mCi	Chem. yield %	Radio-chem. yield %	Production rate mCi/uAh	Spec.Act. mCi/mmol
1	5	79	76	70	12.5	40
2	1	87	80	62	11.0	193
3	1	116	43	52	9.3	401
4	1	152	68	68	12.1	451
5	0.5	45	30	43	7.7	390

- (1) Falconer W.E. and Sunder W.A., J. Inorg. Nucl. Chem., 29, 1380 (1967).
- (2) Korytnyk W. and Valentekovic-Horvat S., Tetrahedron Lett., 21, 1493 (1980).
- (3) Filler R., Isr. J. Chem., 17, 71 (1978).
- (4) Schrobilgen G., Firnau G., Chirakal R. and Garnett E.S., J.C.S. Chem. Comm., 198 (1981).
- (5) Firnau G., Chirakal R., Sood S. and Garnett, E.S., Can. J. Chem., 58, 1449 (1980).



INTERFEROMETRIC STUDIES OF THE INFLUENCE OF AN INTENSE ION BEAM ON HIGH PRESSURE GAS TARGETS

S.-J. Heselius, P. Lindblom, and O. Solin.  
Department of Physics, Åbo Akademi, Porthansg. 3,  
SF-20500 Turku 50, Finland.

In the production of radionuclides from gas targets a non-linear relationship between radionuclide yield and particle beam current at a fixed particle entering energy has been observed (1-3). One of the reasons for this non-linearity is density reduction in the beam volume of the target gas when the beam current is increased (1-3). There is a lack of information on the effects causing the density reduction (3).

Interferometric studies of the influence of an intense ion beam on high pressure gas targets have been made (4). A double-windowed target chamber equipped with optical windows (Melles Griot B.W., 02 WBK 009) was used. The irradiations were carried out with the Åbo Akademi 103 cm isochronous cyclotron (18 MeV protons, external beam of 50  $\mu$ A current). Helium, neon and argon gas targets at 420-960 kPa pressures were bombarded with protons, deuterons and alpha-particles in the energy range 2-18 MeV. The particle beam was collimated by an aperture of 1.5 mm diameter before entrance into the target chamber.

Through an interferometric arrangement (Fig. 1), using a He-Ne laser, interferograms of the target gas were recorded showing variations in the refractive index of the gas caused by the particle beam. The He-Ne laser beam is transformed by a focusing lens to a spherical light beam; this is split into two light beams by the beam splitter. The light beam is collimated by the paraboloidal mirror and sent through the target chamber. The plane mirror reflects the light beam back through the target chamber on to the paraboloidal mirror which in turn transforms the returning light beam to a convergent spherical light beam. This light beam interferes with the reference light beam from the spherical mirror and the interferograms are recorded photographically. The camera lens focuses an image of the target chamber on the film plane. When the interferometer is properly adjusted, the recorded interferograms map the variations in optical path length caused by the particle beam.

By measuring the position of the interference fringes in the vertical plane from the bottom to the top of the chamber, a cross-sectional plot of the variation in optical path length in relation to the conditions at the bottom can be made. At each fringe a constant increment in the ordinate is made corresponding to  $\lambda/2$  in the optical path length. The obtained diagrams of fringe number against vertical fringe position for Ar at 675 kPa initial pressure bombarded with 17.7 MeV alpha-particles of 1-6  $\mu$ A beam current are shown in Fig. 2. As can be seen, an almost linear change takes place in the beam region showing an upward increasing density reduction in the beam.

With the help of photographs taken of the beam in the light

emitted by atoms of the target gas the temperature in the target can be estimated from the interferograms. Figure 2 shows the temperatures calculated for Ar at 675 kPa bombarded with 17.7 MeV alpha-particles. The interferograms show that there is a strong upward gravitational transport of the heated gas in the target chamber.

This work has been partly sponsored by the Finnish Academy of Sciences and by the Swedish Academy of Engineering Sciences in Finland.

- (1) Oselka M., Gindler J.E. and Friedman A.M., *Int. J. Appl. Radiat. Isotopes* 28, 804 (1977).
- (2) Casella V., Ido T., Wolf A.P., Fowler J.S., MacGregor R.R. and Ruth T.J., *J. Nucl. Med.* 21, 750 (1980).
- (3) Wieland B.W., Schlyer D.J., Ruth T.J. and Wolf A.P., *J. Labelled Comp. Radiopharm.* 18, 27 (1981).
- (4) Heselius S.-J., Lindblom P. and Solin O., Manuscript accepted for publication, *Int. J. appl. Radiat. Isotopes*.

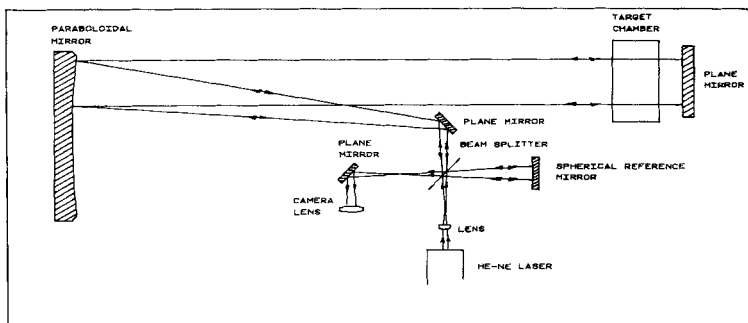


Fig. 1. Interferometric arrangement (4).

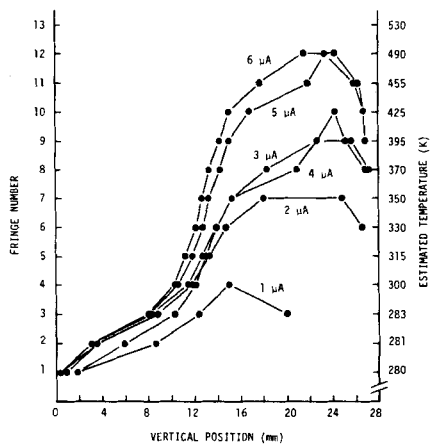


Fig. 2. Fringe number and estimated temperature as function of vertical position in an Ar target at 675 kPa initial pressure bombarded with 17.7 MeV alpha-particles of 1.0 - 6.0  $\mu\text{A}$  beam current (4).

A POSITRON DETECTOR SUITABLE FOR AUTOMATED RADIOPHARMACEUTICAL PRODUCTION

R.D. Hichwa and C. Tsang. Division of Nuclear Medicine, University Hospital, Box 21, University of Michigan, Ann Arbor, MI 48109.

A low cost, low voltage, positron detection system has been developed to aid in the automated synthesis of short-lived cyclotron produced radiopharmaceuticals.

The detector consists of a disk of rare earth x-ray intensifier screen (2.5mm dia.) optically coupled to an integral silicon photodiode and operational amplifier (1). Plastic scintillators (NE-102, NE-110) and other intensifier screens ( $\text{CaWO}_4$ ,  $(\text{ZnCd})\text{S}$ ) were investigated as possible  $\beta^+$  scintillators; however, the gadolinium ( $\text{Gd}_2\text{O}_2\text{S}$ ) screen produced the greatest light output while providing the best match of the intensifier screen emissions to the photodiode spectral response (2,3). Operation depends upon a useful signal-to-noise ratio and ranges from a lower limit of 0.5 mCi to an upper bound of greater than 100.0 mCi of  $\beta^+$  activity.

The entire system is designed to be installed in a hot-cell or shielded chemical hood and operated in a highly radioactive and corrosive environment. The large  $\gamma$ -ray background from positron annihilation is effectively eliminated by combining the outputs of two such detectors into a low noise, high gain, differential operational amplifier (4). Light from gammas impinging upon the intensifier screen as well as direct high energy photon interactions with the 5.0 mm<sup>2</sup> active diode area contributes to the background signal (5,6). A 0.5 mm thick lead absorber placed in front of one detector attenuates the positron flux by  $10^4$  while having little effect on the 0.511 MeV  $\gamma$ -rays. The high common mode rejection of the differential amplifier for the gamma noise present at the output of both detectors allows determination of the  $\beta^+$  signal.

The optical detectors, intensifier screens,  $\beta^+$  absorber and op-amp are mounted in a small aluminum box fashioned from square aluminum tubing (19.0 mm x 19.0 mm x 50.0 mm). A 6.4 mm slot in the box between the detectors facilitates clamping the unit to the appropriate chemical plumbing. Positron activity is assessed in the tube volume viewed by the detector pair. Large quantities of Pb shielding about the detectors are unnecessary. Shielding of the detector system provided by the 3.2 mm Al wall tubing is sufficient to permit quantitation of local  $\beta^+$  activity at any point in the radiopharmaceutical synthesis apparatus. A single low voltage supply operating at +15.0 V provides sufficient power to operate several detectors simultaneously. The analog outputs corresponding to the positron activity are then routed to a multiplexed analog-to-digital converter (ADC) which in turn is interfaced to a microcomputer. Real-time processing of the  $\beta^+$  activity, consistent with the radiopharmaceutical synthesis scheme, controls the procedure by optimizing the process flow rates and by synchronizing the addition of reagents as well as the simpler tasks of heating, cooling and drying.

These positron detectors, enhanced by their compact design and relative  $\gamma$ -ray immunity, supply input to a multifaceted automated radiopharmaceutical production system. Their incorporation into automated laboratory chemistry enables the radiochemist to pass the burden of routine production to the realm of high technology and computers thereby freeing valuable time to explore new research avenues.

- (1) Devar 529-2-5, Devar Inc., Control Products Division, 706 Bostwick Ave., Bridgeport, CT 06605.
- (2) Coltman J.W., Ebbighausen, E.G. and Altar W., J. Appl. Physics, 18, 530 (1947).
- (3) Ludwig G.W., J. Electrochem. Soc: Solid State Science, 118, 1152 (1971).
- (4) National Semiconductor LM 363, National Semiconductor Corporation, 2900 Semiconductor Drive, Santa Clara, CA 95051
- (5) Melchior H., Physics Today, 30, 32 (1977).
- (6) Wiczler J.J., Dawson L.R. and Barnes C.E., IEEE Trans. Nucl. Sci., NS-28, 4397 (1981).

## AUTOMATED PHOTOSYNTHESIS OF $^{11}\text{C}$ -GLUCOSE

K. Ishiwata, M. Monma, R. Iwata, and T. Ido  
Cyclotron and Radioisotope Center, Tohoku University, Sendai, 980,  
Japan.

The positron-emitting carbon-11 labeled glucose is significantly useful in studying the *in vivo* metabolism of glucose. We synthesized a mixture of  $^{11}\text{C}$ -labeled glucose and fructose by the photosynthesis method of Lifton and Welch (1) with some modifications and have automated the whole procedure.

The system for the photosynthesis of  $^{11}\text{C}$ -glucose and  $^{11}\text{C}$ -fructose was shown in Fig. 1 and the sequence program of it is summarized in Table 1. Each step of the procedure is proceeded by using a timer, a limit switch or a photo-level sensor.  $^{11}\text{CO}_2$  was produced by the proton irradiation of  $\text{N}_2$  via the  $^{14}\text{N}(p,\alpha)^{11}\text{C}$  reaction using the Tohoku University cyclotron and was concentrated on Molecular Sieve 4A for 10-15 min. After heating it in a glass tube oven at  $250^\circ\text{C}$ ,  $^{11}\text{CO}_2$  was swept with about 100 ml of He into a first glass chamber preevacuated, in which spinach leaves (1g) were placed. The photosynthesis was carried out by illuminating with a day light lamp and cooling with a fan for 10 min and  $^{11}\text{CO}_2$  unabsorbed into leaves was wasted through a soda lime trap with a suction pump. 10 ml of 90 % ethanol was injected into the vessel by evacuating it with a suction pump and sugars were extracted by refluxing the mixture with a fan-heater for 7 min. The alcoholic extract was filtered with a glass sinter and transferred into the second vessel by suction. The first vessel was washed with 3 ml of 90 % EtOH and the washings was also transferred. After the extract was concentrated to about 2 ml, 2 ml of 2 M HCl was injected into it and sucrose was hydrolysed by boiling with a fan-heater for 4 min. The hydrolysate was filtered through SEP PAK C18 cartridges and an activated charcoal column (0.9x1cm) and transferred on AG 11A8 (self adsorbed form) column (0.9x10cm) equilibrated with  $\text{H}_2\text{O}$ . Above step was carried out with the pressure of He gas. Wash water (2 ml) was also loaded on a column. A mixture of  $^{11}\text{C}$ -glucose and  $^{11}\text{C}$ -fructose was eluted with  $\text{H}_2\text{O}$  by using a perista pump. The first 4 ml of effluent was discarded and the next 5-10 ml was obtained as a mixture of  $^{11}\text{C}$ -glucose and  $^{11}\text{C}$ -fructose and sterilized by a membrane filtration (0.22  $\mu\text{m}$ ).

Molecular Sieve 4A was activated before use and 85-95 % of  $^{11}\text{CO}_2$  was usually released from it. Spinach leaves absorbed 75-95 % of the  $^{11}\text{CO}_2$  and 70-80 % of the radioactivity in leaves was extracted in ethanol as sugars. Photosynthesis seemed to be more effective by using leaves placed in dark overnight. The final products were obtained with the radiochemical yield of 30-50 % within 60 min from the end of bombardment. The radiochemical purity of products was analyzed by high-performance liquid chromatography on a  $\mu\text{BONDAPAK}$ -Carbohydrate column (Fig. 2). About 90 % of the radioactivity was observed in  $^{11}\text{C}$ -glucose and  $^{11}\text{C}$ -fructose and two sugars were found to be present in a ratio of approximately 1 : 1. However, fructose tended to be more degradative in HCl-hydrolysis than glucose, so the ratio was more or less variable. An unknown radioactive material was eluted at 30 min and was found to be adsorbed on a cation-exchange resin (AG 50W). Small amounts of impurities, eluted before fructose, were also removed with an anion exchange resin (AG 1). For the

removal of pigments of leaves, we used SEP PAK C18 cartridges and charcoal instead of extraction in chloroform or ether (1), which enabled the in-line system. An ion retardation resin (AG 11A8) was used for the isolation of glucose and fructose from HCl and salts.

In the automated system the whole procedure is mainly controlled with timers except for the chromatography, which can not necessarily ascertain the completion of each step and is apt to be too time-consuming to process control. In the chromatographic system, though a mixture of  $^{11}\text{C}$ -glucose and  $^{11}\text{C}$ -fructose is collected empirically with a photo-level sensor, a in-line detector of radioactivity is of greater advantage. Although there is room for modification, our system can be used for the routine synthesis of a mixture of  $^{11}\text{C}$ -glucose and  $^{11}\text{C}$ -fructose.

(1) Lifton J.F. and Welch M.J., *Radiat. Res.*, 45, 35 (1971).

Table 1. Sequence Program of the Automated Photosynthesis System

Step No.	Action	Stepping Method
1.	Concentration of $^{11}\text{CO}_2$	Timer(10-15 min)
2.	Heating of Molecular Sieve 4A and transfer of $^{11}\text{CO}_2$ into the 1st vessel	Timer(2.5 min) Timer(1 min)
3.	Photosynthesis	Timer(10 min)
4.	Removal of $^{11}\text{CO}_2$	Timer(1 min)
5.	Injection of ethanol	Limit switch
6.	Extraction of sugar	Timer(7 min)
7.	Transfer of the extract to the 2nd vessel	Timer(1 min)
8.	Washing:Injection of ethanol	Limit switch
9.	Transfer to the 2nd vessel	Timer(1 min)
10.	Concentration of the extract	Timer(4 min)
11.	Injection of HCl	Limit switch
12.	Hydrolysis of sucrose	Timer(2 min)
13.	Transfer of the hydrolysate to columns	Photo-level sensor
14.	Fractionation	Photo-level sensor
15.	Washing:Injection of water	Limit switch
16.	Transfer to columns	Photo-level sensor
17.	Fractionation	Photo-level Sensor
18.	Fractionation with water	Photo-level Sensor
19.	End	

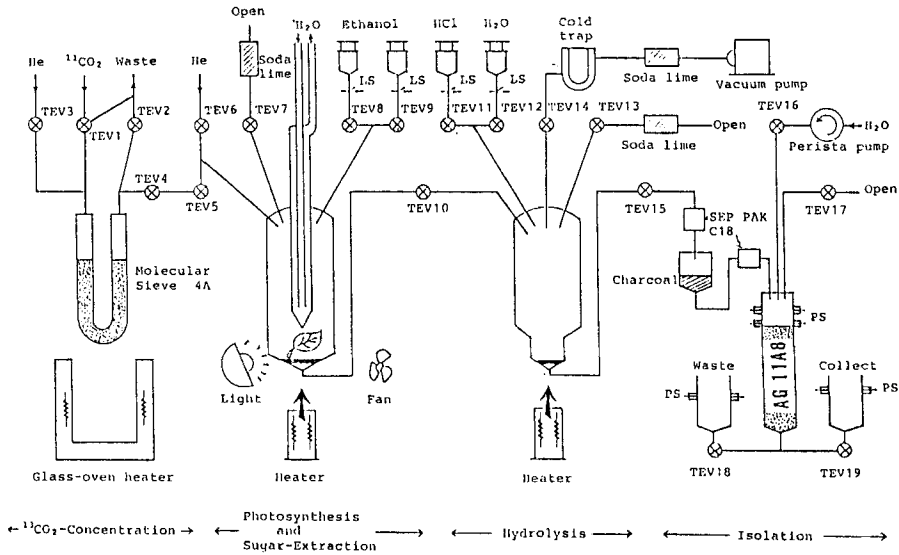


Fig. 1. System for the automated photosynthesis of a mixturer of  $^{11}\text{C}$ -glucose and  $^{11}\text{C}$ -fructose. TEV:teflon electric valve, LS:limit switch, PS:photo-level sensor

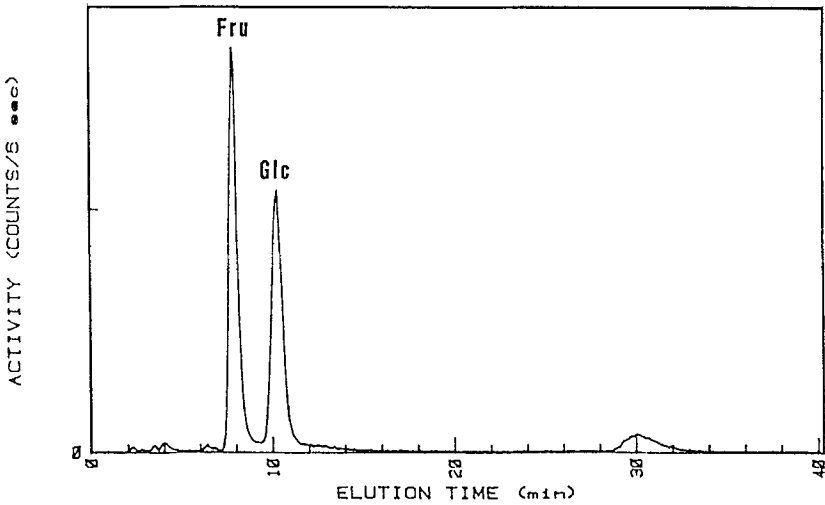


Fig. 2. High-performance liquid chromatography of the photosynthetic products on uBONDAPAK/Carbohydrate column. A 0.4x30 cm column was eluted with  $\text{CH}_3\text{CN}/\text{H}_2\text{O}$ (85/15) at a 2 ml/min of flow rate.

## FULLY AUTOMATED SYNTHESIS SYSTEM OF [ $^{18}\text{F}$ ]-2-DEOXY-2-FLUORO-D-GLUCOSE

---

R. Iwata, T. Takahashi, M. Shinohara, and T. Ido.

Cyclotron and Radioisotope Center, Tohoku University, Sendai, 980, Japan.

[ $^{18}\text{F}$ ]-2-deoxy-2-fluoro-D-glucose ( $^{18}\text{F}$ FDG) is well known as an excellent radio-pharmaceutical. For its frequent medical use, remote-controlled synthesis system has been developed(1,2). We have also started to develop the synthesis system as the fully automated one for the routine production without radiation hazard.

The conventional synthetic procedure(3) was used with some modifications for improving the radiochemical purity. It consisted of the following steps.

Step 1. Reaction of  $^{18}\text{F}\text{-F}_2$  with 3,4,6-tri-O-acetylglucal(TAG).

Step 2. Separation of isomeric  $^{18}\text{F}$ -difluoro adducts by column chromatography on silical gel.

Step 3. Collection of eluted  $^{18}\text{F}$ -difluoro adduct( $^{18}\text{F}$ -glucopyranosyl difluoride) and evaporation of solvent.

Step 4. Hydrolysis of  $^{18}\text{F}$ -difluoro adduct and purification by column chromatography on ion exchange resin, active charcoal and alumina.

Fig.1 shows the flow chart of the system for the automated processing of the former half of the above procedure(step 1 and 2). The gas and liquid flow was controlled with teflon solenoid valves. The liquids were transferred under He pressure. A photo-level sensor was used for detecting a liquid level in a glass vessel from outside as a stepping signal. Thus, the sequence listed in Table 1 could proceed by the signals from the four photo-level sensors.

The automation of the latter half of the procedure is now in progress. The fully automated synthesis system of  $^{18}\text{F}$ FDG controlled with a microcomputer will be presented.

### References

- (1) J.R.Barrio, *et al.*, J. Nucl. Med., 22, 372 (1981).
- (2) J.S.Fowler, *et al.*, J. Nucl. Med., 22, 376 (1981).
- (3) T.Ido, *et al.*, J. Lab. Comp. Radiopharm., 14, 174 (1978).



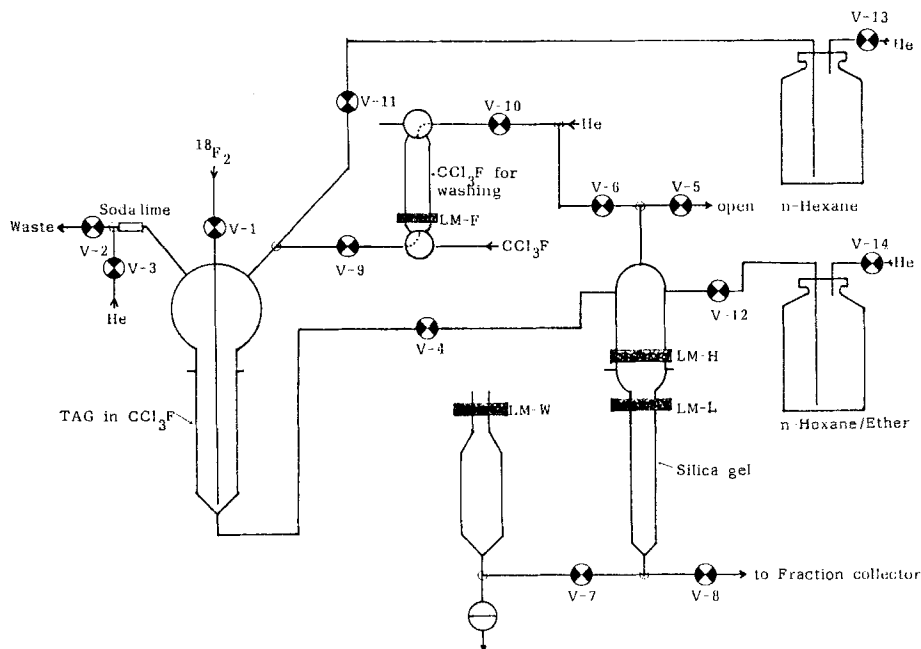


Fig.1 Flow Chart of the Former half of the Automated Synthesis system of  $^{18}\text{F}$ DG  
 V : teflon solenoid valve      LM : photo-level sensor

Table 1 Sequence Program in the former half of the Automated  $^{18}\text{F}$ DG Synthetic Procedure

Step No.	Operation	Stepping method
1	React of $^{18}\text{F}\text{-F}_2$ with TAG(67 mg) in $\text{CCl}_3\text{F}$ (10 ml)	Manual
2	Transfer the reaction mixture to silica gel	LM-H
3	Absorb the reaction mixture on silica gel	LM-L
4	Wash the reaction vessel with fresh $\text{CCl}_3\text{F}$ (5 ml)	LM-F
5	Transfer the $\text{CCl}_3\text{F}$ to silica gel	LM-H
6	Elute TAG with n-hexane (50 ml)	LM-X
7	Elute n-hexane	LM-L
8	Fill a silica gel column with n-hexane/ether(1:1)	LM-H
9	Elute $^{18}\text{F}$ -glucopyranosyl difluoride with n-hexane/ether	Radioactive detector

PRODUCTION OF O-15, C-11 AND F-18 LABELED RADIOPHARMACEUTICALS FOR CLINICAL USE WITH A TANDEM VAN DE GRAAFF ACCELERATOR

---

S.C. Jones, G.D. Robinson, Jr., A. Alavi, E. McIntyre, and M. Reivich, Cerebrovascular Research Center, School of Medicine, University of Pennsylvania, Philadelphia, Pennsylvania 19104.

We have developed a facility for producing positron emitting radiopharmaceuticals with a tandem Van de Graaff accelerator in order to supply the needs of an active positron emission tomography (PET) research center. Carbon-11 labeled carbon monoxide ( $^{11}\text{CO}$ ), oxygen-15 labeled water ( $\text{H}_2^{15}\text{O}$ ) and fluorine-18 labeled 2-fluoro-2-deoxy-D-glucose ( $^{18}\text{F}$ -2FDG) are being produced routinely for the measurement of cerebral blood volume (CBV), blood flow (CBF) and the metabolic rate for glucose (CMRgl), respectively. The problems that have been encountered and solved are the one kilometer separation of the accelerator and clinical area and limited radiochemistry laboratory space and beam current. The solution to these problems has depended to some extent on the radiopharmaceutical.

The University of Pennsylvania tandem Van de Graaff accelerator (FN-6) produces up to 16 MeV protons or deuterons from an ion source (1) capable of putting at least 10  $\mu\text{A}$  on target.

Laboratory space was created by equipping a 3 m by 11 m specially designed trailer as a radiochemistry laboratory. The choice of a trailer allowed the laboratory to be located 22 meters from the target area of the tandem accelerator. The target area was chosen so as not to interfere with the nuclear physics research. Basic equipment includes one shielded fume hood, a hot cell equipped with a master slave manipulator, a radio-gas chromatograph, NaI(Tl) well counter, and a dose calibrator. The distant location of the accelerator and radiochemistry laboratory from our PETT-V facility has complicated the delivery of  $^{15}\text{O}$  and  $^{11}\text{C}$  labeled compounds.

$^{11}\text{CO}$  is produced with the  $^{14}\text{N}(p,\alpha)^{11}\text{C}$  reaction on  $\text{N}_2$  with 0.01%  $\text{O}_2$  in a flow system with 12 MeV protons incident on the gas. Special consideration was given to the need to transport the  $^{11}\text{CO}$  in public areas via hand cart to the PETT-V facility 1000 meters away. The  $^{11}\text{CO}_2$  exiting from the target is collected in a coil of tubing at  $-196^\circ\text{C}$ . A 25 minute bombardment with a beam current of 10  $\mu\text{A}$  results in a 150 mCi collection of  $^{11}\text{CO}_2$ . After the collection is finished, helium flow is established through a flow path which includes zinc at  $395^\circ\text{C}$ , a  $\text{CO}_2$  absorber and a molecular sieve (13X) trap at  $-196^\circ\text{C}$ . This allows the collection of  $\sim 100$  mCi of  $^{11}\text{CO}$  in the molecular sieve trap at a pressure after warming of 3.4 atm absolute. Routine radio-gas chromatography is performed to verify the presence of  $^{11}\text{CO}$  and absence of  $^{11}\text{CO}_2$ . The molecular sieve trap is then transported to the hospital in a shielded container mounted on a hand cart and 20 mCi of  $^{11}\text{CO}$  is dispensed into an evacuated U-tube (200 ml volume) for a CBV study. The U-tube is designed to replace a section of tubing connecting a patient to a respirator, so that the CBV of brain trauma patients can be studied.

Oxygen-15 labeled water vapor is produced in a flowing gas target of 5%  $\text{H}_2$  in  $\text{N}_2$  (2) using the  $^{14}\text{N}(d,n)^{15}\text{O}$  reaction with 10 MeV deuterons incident on the gas. Radio-gas chromatography using Chromosorb 104 at  $130^\circ\text{C}$  with a helium carrier gas flow of 20 ml/min demonstrates that 95% of the activity is present as  $\text{H}_2^{15}\text{O}$  with the balance appearing as  $^{15}\text{O}$  labeled  $\text{O}_2$ . Distillation after bubbling the target gas effluent through water was performed and showed that 100% of the activity distilled at  $100^\circ\text{C}$ .

A gas transport system consisting of 1000 m of 3.2 mm inside diameter teflon tubing connects the  $^{15}\text{O}$  target and the PETT-V facility. The transport parameters of this line were established by measuring the transit time of a helium bolus in  $\text{N}_2$  carrier at drive pressures of 0 to 8 atmospheres. The arrival time of the helium bolus was sensed with a thermal conductivity detector. Figure 1 is a plot of

measured transit time and gas flow rate as a function of drive pressure. For Fig. 1, these parameters are also calculated from laminar flow theory (3). The transit time does not decrease below 3.8 minutes as the drive pressure is increased above 2.4 atm presumably because turbulent flow predominates; the Reynold's number,  $Na$ , is greater than 2000 above a pressure of 2.4 atm. The gas flow rate increases linearly over the same pressure range. Both the measured transit time and gas flow rate depart from the predictions of laminar flow theory at  $Na = 2000$ . Gaseous radioactivity, gas flow rate and gas pressure are monitored at each end of this transport system during operation. The integrity of the line is insured with a fourteen hour pressure test the night before a run. Pressure losses are consistent with the permeability of teflon to nitrogen. Typical operation is at a drive pressure of 3.7 atm and a gas flow rate of 5 l/min.

A bubbling system (Fig. 2) to entrap the  $H_2^{150}$  vapor in saline consists of two precision pumps for saline, a bubbling tube and overflow trap, and a saline radioactivity monitor. The bubbler tube and saline overflow trap are shielded with 2.5 cm of lead. The saline flow rate is 2 ml/min. The saturation activity delivered is typically 6 mCi with a beam current of 1  $\mu A$ . A terminal membrane filter (0.22  $\mu m$ ) assures sterility. The system satisfies electrical safety requirements, possesses a suitable appearance for operation in a medical environment, and has been shown to produce a sterile and apyrogenic solution. The bubbler system produces the stable output necessary for equilibrium imaging of CBF. The output stability is monitored by strip chart recordings of the saline radioactivity monitor.  $H_2^{150}$  is produced, delivered, entrapped in saline, and infused continuously for the measurement of CBF using equilibrium imaging.

$^{18}F$ -2FDG is produced from anhydrous  $^{18}F_2$  produced in a high pressure target (4) containing  $\sim 0.2\%$   $F_2$  in Ne. The  $^{20}Ne(d,\alpha)^{18}F$  reaction with 10  $\mu A$  of 10.5 MeV deuterons (after the target entrance window) produces a thick target saturation activity of 55 mCi/ $\mu A$ . Typically, 40% of the  $^{18}F$  is available as  $^{18}F_2$  for the initial reaction with tri-acetyl glycol. The target is filled to 37 atm absolute with both pure Ne and a 1%  $F_2$  in Ne mixture using a procedure designed to minimize contamination with air. Chemically, the syntheses of  $^{18}F$ -2FDG proceeds as has been reported elsewhere (5). Procedurally, a simple remote synthesis system (Fig. 3) is used to produce 8-12 mCi of  $^{18}F$ -2FDG for injection for the measurement of CMRgl.

This facility serves as a temporary and not completely ideal "factory" for the production of a limited number and quantity of radiopharmaceuticals. Of particular importance in our laboratory is the ability to mesh the needs of radiopharmaceutical production with the normal operation of an accelerator used primarily for nuclear physics research. This has been accomplished by using a dedicated ion source and a schedule which allows a radiopharmaceutical production run the morning before a one to four day nuclear physics experiment. Thus, we have been able to use the accelerator 2 to 3 times a week. Under these scheduling conditions, radiopharmaceutical research must take second priority to the supply of useful radiopharmaceuticals for the study of cerebral hemodynamics and metabolism.

- (1) Middleton, R., Proceedings of the Symposium of Northeastern Accelerator Personnel; SNEAP 80. University of Wisconsin, Madison, Wisconsin.
- (2) Harper, P.V. and Wickland, T., J. Label. Compound. Radiopharm., 18, 186 (1981).
- (3) Hichwa, R.D. and Nickles, R.J., IEEE Trans. Nucl. Sci., NS-26, 1707 (1979).
- (4) Cassela, V., Ido, T., Wolf, A.P., Fowler, J.S., MacGregor, R.R. and Ruth, T.J., J. Nucl. Med., 21, 750 (1980).
- (5) Barrio, J.R., MacDonald, N.S., Robinson, G.D., Jr., Najafi, A., Cook, J.S. and Kuhl, D.E., J. Nucl. Med., 22, 372 (1981).

Supported by United States Public Health Service Program Project Grant Ns-14867-03.

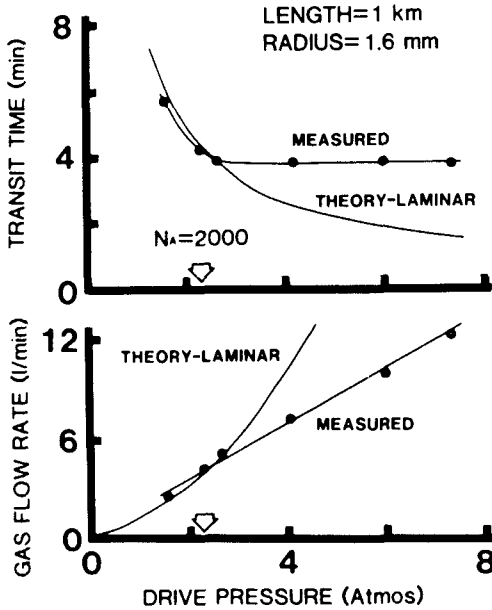


Fig. 1. In the top section, the measured and theoretical (laminar flow) transit time are compared as a function of drive pressure for the 1 km long, 1.6 mm radius 0-15 transport system. In the bottom section, the gas flow rates are compared. Laminar flow theory departs from measurement above a Reynold's number (Na) of 2000. Decay losses during transit cannot be reduced below a factor of  $\sim 4$ .

Fig. 2. The schematic diagram of liquid and gas flow for the bubbler system used to produce  $H_2^{15}O$  in saline for continuous infusion.

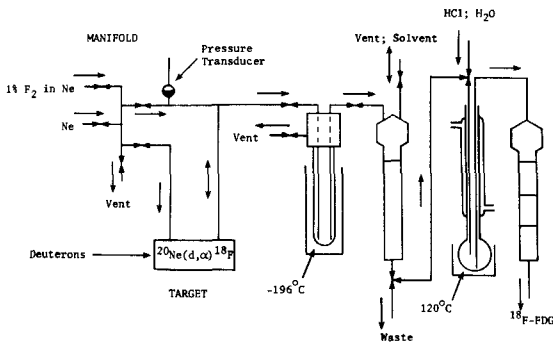
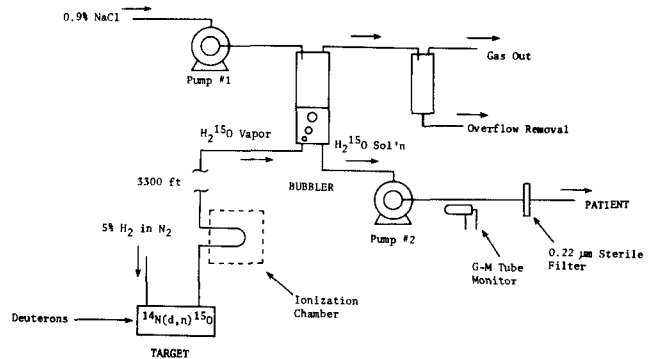


Fig. 3. The  $^{18}F_2$  and  $^{18}F$ -2FDG system. The first column contains silica gel and the second contains ion retardation resin in the top and bottom section with alumina in the middle. For the  $^{18}F$ -2FDG synthesis system, valves are solenoid actuated and reagents are added remotely via teflon tubing.

AN AUTOMATIC TARGET SYSTEM FOR HIGH CURRENT IRRADIATIONS IN THE  
INTERNAL BEAM OF A COMPACT CYCLOTRON

---

W. Stellmacher\*, W. Kogler\*, H. Cremer\*, W. Bolten\*\*, and  
G. Blessing\*\*.

\* Bestrahlungsgruppe des Instituts für Festkörperforschung, and

\*\* Institut für Chemie 1 (Nuklearchemie), Kernforschungsanlage Jülich  
GmbH, D-5170 Jülich, FRG.

The cyclotron production of medically important radioisotopes in quantities sufficient for diagnostic purposes, especially for positron emission computed tomography (PECT), requires development of high current target materials and suitable irradiation facilities so that beam currents  $> 100 \mu\text{A}$  can be used. High currents are generally achieved using internal beams. The irradiated material, however, is strongly radioactive and radiation doses on the order of 500 R/h are expected. It is therefore absolutely necessary that remote controlled and automatic systems for removing the target are developed.

In order to meet the above requirements, especially in the production of  $^{75}\text{Br}$  ( $T_{1/2}$ : 1.6 h), an internal target system has been developed at our Compact Cyclotron CV 28, replacing the older pneumatic tube system. A sketch of the system is shown in Fig. 1. There are three major components of the system:

- 1) Target drive system.
- 2) Vacuum lock system with removal station.
- 3) Target holder.

The target is placed manually in the target holder and then brought to the appropriate position using a definite torque from a motor. Thereafter, the following subsequent steps are controlled by a program:

- Vacuum shutter lid closes pneumatically.
- On reaching the threshold value of the vacuum, flow of cooling water sets in.
- A check against leakage is carried out.
- The high vacuum lock opens up.
- The target head is moved to the internal irradiation position by means of a target drive system.

At the end of the irradiation the removal of the target takes place in the opposite sequence. The vacuum chamber is ventilated, the cooling water is blown out and the irradiated target is removed from the target holder using the mechanics of the target clamp system. The lower target clamp is tilted at the hinge downwards and the target now falls through a photoelectric barrier into a target catcher placed in a lead container. The lid of the container is then closed using a rotating pneumatic elevator.

All the stages of the process can be followed optically using a control and signal panel installed in the control room of the cyclotron.

The system has the following advantages over a conventional pneumatic tube system:

- a) High operational safety and reliability.
- b) Elimination of danger of external contamination.
- c) Strong reduction in the radiation dose to the worker.
- d) Automatic target removal through the use of a computer program (Texas Instruments).
- e) Indication of the beam spot on the silver plated backing of the target.

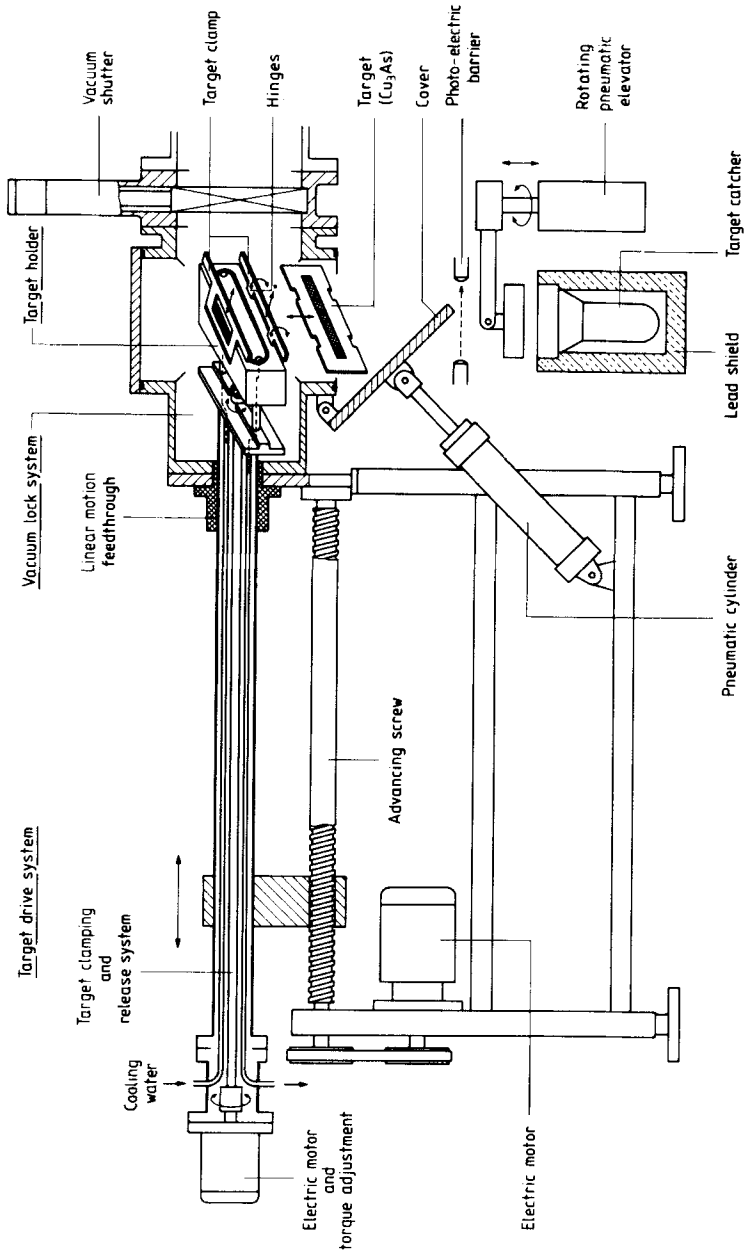


Fig. 1. Sketch of the target system for irradiations in the internal beam.

Working Experience

- i) Radiation dose effects require the change of the O-rings at the target holder every 10 hours of operation.
- ii) In order to avoid high-voltage flashes on the Dee-insulators it is essential that the evaporation of the target material should be negligible.

Typical Use in Production Runs

$^{75}\text{Br}$  (1.6 h) : 36 MeV  $^3\text{He}$ , 100  $\mu\text{A}$ , 2 h irradiation,  $\text{Cu}_3\text{As}$  target  
 $^{77}\text{Br}$  (56 h) : 28 MeV  $^4\text{He}$ , 100  $\mu\text{A}$ , 5 h irradiation,  $\text{Cu}_3\text{As}$  target  
 $^{97}\text{Ru}$  (2.9 d) : 36 MeV  $^3\text{He}$ , 100  $\mu\text{A}$ , 5 h irradiation, Mo target

We thank Prof. G. Stöcklin and Dr. S.M. Qaim for their active support of this work and for fruitful discussions.

DEVELOPMENT OF Na<sup>123</sup>I PHARMACEUTICAL FROM ANTIMONY TARGET

Li Yongjian, Sun Qixun, Shen Dequn, Fan Fasheng, Lan Yunxia, Zhao Zhaoyi, Weng Shouqing, He Weiyu, Lu Jiexi, Yu Yingen, Yang Lanping, Wang Yongchuan, and Ji Qianmei.  
Shanghai Institute of Nuclear Research, Academia Sinica, P.O.Box 8204, Shanghai, The People's Republic of China.

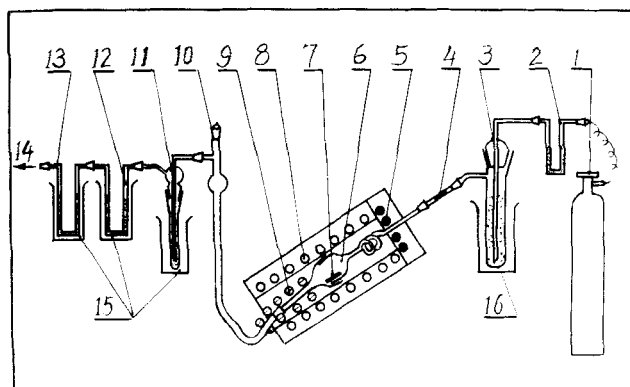
The application of excellent medical radionuclide <sup>123</sup>I progresses quickly and tends to take over most part of reactor-produced <sup>131</sup>I in clinical diagnosis. The demand of more and more sources of <sup>123</sup>I supply becomes remarkable. The conventional methods consisting mainly of <sup>124</sup>Te(p,2n)<sup>123</sup>I reaction and indirect production via <sup>123</sup>Xe parent (1) are restricted by their highly enriched <sup>124</sup>Te target and high energy proton beam. In this paper we describe an alternative new method developed for the production of Na<sup>123</sup>I radiopharmaceutical by <sup>121</sup>Sb(α,2n)<sup>123</sup>I reaction (2,3,4) using natural target with dry separation process to meet local situation.

The Sb target is prepared by electroplating in a bath of 60 g Sb<sub>2</sub>O<sub>3</sub> and 144 ml 40 % HF per liter with 7.6x10<sup>-6</sup> M of PEG-400 as additive. Target substrate from ø 38x2 mm Ag-Cu (1:9) complex in a specially designed cell containing 20 ml plating liquor with Pt wire stirrer as anode at a current density about 40-80 mA/cm<sup>2</sup>. This gives firm bright antimony layer of 60 mg/cm<sup>2</sup> thickness with good thermal conductivity. In irradiation with α-particle beam of 32 MeV the target is back cooled by water and covered with a 14.8 mg/cm<sup>2</sup> thick Al foil for α-degradation to around 30 MeV to insure low <sup>124</sup>I contamination.

The bombarded target is transferred immediately to a quartz dry distillation apparatus heated gradiently to 600 °C at the center. The iodine evolved is carried by a hydrogen stream which is treated first by molecular sieves 5 A, Ag-X at a rate of 10-20 ml/min and then absorbed in 0.1 N NaOH. The radiochemical yield reaches 98 % within 1 hr. The quality is controlled by paper chromatography, about 99 % of the activity in the solution exists as iodide, the rest as iodate with principal chemical impurities of < 0.30 ppm Sb and < 0.15 ppm Cu. Radionuclidic purity at E.O.B. is: > 98 % <sup>123</sup>I, < 0.75 % <sup>124</sup>I, < 0.15 % <sup>126</sup>I, < 0.5 % <sup>125</sup>I. For a thick target, the yield is around 0.3 mCi/μAh. The solution adjusted to pH 6-8 and passed through multipore was subjected to preclinical pharmacological tests (5) and clinical uses; it proved to fulfill the requirements for injection, also suitable for labelling of organic radiopharmaceuticals.

- (1) Stöcklin G., *Int. J. appl. Radiat. Isotopes*, **28**, 131 (1977).
- (2) Deglume Ch., *Deutsch J.P.*, Favart D. and Prieels R., *Int. J. appl. Radiat. Isotopes*, **24**, 291 (1973).
- (3) Silvester D.J., Sugden J. and Watson I.A., *Radiochem. Radioanal. Letters*, **2**, 17 (1969).
- (4) Homa Y. and Murakami Y., *Radioisotopes*, **26**, 315 (1976).
- (5) Li Yongjian, Sun Qixun, Shen Dequn, Fan Fasheng, Wang Yongchuan and Ji Qianmei, "Third World Congress of Nuclear Medicine and Biology", Paris, Aug. 29 - Sept. 2, 1982.





Sketch of dry distillation assembly

- |                  |                 |                      |
|------------------|-----------------|----------------------|
| (1) hydrogen     | (2) drier       | (3) deoxidizer       |
| (4) filter       | (5) furnace-1   | (6) quartz vessel    |
| (7) target plate | (8) furnace-2   | (9) furnace-3        |
| (10) absorber-1  | (11) absorber-2 | (12) molecular sieve |
| (13) Si-gel      | (14) exit       | (15) cold bath       |
| (16) warm bath   |                 |                      |

ABOUT THE POSSIBILITY OF PRODUCTION OF  $^{123}\text{I}$  BY A PHOTONUCLEAR REACTION

---

A.B. Malinin, V.T. Kharlamov, N.V. Kurenkov, and V.B. Popovitch.  
 Institute of Biophysics, Ministry of Health, Moscow 123182, USSR.

The paper considers the possibility of production of  $^{123}\text{I}$  by the reaction  $^{124}\text{Xe}(\gamma, n) ^{123}\text{Xe} \xrightarrow[2.08 \text{ hr}]{\text{EC}, \beta^+} ^{123}\text{I}$  with the use of isotopically enriched xenon and bremsstrahlung beams with the energy of about 25 MeV (1). The calculations based on the experimentally measured yield of  $^{123}\text{Xe}$  for a thin target show that  $^{123}\text{I}$  can be generated in comparable or greater amounts at the modern electron accelerators compared with those at powerful accelerators of charged particles. Fig. 1 presents the  $^{123}\text{I}$  activity calculated per 1  $\mu\text{A}$  of electron current and 1 g of  $^{124}\text{Xe}$  as a function of time of irradiation. The activities are given for the optimum waiting time of the irradiated xenon in order to achieve maximum accumulation of  $^{123}\text{I}$ . Fig. 1 also gives the dependence of the optimum waiting time ( $t_{2, \text{opt}}$ ) on the time period of irradiation ( $t_1$ ).

The level of  $^{125}\text{I}$  impurity in the  $^{123}\text{I}$  produced can be estimated from Fig. 1 which shows its values for various irradiation time periods with similar isotopic content of  $^{126}\text{Xe}$  and  $^{124}\text{Xe}$  in the irradiated target. Decrease of the relative fraction of  $^{126}\text{Xe}$  allows to increase the energy of bremsstrahlung beam and, consequently, the yield of  $^{123}\text{I}$  without generating detectable admixtures of undesired  $^{124}\text{I}$  by a direct reaction ( $\gamma, np$ ).

(1) Levin V.I. et al., The Russian Patent no. 671194 (1977).

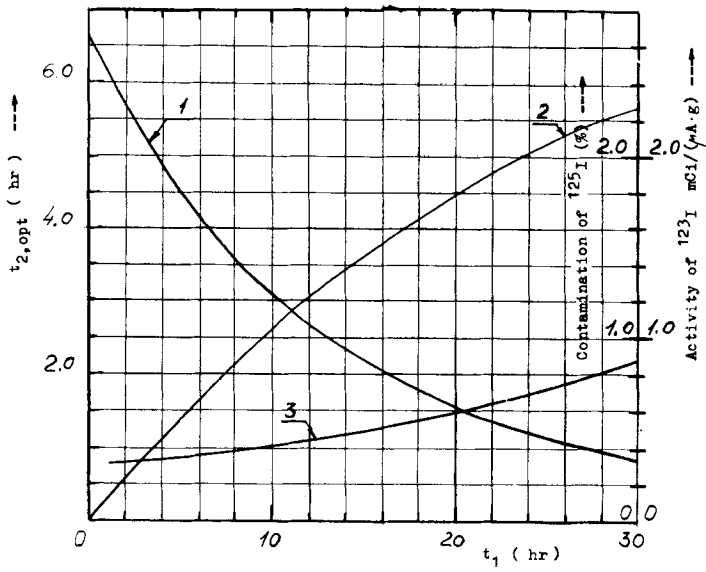


Fig. 1. The optimum waiting time ( $t_{2,opt}$ ) of xenon after the irradiation (curve 1); the activity of  $^{123}\text{I}$  (curve 2) and the contamination of  $^{125}\text{I}$  (curve 3) as a function of the irradiation time ( $t_1$ ).

AN AUTOMATED GAS HANDLING SYSTEM FOR  $^{11}\text{C}$ -LABELED  $\text{CO}$ ,  $\text{CO}_2$ , AND  $\text{HCN}$ 

G.-J. Meyer, T. Harms, and H. Hundeshagen.  
Abteilung Nuklearmedizin und spezielle Biophysik, Medizinische Hochschule Hannover.

$^{11}\text{C}$ -labeled  $\text{CO}$ ,  $\text{CO}_2$ , and  $\text{HCN}$  are the basic precursors for the synthesis of  $^{11}\text{C}$ -radiopharmaceuticals. A vacuum system has been built which allows remote handling of these products in Curie-quantities on a routine production scale. A scheme of the system is given in Fig. 1.

The vacuum line is connected to two gas targets, one for  $^{11}\text{CO}_2$  production, the other one for  $^{11}\text{CH}_4$  production according to the method of Christman et al. (1). The main functions of the system are described below.

 $^{11}\text{CO}_2$  collection

$^{11}\text{CO}_2$  is produced via the  $^{14}\text{N}(\text{p},\alpha)^{11}\text{C}$  nuclear reaction in a  $\text{N}_2$  gas target at 7 bar. After the end of bombardment (EOB) the target is depressurized via the flow controller, valve no. 1, valve no. 2, the Ni-plated glass trap (at liq.  $\text{N}_2$  temp.), valve no. 4, and the flow meter. Then the system is closed against the target, excessive dead volume, and the outlet by valves no. 1, no. 2, and no. 4. By opening valve no. 3 the system is evacuated to  $10^{-3}$  torr. After the vacuum is reached valve no. 3 is closed again. Valve no. 5 is connected to a preevacuated reaction vessel which is cooled with liq.  $\text{N}_2$ . Upon opening of valve no. 5 the cooling of the Ni-plated glass trap is lowered and the trap heated at  $100^\circ\text{C}$  by a direct electrical current.  $^{11}\text{CO}_2$  distills into the reaction vessel which can be closed and detached from the line easily by a manipulator. The whole process takes 5-6 min from EOB and yields ca. 1.5 Ci for a 20 min irradiation at 40  $\mu\text{A}$  beam current.

 $^{11}\text{CO}$  production

The procedure follows the one for  $\text{CO}_2$  collection until the evacuation step. After the vacuum is reached valve no. 3 is closed and the system filled with He by opening valves no. 8 and no. 9. When the He pressure has reached 0.5 bar valves no. 6 and no. 7 are opened and valve no. 9 is closed in order to restrict the He flow to a precalibrated value of 25 ml/min. Lowering of the liq.  $\text{N}_2$  cooling of the Ni-plated glass trap and heating leads to the release of  $^{11}\text{CO}_2$  and its subsequent reduction to  $^{11}\text{CO}$  by passing the  $400^\circ\text{C}$  Zn-catalyst.  $^{11}\text{CO}$  is either collected in a 100 ml syringe or is bubbled through a reaction mixture. The total time required for the production is ca. 10 min from EOB. The amount of  $^{11}\text{CO}$  is ca. 1 Ci in 100 ml He, for a 20 min irradiation at 40  $\mu\text{A}$ .

 $\text{H}^{11}\text{CN}$  production

$^{11}\text{CH}_4$  is produced in a separate gas target by irradiation of a 95 %  $\text{N}_2$  + 5 %  $\text{H}_2$  gas mixture. The target is depressurized via the flow controller, valve no. 1, the  $1000^\circ\text{C}$  Pt-catalyst, the  $\text{P}_2\text{O}_5$  trap, valve no. 2, the Ni-plated glass trap (at liq.  $\text{N}_2$  temp.), valve no. 4, and the flow meter. Upon passing the Pt-catalyst  $^{11}\text{CH}_4$  is converted to  $\text{H}^{11}\text{CN}$  by the action of radiolytically formed  $\text{NH}_3$ . The  $\text{H}^{11}\text{CN}$  is trapped in the Ni-plated glass trap and worked up in the same way as  $^{11}\text{CO}_2$ . Because of a reduced flow during the release from the target and a somewhat slower distillation of  $\text{HCN}$  when compared with  $\text{CO}_2$  the whole procedure takes ca. 10-12 min from EOB to detachment of the reaction vessel from the line. The overall yield is ca. 1 Ci for a

20 min irradiation at 40 uA beam current.

- (1) Christman D.R., Finn R.D., Karlstrom K.I. and Wolf A.P.,  
 Int. J. appl. Radiat. Isotopes, 26, 435 (1975).

Acknowledgement

A prototype gas handling system was built by G.J.M. and the technical staff of the chemistry department, Brookhaven Nat.Lab., unter supervision of Dr. A.P. Wolf. The version presented here is based on the same concept; however, it is improved in many respects. The authors are indebted to Dr. A.P. Wolf and the technical staff of the Brookhaven Nat.Lab's chemistry department for their advice and help in building the prototype version.

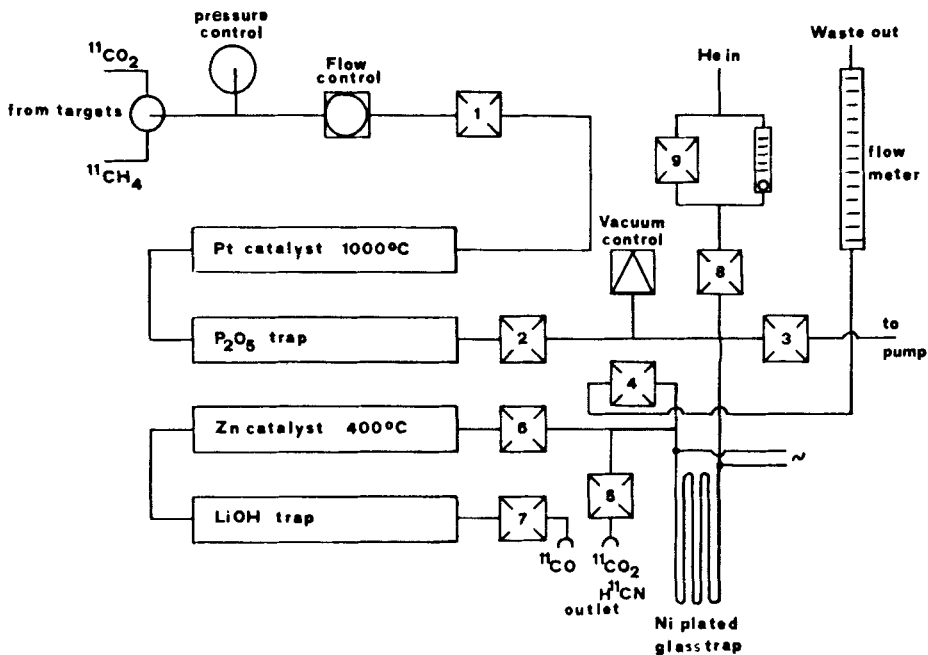


Fig. 1 Scheme of gas handling system for  $^{11}\text{CO}$ ,  $^{11}\text{CO}_2$ , and  $\text{H}^{11}\text{CN}$ .

SMALLER, COLDER TARGETS

R.J. Nickles, M.F. Daube, and G.D. Hutchins.

Department of Medical Physics, University of Wisconsin, Madison, WI 53706.

The clinical application of positron emission tomography at the Wm. S. Middleton VA Hospital utilizes an Ortec ECAT scanner with radiotracers originating from generators ( $^{68}\text{Ge}/^{68}\text{Ga}$ ,  $^{82}\text{Sr}/^{82}\text{Rb}$ ) or the UW EN tandem accelerator. The tandem constraints on beam current and energy are severe (4 uA protons or deuterons, 11 MeV), calling for high-yield reactions on enriched targets. This leads logically to small-volume, high-pressure cryogenic targets sealed with a single, thin (25 um) entrance foil (1). These small, cold targets offer advantages to cyclotrons now being developed for "turn-key" installations, namely

- small proton-only machines needing enriched targets and
- self-shielded machines with targets re-entrant into the magnet gap.

A number of special purpose targets have evolved, characterized in Table 1 along with the previously-reported (2)  $^{80}\text{Kr}$ -target (E) for comparison.

TABLE 1.

TARGET:	<u>A</u>	<u>B</u>	<u>C</u>	<u>D</u>	<u>E</u>
Designed for:	$^{18}\text{F}^-$	$^{18}\text{F}_2$	$^{15}\text{O}_2$	$^{13}\text{NO}_3^-$	$^{81}\text{Rb}; ^{38}\text{K}$
Target material:	$^{18}\text{O}_2$ (pure)	$^{18}\text{O}_2 + \text{F}_2$	$^{15}\text{N}_2$	$\text{H}_2\text{O}$	$^{80}\text{Kr}; ^{38}\text{Ar}$
Static?/Recovered?	yes/yes	yes/no	yes/no	flow-loop	yes/yes
Product form:	$^{18}\text{F}$ -on-liner	$^{18}\text{F}_2$	$^{15}\text{O}_2$	$^{13}\text{NO}_3^-$	$\text{Rb}^+; \text{K}^+$
Recovered yield: (mCi/uA EOSB 10 MeV)	150	50*	70	10	15; 2
Material:	SS	Ni	quartz	SS	SS
Entrance foil:	Nb	Ni	SS	Nb	Nb
Sealed by:	O-ring	Pb-gasket	Ag-braze	O-ring	In-gasket
Volume (ml):	25	4	5	1	2
Length (cm):	15	6	5	1	3
Diam (mm):	12	6	9	8	4 → 10
Operating					
Pressure (abs atm):	15	< 60	25	1	< 60
Temp max (°C):	100	250	400	100	80
min:	-70	-190	-190	0	-190
Transducers,	P,T, $\beta^+$ ,	P,T	P,T,	fiber-	P,T,
special features:	viewport		view	optics	washable

\* With  $^{20}\text{Ne}(d,\alpha)^{18}\text{F}$ .

Target A was designed for  $^{18}\text{F}$ -fluoride deposition into a pyrex liner. The  $^{18}\text{O}_2$  gas is stored over molecular sieve, with transfer to or from the target by application of a torch or  $\text{LN}_2$ , respectively. The target is thick to incident 10 MeV protons, with 150 mCi/uA saturation yields of  $^{18}\text{F}$  adhering to the liner interior. Eighty percent recovery into hot water is typical, followed by workup to the desired anhydrous tetraethylammonium fluoride.

Target B was designed for  $^{18}\text{F}_2$  production with dimensions scaled down to permit an expendable  $^{18}\text{O}_2$  charge that would be effectively lost in the synthesis of  $^{18}\text{F}$ -2FDG (3). The target gas sees only passivated (4) nickel surfaces. The two seals maintaining target pressure and accelerator vacuum are made by a single Pb-gasket overlapping a single nickel foil, tight over the extended temperature range. Target filling (1 atm Ne+30%  $\text{F}_2$ ; 25-35 atm  $^{18}\text{O}_2$ ) proceeds through separate ports

(passivated manifold for F<sub>2</sub>; low-volume for <sup>18</sup>O<sub>2</sub>) with only 100 ml (STP) of <sup>18</sup>O<sub>2</sub> invested. Initial studies show 80% recovery as useful <sup>18</sup>F<sub>2</sub> at low doses (15 min @ 2 mA; ~ 400 eV/molecule), dropping to 15% at longer irradiations (2 hrs @ 2 uA). Until the O<sub>2</sub>-F<sub>2</sub> interaction is better understood, this target is charged with Ne + 1% F<sub>2</sub> for deuteron irradiation, with reproducible <sup>18</sup>F<sub>2</sub>-fractions in excess of 80% of the total yield.

Target C was designed for the irradiation of <sup>15</sup>N<sub>2</sub> and <sup>13</sup>CH<sub>4</sub>, with special attention paid to TV telemetry of the entire beam path in the gas target. To achieve this, the entrance foil is silver brazed (BT) onto a copper seat which re-enters back into the 12 mm OD quartz tube that comprises the outer wall of the target chamber. The open end of the quartz tube is secured in a cooled metric swage fitting with teflon ferrules. The rear end is flame-sealed around a rhenium wire acting as a feed-through to monitor ionization current.

Target D is a flow-through liquid target, notable for its high-resolution telemetry of the beam strike fluorescence. Target E is suitable for use with such extremely costly gases as <sup>80</sup>Kr and <sup>38</sup>Ar due to its small volume and reliability at pressure and temperature extremes. The modest <sup>38</sup>Ar(p,n)<sup>38</sup>K yield, extrapolated from measurements on natural argon, holds the only hope for <sup>38</sup>K-production on a proton-only machine.

During production, activity buildup is anticipated by a leaky integrator and measured directly at the target by a current-mode plastic scintillator. The emphasis on view ports and pressure transduction reflects the importance of maintaining a gas target thick enough to stop the incident beam. In those targets (B,E) not permitting visual inspection of end-of-range, the fingerprint of a thick target is a monotonically increasing pressure rise  $\Delta P$  at constant current, as the beam energy is raised. Similar assurance is given by the proportionality of the observed scintillator output with beam current.

For positron tomography to reach a wider audience, the production of positron emitters must be broadened through small accelerator facilities. The accelerator enlisted - either old or new - imposes its own unique constraints. By scaling size and temperature down and pressure up, a number of target problems are bypassed, so that full attention can be focussed on the subsequent radiopharmaceutical synthesis.

- (1) Nickles R.J., Nucl. Instr. Methods, 177, 593 (1980).
- (2) Hichwa R.D., Daube M.E. and Nickles R.J., J. Lab. Comp. Radiopharm., 18, 227 (1981).
- (3) Ido T., Wan C.N., Casella V.J., et al., J. Lab. Comp. Radiopharm., 14, 175 (1978).
- (4) Lambrecht R.M., Neirinckx R. and Wolf A.P., Int. J. appl. Radiat. Isotopes, 29, 175 (1979).

$^{52}\text{Fe}$  PRODUCTION AND CHEMICAL RECOVERY FOR MEDICAL USE

H. A. O'Brien, Jr., P. M. Grant, G. E. Bentley, J. W. Barnes, and H. M. Zacharis.  
 Medical Radioisotopes Research Group, Los Alamos National Laboratory,  
 Los Alamos, NM 87545.

Radioiron has been shown to be useful as an *in vivo* imaging agent for erythropoietic bone marrow (1) and is believed to be of greater value than  $^{111}\text{In}$ -transferrin in following the course of radiation/chemotherapy in oncologic patients.  $^{52}\text{Fe}$  (8.28 hr) decays by positron emission and electron capture and emits a 168-keV gamma photon. The radiation dose to the bone marrow from 0.1 mCi of  $^{52}\text{Fe}$  is estimated to be 2.5 rads as compared with 10 rads from 0.02 mCi of  $^{59}\text{Fe}$  (2).

$^{52}\text{Fe}$  decays solely to  $^{52\text{m}}\text{Mn}$  (21.1 min.), which, in turn, decays 98% by a combination of electron capture and positron emission. Thus,  $^{52\text{m}}\text{Mn}$  should be useful in emission computed tomography imaging. In 1977,  $^{54}\text{Mn}$  uptake in canine myocardium was reported to be nearly twice that of  $^{201}\text{Tl}$ , the most widely used radioactive agent in cardiovascular nuclear medicine today (3). It is also noted that the quantity of  $^{54}\text{Mn}$  in the area of infarction was markedly decreased. Mn (II) has been shown to be cleared rapidly from the blood with high uptake in the myocardium within 5 minutes following IV administration (myocardium/blood ratio is 97.5 at 5 minutes) (4).

We have studied the spallogenic yields of  $^{52}\text{Fe}$  in nickel targets irradiated with 800-MeV protons, and previously reported a cross section of  $1.54 \pm 0.13$  mb for this reaction (5). Using 2.54 cm diameter by 1.91 cm thick stacks of 0.05 cm Ni foils, typical 16 hour irradiations at beam currents varying between 250 and 375  $\mu\text{A}$  will yield slightly over 1 Ci of  $^{52}\text{Fe}$  at EOB. Admittedly these conditions are less than optimum, since the size of the proton beam entering our irradiation facility is slightly in excess of 5 cm in diameter. It is necessary to have yields of this magnitude or greater, as chemical processing and transport will require on the order of three  $^{52}\text{Fe}$  half-lives to achieve.

A radiochemical recovery procedure was developed to isolate the radioiron from the target. This procedure gives an overall chemical yield of  $99 \pm 1\%$  for iron. A biomedical generator based on the absorption of iron on an anion exchange resin has been reported to yield approximately 90% of the available  $^{52\text{m}}\text{Mn}$  (4).

- (1) Rayudu, G. V. S., Shirizi, S. P. H., Fordham, E. W., and Friedman, A. M., *Int. J. Appl. Radiat. Isotop.*, **24**, 451 (1973).
- (2) Van Dyke, D., Shkurkin, C., Price, D., Yano, Y., and Anger, H. O., *Blood*, **30**, 364 (1967).
- (3) Chauncey, D. M., Halpern, S. E., Hagan, P. M., McKegney, M. L., Bernstein, K. D., and O'Brien, H. A., *Proceed. West. Reg. Mtg. II, Soc. Nucl. Med.*, p. F-2 (1977).
- (4) Atcher, R. W., Friedman, A. M., Huizenga, J. R., Rayudu, G. V. S., Silverstein, E. A., and Turner, D. A., *J. Nucl. Med.*, **19**, 689 (1978).
- (5) Grant, P. M., O'Brien, H. A., Bayhurst, B. P., Gilmore, J. S., Prestwood, R. J., Whipple, R. E., and Wanek, P. M., *J. Label. Compd. Radiopharm.*, **XVI**, 213 (1979).



CHEMICAL YIELDS MEASURED FOR SPALLOGENIC IRON RADIOCHEMICAL PROCEDURE  
(RESULTS AVERAGE OF 4 EXPERIMENTS)

	OVERALL CHEMICAL YIELD (%)							
	IIA*	Sc	V	Cr	Mn	Fe	Co	Ni
ORIGINAL SOL'N	100	100	100	100	100	100	100	100
AQUEOUS AFTER MIBK	93	98±1	96±4	100	100	0.30±0.5	99±0.2	100
MIBK 1	6.6	2.0±0.8	4.0±4	0	0	100±0.6	1.1±0.2	0
6M HCL WASH	6.6	2.0±0.8	4.0±4	0	0	0.66±0.5	1.1±0.2	0
MIBK 2	0	0	0	0	0	99±1	0	0
MIBK 3	0	0	0	0	0	0	0	0
H <sub>2</sub> O STRIP (FINAL SOL'N)	0	0	0	0	0	99±1	0	0

\*RESULTS OF ONE EXPERIMENT ONLY

RADIOISOTOPE PRODUCTION VIA 500 MEV PROTON-INDUCED REACTIONS

R. Robertson, D. Graham, and I.C. Trevena.

Atomic Energy of Canada Limited, 4004 Wesbrook Mall, Vancouver, B.C.,  
Canada V6T 2A3.

As part of a collaboration between AECL and TRIUMF on commercial radioisotope production, a facility for irradiating targets with 500 MeV protons was built immediately before the beam-stop on beamline 1A of the TRIUMF cyclotron. This facility was commissioned in the spring of 1980 and is described elsewhere (1).

Targetry and chemistry have been developed and measurements on production-rates and impurity-levels have been made with respect to the five radioisotopes listed in the table below. This information, together with the methodology used to derive it, is expanded upon and further quantitative data on by-products and waste-products are given. In some cases the derived information is compared with that of a similar nature from Los Alamos and Brookhaven. Some problems and peculiarities associated with the production of these and other spallation-produced isotopes are outlined.

Isotopes Produced via 500 MeV Protons on 0.8cm Thick Targets

<u>Isotope Product</u>	<u>Target Material</u>	<u>* Practical (Observed) Production-Rate</u>		<u>** Main Impurities</u>		
		<u>(<math>\mu\text{Ci}/\mu\text{A.h}</math>)</u>		<u>Isotope</u>	<u>Level</u>	
<u>(relative to product isotope 100%)</u>						
Cu-67 (61.9h)	High Purity zinc metal (cast)	30	(3d, 7d)	Cu-64	0.5%	(7d)
				Sr-46	0.003%	(7d)
				V-48	0.001%	(7d)
Ge-68 (288d)	Arsenic metal powder (compressed)	3.5	(200d, 60d)	Ge-71	3%	(60d)
Sr-82 (25.0d)	Molybdenum metal powder (compressed)	40	(30d, 15d)	Sr-85	200%	(15d)
				Sr-83	0.1%	(15d)
				Sr-8 <sup>c</sup>	<0.3%	(15d)
				Sr-90	<0.001%	(15d)
Cd-109 (464d)	High purity indium metal (cast)	16	(200d, 150d)	Cd-115m	0.5%	(150d)
				Sn-113	0.01%	(150d)
Xe-127 (36.4d)	Cesium chloride salt (compressed)	50	(30d, 15d)	Xe-129m	20%	(15d)
				Xe-131m	15%	(15d)

\* No adjustments are made to the observed production rates for chemical yield ( $\sim 90\%$ ), or for decay during and after bombardment. The quantities in brackets are the typical irradiation and decay times (days and days after EOB) associated with these rates.

\*\* The quantities in brackets associated with the impurity-levels are days after EOB, the approximate decay times required for effective use of the products and corresponding roughly with the normal times of delivery or precalibration to the end-user.

(1) Burgerjon J.J. et al., Proceedings of 27th Conference on Remote Systems Technology pp. 285-291, San Francisco (1979).

## CRYOSTATS FOR LOW TEMPERATURE CYCLOTRON IRRADIATION OF SOLID TARGETS

M. Vogt, A. Gabrysch, and K. Rössler.

Institut für Chemie 1 (Nuklearchemie), Kernforschungsanlage Jülich GmbH, D-5170 Jülich, FRG.

When irradiating solid targets with ion beams from accelerators or cyclotrons, low temperatures are often necessary in order to prevent thermally activated processes or to maintain a specific structure. They are also applied because of the thermal and/or radiation stability of the target. It should be noted that in the case of insulator materials, the heat conductance increases when going to lower temperatures. Some older cryostat systems for irradiation with low-intensity (about 1 W thermal dissipation) ion beams at 5 K and with beams up to some 100 W at 77 K have previously been reported (1-3). A more recent type with a beaker-shaped target holder, which can be filled with cooling liquid from a liquid N<sub>2</sub> reservoir by means of a stopper system, has been improved (Fig. 1). Mounting and demounting of the target holder is performed by means of a gate valve system without interrupting the vacuum of the cryostat system. Stainless steel, aluminium, pure copper and a copper-2 % beryllium alloy have been tested as materials for the target holder. In general, aluminium is the material of choice since it combines low activation cross section with good heat conductivity and a reasonable mechanical stability. Heating a 1 cm<sup>2</sup> spot with 200 W gave rise to a temperature increase of only 10 K in the immediate vicinity.

For irradiation of frozen gases such as NH<sub>3</sub>, noble gases, volatile methyl halides, etc., two new liquid N<sub>2</sub>-cooled systems have been developed. The first is for proton beams and consists of a metal dewar system with thin windows (20 μ Ti - or 15 μ Havar-foils) which allow the beam to penetrate the dewar (Fig. 2). Target holders of 0.4, 2.5 and 5 ml capacitance made of aluminium or Cu/Be-alloy (Fig. 3) can be mounted inside the vessel in such a way that the ion beam passes directly into the target without interfering with the cooling liquid. Two tubes of 1 mm inner diameter allow the filling of the substrate, removal of the gas phase after irradiation, pipetting or distillation of the products, or solvent rinsing of the walls. 4 g frozen NH<sub>3</sub> had been irradiated for 20 minutes with a 30 μAcm<sup>-2</sup> 20 MeV proton beam without giving rise to any dramatic increase in pressure, i.e. the NH<sub>3</sub> remained solid or at least liquid without evaporating.

For irradiation with 14 MeV deuterons a somewhat modified system has been developed (Fig. 4). After passage through 15 μ Havar foil, the beam reaches the target chamber which contains 0.13 ml CH<sub>3</sub>Cl. The chamber is cooled by a liquid N<sub>2</sub>-bath via a copper rod. For transport, the whole system can be closed by a gate valve. Frozen CH<sub>3</sub>Cl (77 K) remains solid with a 0.1 μAcm<sup>-2</sup> 14 MeV d-beam.

- (1) Pross L., Hemmerich J. and Rössler K., *Rev. Sci. Instrum.*, **47**, 353 (1976).
- (2) Rössler K., Cavallero A. and Vogt M., *Nucl. Instr. Meth.*, **189**, 141 (1981).
- (3) Rössler K., Vogt M. and Gabrysch A., paper presented at the 18th European Cyclotron Progress Meeting, Louvain-la-Neuve, Belgium, March 26-27, 1981.

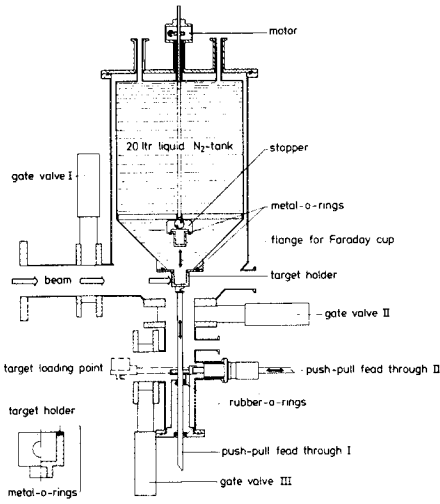


Fig. 1 Cryostat with beaker-shaped target holder.

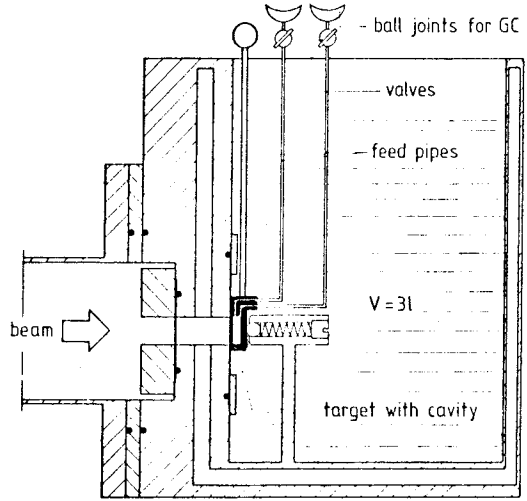


Fig. 2 Cryostat for irradiation of frozen gases with protons.

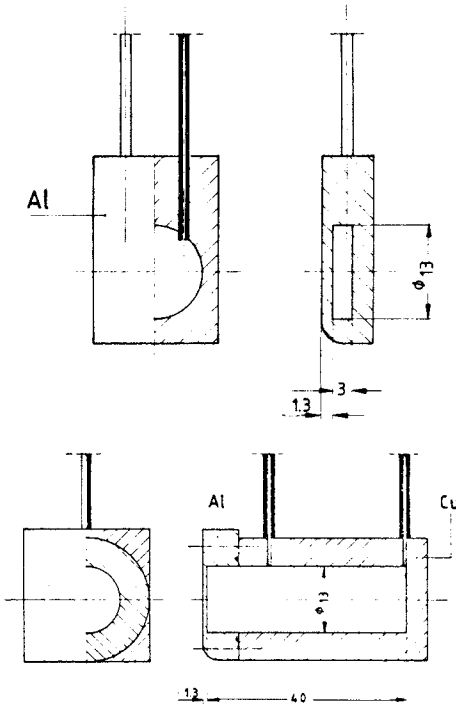


Fig. 3 0.4 ml Al-target chamber and 5 ml Cu/Be-target with 1.3 mm Al window.

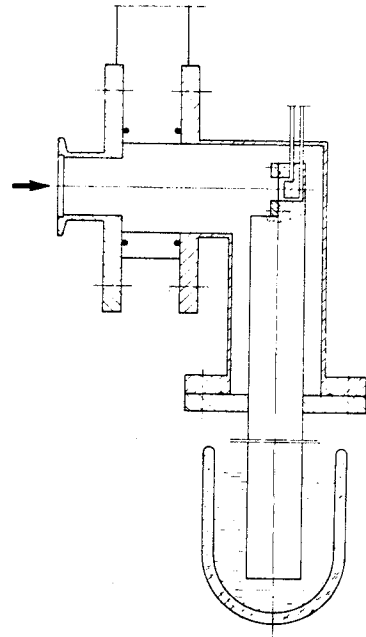


Fig. 4 Cryostat for irradiation of frozen gases with deuterons.

## CHAIN ELONGATION BY RECOILING $^{11}\text{C}$ CARBON ATOMS: A TOOL FOR "NO CARRIER ADDED" LABELING OF BIOMOLECULES

---

G. Gundlach, E.L. Sattler, U. Wagenbach, and K. Wittig.  
Zentrum für Biochemie und Strahlencentrum der Justus-Liebig-Universität, D-6300 Giessen, FRG.

High voltage paper electrophoresis shows in combination with the observation of gaseous products that a good deal of the  $^{11}\text{C}$ -activity produced by the  $\gamma, n$ -process is to be found in compounds, which migrate like amino acid. One part, 5-10% of the total  $^{11}\text{C}$  is trapped by the so-called "retention" or replacement of  $^{12}\text{C}$ -atoms by  $^{11}\text{C}$ . Other attacks of the  $^{11}\text{C}$ -atom lead to cleavage of the bremsstrahlung irradiated target molecule. About 5-10% is found added to the target molecule forming the next homologue.

With the aid of preparative HPLC we have separated these chain elongation products and performed some further chemical analysis and some biological experiments. Both reveal that the optical activity at the  $\alpha$ -C-atom of the amino acid is not changed by the labelling reaction. There is evidence that the C-addition takes place preferentially at the C-atom standing at the end of the target molecule.

Simple aliphatic amines and fatty acids were found to bring about the same amount of labeled higher homologues, namely 5-10%. So, amino acids, fatty acids and amines may be produced by recoil technique without adding carrier and isolated for biological purposes. Starting from one gram "target material" one should expect under optimized conditions one mCi and more of radioactivity ready to use.